# TRANSPORTER-TARGETED PRODRUG DELIVERY TO IMPROVE ORAL BIOAVAILABILITY OF SAQUINAVIR

A DISSERTATION IN

Pharmaceutical Sciences
and
Chemistry

Presented to the Faculty of University of
Missouri-Kansas City in partial fulfillment of
the requirements for the degree

DOCTOR OF PHILOSOPHY

by
ZHIYING WANG

B.S., Pharmacy, China Pharmaceutical University, 1998
M.S., Pharmaceutics, Peking University, 2003

Kansas City, Missouri

2013

TRANSPORTER-TARGETED PRODRUG DELIVERY TO IMPROVE ORAL BIOAVAILABILITY OF SAQUINAVIR

Zhiying Wang, Candidate for the Doctor of Philosophy Degree

University of Missouri-Kansas City, 2013

## ABSTRACT

Saquinavir (SQV) is the first antiretroviral protease inhibitor approved by Food and Drug Administration in the United States for the treatment of HIV infection due to its potent anti-HIV activity. However, some unfavorable properties including low aqueous solubility, low intestinal absorption and fast biotransformation lead to its poor oral bioavailability and limited therapeutic efficacy. The objective of this dissertation project is to investigate whether stereoisomerized peptide prodrugs targeting influx transporter system could improve intestinal absorption and oral bioavailability of SQV.

Four stereoisomeric dipeptide prodrugs of SQV including *L*-valine-*L*-valine-SQV (LLS), *L*-valine-*D*-valine-SQV (LDS), *D*-valine-*L*-valine-SQV (DLS) and *D*-valine-*D*-valine-SQV (DDS) and two amino acid prodrugs including *L*-valine-SQV (LS) and *D*-valine-SQV (DS) were synthesized and investigated using *in vitro* cell culture models. All dipeptide prodrugs exhibit improved aqueous solubility, lowered cytotoxicity, and reduced P-gp/MRP2-mediated efflux activities regardless of stereochemistry in promoieties. SQV attached with *L*-isomers shows higher affinity for peptide transporters but lower stability and higher toxicity, whereas conjugation with *D*-isomers can enhance stability and reduce toxicity, but not be recognized by peptide transporters. Subsequently,

results of metabolism studies performed in rat liver microsomes indicate that elimination half life of SQV was prolonged dramatically by 7- to 40-fold due to prodrug modification with the rank order of DDS > DLS > LDS > LLS > DS > LS > SQV. In comparison with *D*-configuration, *L*-configuration favors the interaction between prodrugs and rat hepatic CYP3A enzymes, resulting in a relatively rapid clearance by CYP3A. Stereoselectivity is also observed in protein binding of prodrugs in rat plasma. Lower protein binding was obtained by LS, LLS and LDS but higher by DS, DDS and DLS as compared with SQV.

Pharmacokinetics studies performed in rats provide further evidences that oral bioavailability of SQV is drastically enhanced by conjugation with dipeptide *L*-valine-*D*-valine. In conclusion, stereoisomeric dipeptide prodrug modification targeting specific influx transporters could be a successful strategy to improve bioavailability of poorly absorbed drug SQV.

Additionally, influence of exogenous human efflux transporters (P-gp, MRP2 and BCRP) on functional activities of endogenous peptide transporters (PepT) was also delineated in *MDR*-transfected MDCK cell lines in this project. Results demonstrate that overexpression of *MDR* genes reduces PepT function probably due to the phenomenon of transporter-compensation resulting in down-regulation of endogenous genes. It may provide some mechanistic insight into possible reasons for underestimation in drug screening using these cell models.

APPROVAL PAGE

The faculty listed below, appointed by the Dean of School of Graduate Studies have examined the dissertation titled “Transporter-Targeted Prodrug Delivery to Improve Oral Bioavailability of Saquinavir” presented by Zhiying Wang, candidate for the Doctor of Philosophy degree, and certify that in their opinion it is worthy of acceptance.

Supervisory Committee

Ashim K. Mitra, Ph.D., Committee Chair

Division of Pharmaceutical Sciences

Chi H. Lee, Ph.D.

Division of Pharmaceutical Sciences

Kun Cheng, Ph.D.

Division of Pharmaceutical Sciences

Zhonghua Peng, Ph.D.

Department of Chemistry

Andrew J. Holder, Ph.D.

Department of Chemistry

CONTENTS

ILLUSTRATIONS

Figure Page

TABLES

Table Page

ACKNOWLEDGEMENTS

I would like to express my sincere thanks and deep appreciation to my advisor Dr. Ashim K. Mitra for giving me a great opportunity to work in his laboratory. I would like to thank him for his excellent guidance, persistent encouragement, and continuous support in my research. I am also thankful to the members of my supervisory committee, Dr. Chi H. Lee and Dr. Kun Cheng of the Division of Pharmaceutical Sciences, Dr. Zhonghua Peng and Dr. Andrew J. Holder of the Department of Chemistry for both kindly serving in my committee and all their help and guidance throughout my graduate work.

I would especially like to thank Dr. Dhananjay Pal for his guidance and support not only on the research but also in the daily life. I would also like to thank Dr. Shuanghui Luo, Dr. Xiaodong Zhu, and Dr. Swapan Samanta for teaching me synthesis, Mass spectrometry and other laboratory techniques essential for successful completion of doctoral degree. Also I am thankful to Mrs. Ranjana Mitra in particular for her cheerful encouragement and support during my stay at UMKC.

I would like to give my deep thanks to Joyce Johnson and Sharon Self for their help through the years. I would also like to express my gratitude towards all the other professors, staff members, and graduate students in the Division of Pharmaceutical Sciences for their help and friendship.

I would like to acknowledge National Institute of Health (NIH) for funding my research.

DEDICATED TO MY PARENTS, MY HUSBAND CHENGLIN AND MY DAUGHTER SHUYA

# CHAPTER 1

# INTRODUCTION

## Overview

HIV protease inhibitors (PIs) are currently considered to be the most important therapeutic agents for the treatment of human immunodeficiency virus (HIV) infection. Their anti-HIV activities result from the blockage of the active site of HIV aspartyl protease, which cleaves the viral gag and gag-pol precursor polyproteins, and the consequent inhibition of production of infectious virions. Saquinavir (SQV) is the first antiretroviral PI drug approved by Food and Drug Administration (FDA) in the United States with significant activity against HIV. Hard gelatin capsule formulation of SQV mesylate (Invirase®) and SQV soft gelatin capsule (Fortovase®) developed by Roche Pharmaceuticals were marketed in the US for the treatment of HIV/AIDS in 1995 and 1997, respectively. However, some unfavorable properties, such as low aqueous solubility, low intestinal absorption and fast biotransformation into inactive metabolites, contribute to its poor oral bioavailability and limit its clinical outcomes. Oral bioavailability of SQV was reported to be only 4% for 600-mg hard gelatin capsules (Invirase®) and around 12% for 1200-mg soft gelatin capsules (Fortovase®) in healthy adults after a single dose administration.

Transporter-targeted prodrug modification could be a viable option for improving cellular permeation of SQV. Recently the influx transporter has attracted a lot of attention since it could be used as target ligand for drug delivery. Oligopeptide transporters such as PepT1 and PepT2 expressed in intestinal and renal epithelial cells transport not only small peptides but also peptide-mimetic drugs like lactam antibiotics and antiviral drug.

We hypothesize that, by conjugating of SQV molecule with proper dipeptides such as stereoisomeric valine-valine, prodrugs could be converted to the substrates for influx transport system and undergo facilitated transport to permeate endothelial cells efficiently. In addition, this drug-peptide conjugate will bypass the recognition by membrane efflux pumps and metabolizing enzymes. Following transport across cellular membrane, active parent drug SQV can be regenerated through the cleavage of covalent bond between drug and pro-moieties catalyzed by hydrolytic enzymes, specifically the intracellular cholinesterases, dipeptidases and aminopeptidases.

All amino acids (except for glycine) have a chiral center. Therefore dipeptide prodrugs derived from SQV containing two chiral centers are found to be stereoisomeric. Generally stereoisomers of drug molecules possess differing potencies for pharmacokinetic processes and pharmacological effects. This "stereoselectivity" have been observed in many aspects in pharmaceutical research, such as affinity for certain receptors or enzymes, drug distribution, metabolism, excretion, and toxicity. Therefore, we hypothesize that derivatives of SQV conjugating with different stereoisomeric dipeptide promoieties are featured with varied physicochemical properties, as well as different pharmacokinetic and pharmacological effects. Based on previous results demonstrating that valine-based dipeptide prodrugs exhibited a 4.6-fold enhanced absorption relative to parent drug in rat jejunum, we developed a series of SQV prodrugs conjugated with various stereoisomeric amino acids and dipeptides (*L*-Val-, *D*-Val-, *L*-Val-*L*-Val-, *L*-Val-*D*-Val-, *D*-Val-*L*-Val-, and *D*-Val-*D*-Val-), and the *in vitro/in vivo* evaluations regarding to targeting to peptide transporters, evasion of P-gp- or MRP-

mediated efflux and CYP-mediated biotransformation, and subsequent oral bioavailability are illustrated in this dissertation project.

## Statement of the Problem

Although SQV possesses high anti-HIV potency, its therapeutic efficacy is very limited. One major obstacle is that SQV shows high affinity for ATP dependent efflux pumps like P-glycoprotein (P-gp) and multidrug resistance associated proteins (MRP). Efflux pumps are membrane transporters which bind and translocate molecules against a concentration gradient at the expense of ATP hydrolysis. Drug accumulation in cells is result of dynamic balance between influx, efflux and sequestration. Therefore, both P-gp and MRP play an important role in drug disposition through limiting the absorption and accumulation of xenobiotics and conferring resistance to a diverse range of compounds. Another main obstacle is rapid cytochrome P450 (CYP)-mediated metabolism. CYP is the most abundant drug metabolizing enzyme family and is present predominantly in intestine and liver. A significant amount of CYP3A, one of major subtype of CYP, is expressed in the enterocytes metabolizing xenobiotics including SQV during their transit across intestinal epithelium. In addition, poor solubility (2.47 μg/ml in water) and high plasma protein binding (98% in human) also partly result in poor oral bioavailability of SQV.

In order to reach its efficient inhibitory levels against virus in human, high doses of SQV have to be administered with food and fluid restrictions. However, drug-resistance can be developed due to this high-dose treatment, which also leads to the development of serious long-term metabolic complications, such as atherosclerosis, hyperlipidemia,

lipodystrophy, insulin resistance, and diabetes. Another efficient way to enhance drug exposure is the application of a "boosting agent", typically small dose (50–200 mg) of ritonavir (RTV), to boost therapeutic concentration of the co-administered PI like SQV in PI-based regimens for the treatment of HIV/AIDS. Subtherapeutic RTV appears to potently inhibit both P-gp-mediated efflux and CYP-mediated metabolism, consequently increases the bioavailability and cellular penetration of the "boosted" SQV. However, coadministration of RTV and SQV leads to some side effects like increased serum lipids levels and higher risk of coronary disease and stroke, and long-term inhibition of metabolizing enzymes.

Therefore, new approaches to increase SQV bioavailability are necessary. The primary objective of this dissertation project is to develop a novel drug delivery strategy to circumvent the unfavorable physicochemical and biological barriers of SQV, consequently enhance its intestinal obsorption and oral bioavailability.

## Objective

The objectives of this dissertation are:

1. To synthesize, purify and identify SQV prodrugs, including stereoisomeric amino acid conjugated SQV (*L*-Val, *D*-Val), and stereoisomeric peptide conjugated SQV (*L*-Val-*L*-Val, *L*-Val-*D*-Val, *D*-Val-*L*-Val, and *D*-Val-*D*-Val). Quantitative analytical methods such HPLC and LC-MS/MS will be developed.
2. To conduct *in vitro* uptake and transport studies using P-gp and MRP overexpressiong cell lines to investigate the affinity of synthesized prodrugs for efflux pumps and peptide transporters. Physicochemical and biological properties including aqueous

solubility, chemical/enzymatic stability, cytotoxicity and protein binding will be evaluated.

3. To investigate CYP-mediated metabolism of the synthesized SQV prodrugs in rat liver microsomes, and to compare the kinetics of biotransformation of SQV with its prodrugs. Hydrolysis of dipeptide prodrugs will also be evaluated in rat plasma and intestinal homogenates to predict drug degradation *in vtro*.
4. To study oral bioavailability of SQV and prodrugs following oral administration in Sprague-Dawley rats. Pharmacokinetic parameters such $C_{max}$, AUC, clearance and MRT will be calculated with noncompartmental analysis (NCA) of plasma drug concentration-time profiles.

# CHAPTER 2

# LITERATURE REVIEW

## Overview of HIV Infection

Human immunodeficiency virus (HIV) is a member of the retrovirus family. It gradually infects immune cells such as lymphocytes and monocytes, produces massive numbers of new viral particles, causes the death of the infected cells, and ultimately destroys immune system. People infected with HIV usually develop slowly progressive (10-15 years) but life-threatening diseases such as acquired immunodeficiency syndrome (AIDS). About 33.3 millions of people worldwide have been infected with HIV in 2009, and at least 25 million people have died due to HIV associated diseases (Adamson et al., 2009). In the United States, approximately more than 56,000 people are infected each year, and more than one million people are now living with HIV (Figure 1). Since the epidemic began, 641,976 Americans living with HIV/AIDS have died by the year of 2009 (Hall et al., 2008; Hall HI, 2008).

Three stages of HIV infection have been identified currently. The initial stage (primary infection), that generally occurs within weeks of acquiring virus, is characterized by a flu- or mono-like illness. During this period, large amount of virus are producing in human body. The second stage is chronic asymptomatic infection. HIV reproduces at very low levels but it is still alive during this period. The patients may not have any symptoms for 8 to 10 years. The third stage is symptomatic infection. The human's immune system has been severely damaged by HIV and complications of AIDS have developed. Symptoms in this stage include severe loss of weight, and one or more unusual opportunistic infections or cancers in skin, respiratory system, gastro-intestinal

(GI) system and central/peripheral nervous system. Without treatment, the patients typically can survive about 3 years (Bartlett, 1990; Belman, 2002; O'Brien et al., 2004).

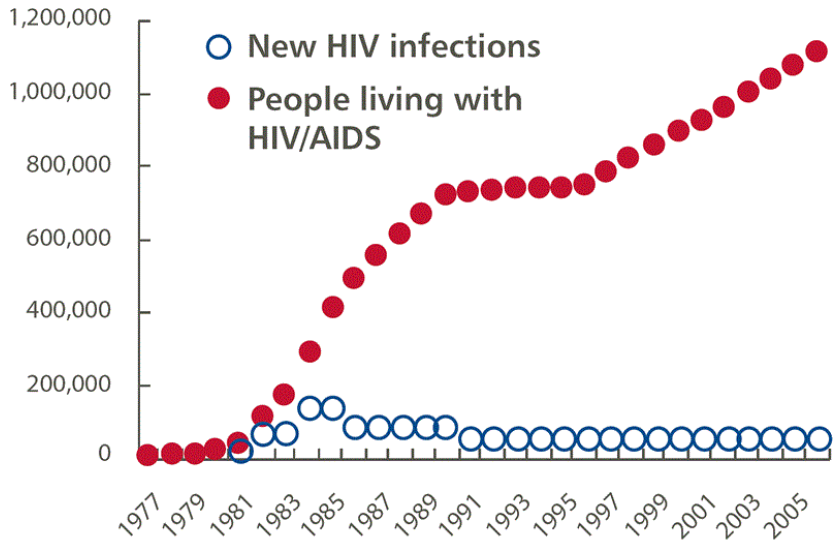


Figure 1. Estimation of population of HIV infections and living with HIV/AIDS in US (1977–2006). Adapted from United States Centers for Disease Control and Prevention website.

## HIV-1 Structure and Replication Cycle

HIV is divided into two strains, HIV type 1 (HIV-1) and HIV type 2 (HIV-2), and both can cause HIV infection in humans. HIV-1 originated from chimpanzees and gorillas living in central Africa, and HIV-2 has been identified as the virus that infect sooty mangabeys (Cercocebus atys) in western coast of Africa (Robertson et al., 1995; Gao et al., 1999). Genetically, HIV-1 and HIV-2 are superficially similar, but HIV-1 is considered to be principle cause of AIDS globally. Structure of HIV-1 shows the characteristics of a typical lentivirus retroviridae (Figure 2). It is a 120-200 nm roughly spherical virion enveloped with 2 single RNA strands. It uses the host cell membrane to

form the viral envelope covered by gp41 and gp120 surface proteins which inserting into the lipid envelope. Inside the envelope, the matrix formed by Gag protein p17 holds a cylindrical core, which not only stores the viral RNA and various proteins, but also contains complementary RNA synthesized by the viral reverse transcriptase (Zhu et al., 2003; Karlsson Hedestam et al., 2008; White et al., 2008).

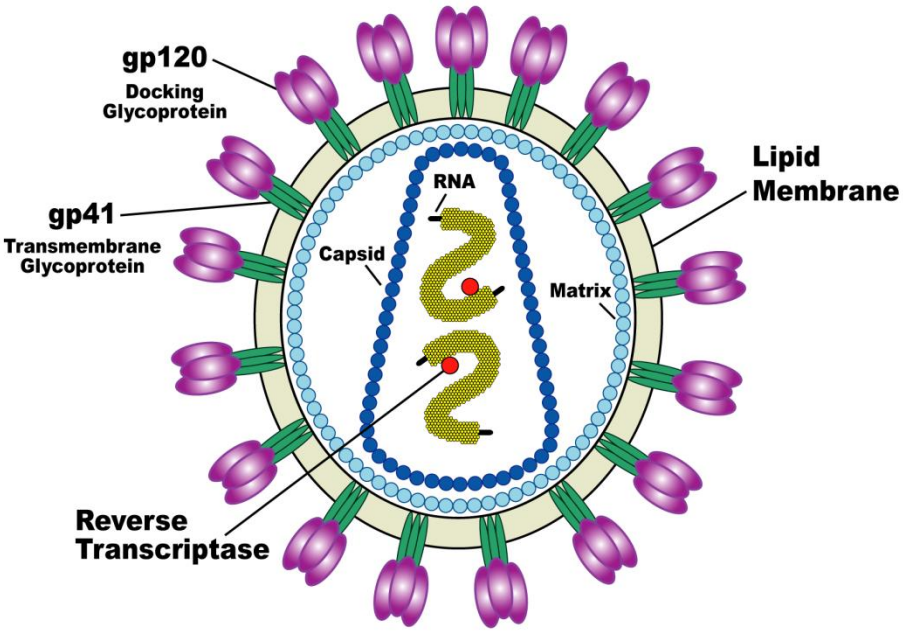


Figure 2. Structure of HIV-1 virion. Adapted from NIAID.

HIV can only replicate inside human cells, therefore HIV life cycle can be divided into 4 steps: entry to the cell, reverse transcription and integration, transcription and translation, and assembly and maturation (Figure 3). First, HIV enters host cell by the binding of glycoproteins (gp120) present on its surface to CD4-receptor on cell membrane which allows the viral envelope to fuse with cell membrane and subsequently

release HIV capsid into the cell (Chan and Kim, 1998; Wyatt and Sodroski, 1998). Once inside the cell, the HIV enzyme reverse transcriptase converts viral single-strand RNA genome into double-strand DNA. Then the DNA is transported to the cell's nucleus where it is integrated into the human DNA by integrase (Zheng et al., 2005). This integrated viral DNA provirus may lie dormant within a cell for a long time in the latent stage of HIV infection. When the cell becomes activated, a certain cellular transcription factors like NF-κB is up-regulated (Hiscott et al., 2001). Then HIV DNA provirus is converted into mRNA and spliced into smaller pieces. These small mRNA pieces are transported from the nucleus into the cytoplasm, where they are translated into the regulatory proteins Tat and Rev (Pollard and Malim, 1998). The final stage of HIV replication cycle is assembly of new HIV virions. Enzyme protease plays a vital role at this stage by cleaving the polyproteins into individual functional HIV proteins. This cleavage step can be inhibited by protease inhibitors (Hallenberger et al., 1992). The newly matured HIV virions are ready to infect another cell and begin the replication process all over again. In this way the virus quickly spreads through the human body.

## Current Treatment for HIV Infection

To date, totally 31 antiretroviral (ARV) drugs belonging to six mechanistic classes have been approved by FDA for the treatment of HIV infection in the United States (Table 1). These medicines have greatly increased patient survival.

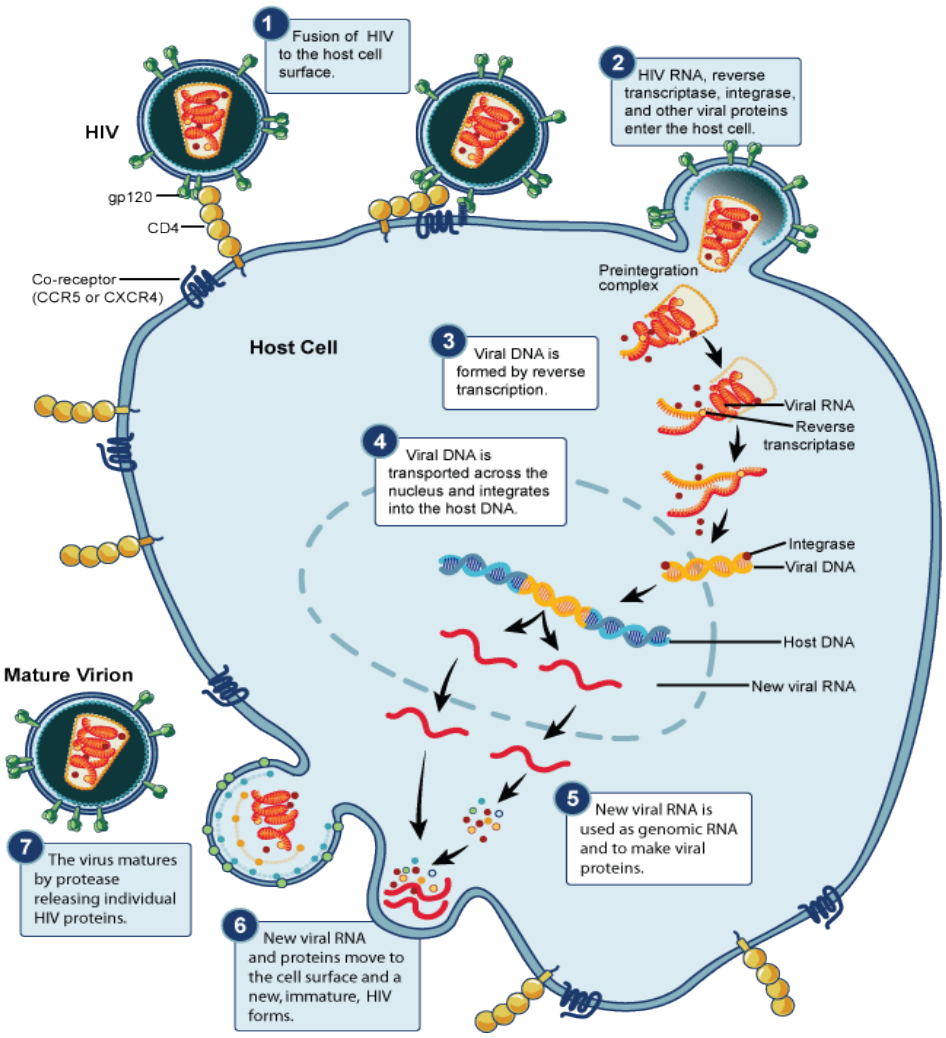


Figure 3. Steps in the HIV Replication Cycle. Adapted from NIAID.

Table 1. Antiretroviral drugs approved by FDA for the treatment of HIV infection by 2012.

| Drug Class | Brand Name | Generic Name |
|---|---|---|
| Non-nucleoside Reverse Transcriptase Inhibitors (NNRTIs) | Viramune | Nevirapine (NVP) |
| | Rescriptor | Delavirdine (DLV) |
| | Sustiva | Efavirenz (EFV) |
| | Intelence | Etravirine (ETV) |
| | Edurant | Rilpivirine (RPV) |
| Nucleoside Reverse Transcriptase Inhibitors (NRTIs) | Retrovir | Zidovudine (ZDV, AZT) |
| | Ziagen | Abacavir (ABC) |
| | Videx<br>Videx EC (enteric-coated) | Didanosine (ddl) |
| | Zerit | Stavudine (d4T) |
| | Epivir | Lamivudine (3TC) |
| | Viread | Tenofovir DF (TDF) |
| | Emtriva | Emtricitabine (FTC) |
| Protease Inhibitors (PIs) | Invirase | Saquinavir (SQV) |
| | Ritonavir | Ritonavir (RTV) |
| | Crixivan | Indinavir (IDV) |
| | Viracept | Nelfinavir (NFV) |
| | Reyataz | Atazanavir (ATV) |
| | Lexiva | Fosamprenavir (FPV) |
| | Aptivus | Tipranavir (TPV) |
| | Prezista | Darunavir (DRV) |
| Fusion Inhibitors | Fuzeon | Enfuvirtide (T-20) |
| CCR5 Antagonists | Selzentry | Maraviroc (MVC) |
| Integrase Inhibitors | Isentress | Raltegravir (RAL) |
| Fixed-Dose Combination (contain two or more anti-HIV medications from one or more drug classes) | Combivir | Lamivudine, Zidovudine |
| | Kaletra | Lopinavir, Ritonavir |
| | Trizivir | Abacavir, Lamivudine, Zidovudine |
| | Epzicom | Abacavir, Lamivudine |
| | Truvada | Emtricitabine, Tenofovir DF |
| | Atripla | Efavirenz, Emtricitabine, Tenofovir DF |
| | Complera | Emtricitabine, Rilpivirine, Tenofovir DF |
| | Stribild | Elvitegravir, Cobicistat, Emtricitabine, Tenofovir DF |

Highly active antiretroviral therapy (HAART), the recommended treatment for HIV infection, involves taking a combination of three or more anti-HIV drugs (a regimen) from at least two different drug classes daily. These treatments prevent HIV from multiplying and thereby suppress viral levels in the body. Multi-drug HAART regimens do not cure the people infected with HIV but help them live longer, healthier lives (Clotet, 2004; Peters and Conway, 2010; Spaulding et al., 2011; Stock, 2011). However, HAART was observed to be associated with some problems, including drug-resistance, side effects of the medication, drug interactions with one another as well as non-HAART drugs, and the high cost of treatment (Belman, 2002; Lambotte et al., 2003; Sunner et al., 2008; Peters and Conway, 2011). The emergence of drug-resistance occurs very rapidly and leads to treatment failure, therefore it must be suppressed. Usually drug-resistance emerges during drug mono-therapy, but it can still be developed even in the face of multi-drug HAART therapy (Richman, 2001; Simon et al., 2006; Temesgen et al., 2006; Chen et al., 2007).

Development of drug-resistance by HIV is similar to the way in which bacteria develop resistance to antibiotics. The virus population in the patient with HIV exists as a diverse but related viral swarm, known as a quasi-species (Thomson et al., 2002). A rapid viral replication combined with the error-prone nature of viral reverse transcriptase leads to the high degree of genetic diversity, which results in nucleotide substitutions, insertions and deletions (Svarovskaia et al., 2003). When the viral population is placed under ARV drugs, these mutant strains of HIV replace wild-type virus due to their selective replication advantage in the face of drug pressure, thereby drug-resistance develop to the medications administered to the patient (Thomson et al., 2002). Generally

ARV drug resistance within drug classes is common. It has been reported that HIV-1, which is resistant to nevirapine (NVP), is very likely to be highly resistant to etravirine (ETV), both belonging to NNRTI agents (van Zyl et al., 2011). Therefore considerations of potential drug-resistance must be incorporated into the design of treatment regimens for HIV infections.

## Saquinavir

HIV protease is an enzyme required to cleave viral *gag* and *gap-pol* polyprotein precursors into individual functional proteins found in infectious virions. Inhibition of HIV protease is considered to be the most important therapeutic approach to date in the treatment of HIV infection since protease inhibitors (PI) prevent the early stage assembly and maturation of infectious virions and effectively block virus replication (Markowitz et al., 1995; 1998; Garcia-Lerma and Heneine, 2001). Therefore discovery of PIs, including saquinavir, lopinavir, ritonavir, nelfinavir and amprenavir, has introduced a new class of first-line drug therapies for mid-stage and advanced-stage HIV-infected patients.

Saquinavir (SQV) is the first PI drug marketed in the United States in 1995 (Figure 4). Hard gelatin capsule formulation of SQV mesylate (Invirase®) and SQV soft gelatin capsule (Fortovase®) discovered by Roche Pharmaceuticals were approved by FDA for the treatment of HIV/AIDS in 1995 and 1997, respectively. Results of *in vitro* studies indicated that SQV is highly active against HIV in human cells, results in the formation of immature, noninfectious virus particles (Kohl et al., 1988; Plosker and Scott, 2003). Clinical trials have shown that 600 mg SQV (mesylate salt) administered orally three times per day is effective in both raising CD4 cell counts and reducing HIV viral load

(Vella, 1995; Noble and Faulds, 1996). Currently Invirase in 200 mg capsules and 500 mg tablets are still widely used in combination with other ARV drugs for the prevention and treatment of HIV infection in adults and children.

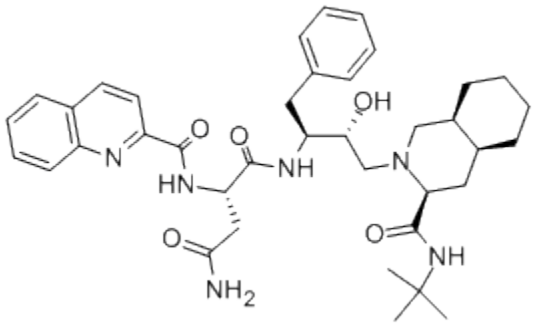


Figure 4. Chemical structure of saquinavir

Although SQV has been reported for its potent activity against HIV, its therapeutic efficacy is limited in clinical application due to its unfavorable properties such as low oral bioavailability, low plasma levels, and poor penetration into central nervous system (CNS) (Kim et al., 1998a; Kim et al., 1998b; Williams and Sinko, 1999). Oral bioavailability of SQV is very limited, only 4% for 600-mg hard gelatin capsules (Invirase) and about 12% for 1200-mg soft gelatin capsules (Fortovase) in healthy adults after single-dose administration (Kaul et al., 1999; Figgitt and Plosker, 2000). In order to increase its efficient inhibitory levels against virus in human cells, high daily doses must be administered, and with food and fluid restrictions. Consequently it contributes to the development of drug-resistance and leads to the appearance of serious long-term metabolic complications, such as atherosclerosis, hyperlipidemia, lipodystrophy, insulin resistance, and diabetes (Gyalrong-Steur et al., 1999; Kaul et al., 1999; Penzak and

Chuck, 2002; McComsey et al., 2003; Duong et al., 2006; Chandra et al., 2009), thereby lowers its clinical outcomes.

Another efficient way to enhance adequate drug exposure is the application of "boosting agent", typically small dose of ritonavir (RTV), to boost therapeutic concentration of the second PI such as SQV in PI-based regimens for the treatment of HIV/AIDS (Llibre, 2009; Holmstock et al., 2012; Tomaru et al., 2013). Since all PIs are substrates of both cytochrome P450 isoenzyme 3A4 (CYP3A4), one of key enzymes associated with drug metabolism, and P-glycoprotein (P-gp), an efflux transporter that can effectively pump drugs out of the gut wall and back into the intestinal lumen (Kaul et al., 1999; Eagling et al., 2002; Plosker and Scott, 2003; Pal et al., 2011). Subtherapeutic RTV (50–200 mg) appears to inhibit potently both of these proteins and, consequently, can increase the bioavailability and cellular penetration of the "boosted" PI as well as reduced doses and less frequent administration, the antiretroviral activity of the second PI is, consequently, enhanced (Rathbun and Rossi, 2002; Gallant, 2004; Youle, 2007; Ananworanich et al., 2008). It has been reported that the area under plasma concentration-time profile curves (AUC) of SQV delivered orally remarkably increased 325-fold by coadministration with 50 mg RTV, from 165.6±128.7 ng ħ/ml to 53850.1±12758.9 ng ħ/ml, in mice. Moreover, oral bioavailability of SQV was observed to be enhanced from 0.0093 to 0.675 under the boosting effect of RTV (Tomaru et al., 2013).

However, SQV concentration in cerebrospinal fluid was not observed to be enhanced to any significant extent in the presence of boosting agent RTV (Gisolf et al., 2000). Hence RTV/SQV cannot inhibit the infection of HIV-1 in brains efficiently. Additionally,

coadministration of low dose of RTV with "boosted" lopinavir and SQV leads to an increase in serum lipids to a more extent in comparison with application of these PI alone (Buss et al., 2001; Arnaiz et al., 2003). These side effects may lead to higher risk for coronary disease and stroke. Other drawbacks to RTV boosting include high cost and the long-term inhibition to metabolic enzymes CYP3A4 (Gallant, 2004).

## Various Factors Contributing to Poor Oral Bioavailability of Saquinavir

Bioavailability (F) of a drug is defined as the fraction of the dose that appears intact in the systemic circulation. Various factors may influence intestinal drug absorption and oral bioavailability after oral administration.

$$F = f_a \cdot (1-E_G) \cdot (1-E_H)$$

where $f_a$ is the fraction of the drug absorbed across intestinal mucosa, $(1-E_G)$ is the fraction that bypasses the degradation in gut wall, and $(1-E_H)$ is the fraction that escapes the metabolism and biliary excretion occurring in liver (Wu et al., 1995).

Absorption of drugs delivered orally is very complicated and influenced by many possibilities. These causative factors include physiological factors (absorption sites, length of absorbing surface, blood circulation at the absorption site, pH in GI tract, gastric emptying rate, permeability of absorbing membrane, transit time in intestinal lumen, active influx and efflux transporters as well as metabolic enzymes in gut lumen), physicochemical properties of drugs (solubility, pKa, chemical stability, and salt forms), and formulation factors (drug particle size and dosage forms, etc.) (Agoram et al., 2001; Lipinski et al., 2001; Pang, 2003; Severijnen et al., 2004; Pang et al., 2007). Diminished access for absorption site due to physical inactivation and chemical degradation in gut

lumen, poor permeability across GI tract mucosa, and fast elimination by first-pass effects occurs in intestine and liver may also contribute to poor oral bioavailability of the delivered therapeutic agents and thereby limit their clinical outcomes.

## Key Physiological Factors Influencing Drug Oral Bioavailability

### Structure of Small Intestine

Small intestine is the major site for drug oral absorption. Its length (around 7 meters for adult human) and wall structure formed by mucosal folds, villi and microvilli provide a large surface area (about 250 square meters) for absorption and digestion. Small intestine is made up of three segments: duodenum, jejunum and ileum. In which duodenum and jejunum, the upper section of small intestine, is the main drug absorption site due to its large surface area, generous blood supply and permeable mucosa (Severijnen et al., 2004). Epithelium of the intestinal mucosa consists of simple columnar epithelium which contains three types of cells with distinct functions: endocrine, exocrine and absorptive cells. Endocrine cells secrete digestive hormone peptides, while exocrine cells (goblet cells) secrete mucus or antimicrobial peptides. Absorptive cells (also called enterocytes), the most abundant epithelial cells, contribute to the translocation of compounds and nutrients across intestinal epithelium (Wu et al., 1995).

Compounds passing from the bulk phase of the intestine to epithelial cell apex encounter two distinct regions, the unstirred water layer (USWL) and the acidic microclimate (Collet et al., 1992; Sanderson, 1999). The USWL, with the thickness of about 530 μm in small intestine, is known to be a significant barrier to the highly lipiphilic molecules which exhibit much greater membrane permeation than hydrophilic

agents, hence absorption is rate-limited by the inability of traversing the USWL for these lipiphilic drugs (Ungell et al., 1998; Pang, 2003). However, hydrophilic or polar molecules are not significantly impeded by the lipid layer. Therefore only drugs possess both hydrophilic and lipiphilic properties can permeate the USWL and cellular membrane well. The mucus coat and outer glycocalyx of the intestinal epithelium are composed of negatively charged carbohydrate side chains, thus it forms an acidic microclimate region on the surface layer of epithelial cells. It has been reported that the pH of microclimate in proximal small intestine is significantly more acidic than in bulk phase (Sanderson, 1999), and a pH-dependent transport process through intestinal epithelial cells can be observed especially for weak electrolytes.

Transporters and Metabolic Enzymes in Intestine

Being a major absorption site for orally administered drugs, expression of various influx and efflux transporters as well as drug metabolizing enzymes in small intestine influences its absorptive function (Pang, 2003; Pang et al., 2007). A variety of influx transport systems, illustrated in Figure 5, facilitate the translocation of amino acids, peptides, hexose, organic anions, organic cations, nucleosides and other nutrients across intestinal epithelium. Among these influx transport systems, peptide transporter 1 (PepT1) has attracted a special attention recently. PepT1 is one of identified members of proton-dependent oligopeptide transporter (POT) family, and shows broad substrate specificity. Generally proteins are digested in GI tract and produce a huge number of short-chain peptides, like di- and tri-peptides, which can be translocated across intestinal epithelium by PepT1 localized on the brush-border membrane (Thamotharan et al., 1997; Terada and

Inui, 2004). It has been reported that, in comparison with *L*-alpha-methyldopa, a 4- to 20-fold increase in intestinal permeabilities was achieved for five dipeptidyl derivatives targeting the peptide transport system (Hu et al., 1989).

In contrast with influx transporters, the role of efflux transporters is to limit influx and facilitate efflux to prevent the intracellular accumulation of their substrates, consequently effectively reduce drug translocation within the enterocyte. Drug exsorption occurs at apical cell membrane of enterocytes at the villous tips via ATP-binding cassette (ABC) efflux transporters including P-glycoprotein (P-gp), multidrug resistance-associated protein 2 (MRP2) and breast cancer resistance protein (BCRP) (Saitoh and Aungst, 1995; Takano et al., 2006; Constantinides and Wasan, 2007). These efflux transporters delimit intestinal absorption of a variety of drugs due to their broad substrate specificity. P-gp recognizes neutral and positively charged hydrophobic compounds, MRP2 effluxes relatively hydrophilic compounds such as glucuronide, glutathione and sulfate conjugates, and BCRP recognizes relatively hydrophilic anticancer compounds. The detailed characteristics of these efflux transporters will be described in the following section.

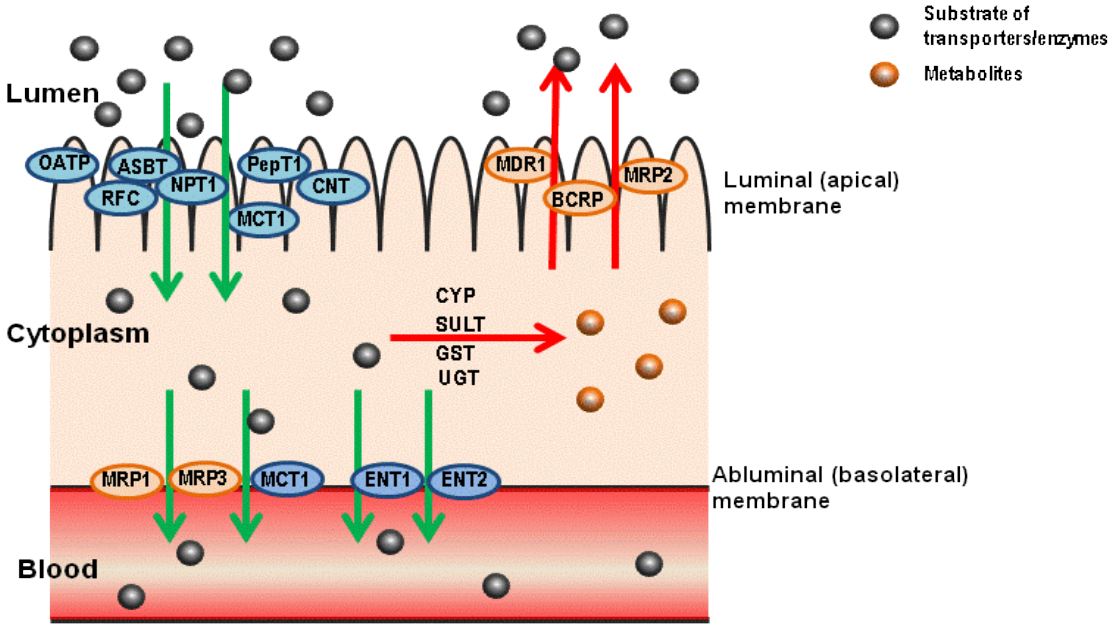


Figure 5. Distribution of metabolic enzymes and transporters present in intestinal epithelial cells.

Influx transporters: PepT1: Oligopeptide transporter 1; ASBT: Apical sodium-dependent bile acid transporter; RFC: Reduced folate transporter; NPT1: Sodium-dependent phosphate cotransporter type 1; CNT: Concentrative nucleoside transporters; MCT1: Monocarboxylic acid transporter 1; OATP: Organic anion transporting polypeptide; ENT1/ENT2: Equilibrative nucleoside transporter 1/2. Efflux transporters: MDR1 (P-gp): Multidrug resistance-associated protein; MRP2: Multidrug resistance-associated protein 2; BCRP: Breast cancer resistance protein. Enzymes: CYP: Cytochrome P450; SULT: Sulfotransferase; UGT: UDP-Glucuronosyltransferase; GST: Glutathione S-transferase.

Intestinal metabolism plays an important role in limiting the systemic uptake of orally ingested therapeutic compounds. Both phase I and phase II enzymes are expressed in intestinal tissue, although at lower levels than those in liver. These enzymes include

cytochromes P450 (CYP) (Watkins et al., 1987; Paine et al., 2006), uridine diphosphate glucuronosyltransferases, sulfotransferases (UGT) (Czernik et al., 2000; Strassburg et al., 2000), sulfotransferase (SULT) (Chen et al., 2003), glutathione S-transferases (GST) (Gibbs et al., 1998), hydrolase (Peters, 1970) and alcohol dehydrogenase (Engeland and Maret, 1993). CYP3A, including CYP3A4, CYP3A5, CYP3A7, and CYP3A43 etc, is considered as the predominant subfamily (about 70-80%) of P450 enzymes in the enterocytes (Peters and Kremers, 1989; Kaminsky and Zhang, 2003; Thelen and Dressman, 2009; Honda et al., 2011). CYP3A content in human intestinal microsomes has been reported to be 30.6 pmol/mg protein in duodenum, 22.6 pmol/mg protein in jejunum, and 16.6 pmol/mg protein in ileum, respectively (Paine et al., 1997). Additionally, the median microsomal CYP3A content in these intestinal sections is observed to be 44%, 32% and 24% of the median hepatic CYP3A content, respectively (Paine et al., 1997). Pharmacokinetic studies of CYP3A4 substrate midazolam after oral administration to healthy human subjects indicate that the intestinal extraction ratio of midazolam ($0.43 \pm 0.24$) is similar to that of liver ($0.44 \pm 0.14$), suggesting that intestinal elimination contributes significantly to the first-pass metabolism of orally delivered CYP3A substrates (Thummel et al., 1996). Apart from CYP3A, only limited types of CYP enzymes are expressed in human small intestine. These enzymes include CYP2C, CYP2J, CYP2D6, CYP1A and CYP4F12, etc (Hashizume et al., 2002; Thelen and Dressman, 2009). Generally, the range of different CYP enzymes expressed in human intestine is markedly less than the range in liver. In comparison with other organs of GI tract, small intestine exhibits higher expression levels of phase II enzymes including GST,

UGT, and SULT. Interaction between xenobiotic compounds and these enzymes facilitates their elimination from the lumen of intestine.

**Unfavorable Properties of Saquinavir**

Although SQV exhibits potent activity against HIV-1, its therapeutic efficacy is limited in clinical application due to some undesirable properties like poor aqueous solubility as well as high affinity for efflux transporters and metabolic enzymes (Kim et al., 1998a; Plosker and Scott, 2003).

Low Solubility:

*In vivo* efficiency of SQV not only depends on its intrinsic anti-HIV activity, but also on its biopharmaceutical availability, i.e. the ability to reach HIV-infected cells after oral administration. Therefore a high concentration in intestinal fluid in GI tract is required to provide sufficient driving force to penetrate the underlying tissue. SQV is a lipophilic (log*P* = 4.2) and weakly basic (p*Ka* ~ 2 and 7) compound with a very poor aqueous solubility (2.47 μg/ml) (Cheng et al., 2007; Buchanan et al., 2008). The mesylate salt of SQV shows an improved but still limited solubility in water (2.22 mg/ml at 25°C). It significantly limits its therapeutic efficacy during its clinical application.

High Affinity for Efflux Pumps:

ATP binding cassette (ABC) efflux pumps, including multidrug resistance proteins – P-glycoprotein (P-gp, MDR1, ABCB1), multidrug resistance-associated protein 2 – MRP2 (ABCC2), and breast cancer resistance protein –BCRP (ABCG2), have been

widely accepted as important defense against exogenous compounds encountered in daily life (Ito et al., 2005). Efflux pumps are responsible for imparting drug resistance by actively effluxing out drug molecules out of cytoplasm, thus protect the cells from endogenous or exogenous toxins. Due to their broad substrate specificity and high expression at apical membranes of epithelial barriers like intestine, blood-brain barrier (BBB), liver and kidney, these efflux proteins regulate the pharmacokinetic and pharmacodynamic processes of numerous therapeutic compounds. Efflux activity of these transporters is the major factor responsible for the poor absorption, low bioavailability, and high metabolism of a variety of PIs, consequently exhibits a dramatic impact on their therapeutic outcomes and clinical application (Kim et al., 1998a; Pal and Mitra, 2006; Thuerauf and Fromm, 2006; Pal et al., 2011).

*P-glycoprotein (P-gp):*

P-gp, a transmembrane glycosylated protein and gene product of MDR1, is one of the major efflux transporters located on the luminal (apical) surface of epithelial and endoethelial cells in a variety of tissues including intestine, liver and blood-brain-barrier. P-gp consists of a duplicated structure (tandem structure) composed of around 1,280 amino acids with a molecular weight of 170 kDa. Each half of the molecule contains a nucleotide-binding domain (NBD) including six highly hydrophobic transmembrane domains (TMDs) followed by a large cytoplasmic domain with an ATP-binding site (Figure 6). The second half of P-gp shows over 65% of amino acid similarity with the first half of the polypeptide (Sharom, 1997; Wacher et al., 1998).

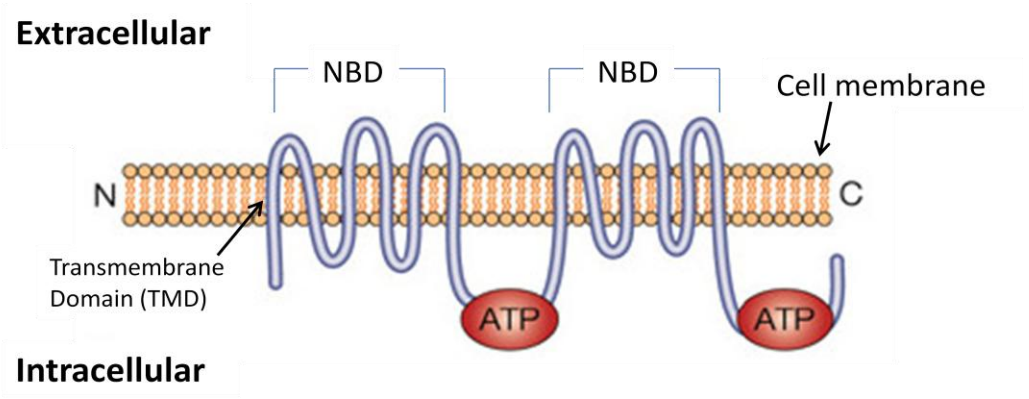


Figure 6. Topological structure of P-glycoprotein

Compounds with large, amphipathic and aromatic structures tend to be interacted with P-gp. This ATP-driven protein binds and translocates these hydrophobic compounds from plasma membrane back into extracellular fluid and thereby restricts their entry into epithelial cells, subsequently diminishes drug efficacy. Previous research on MDR1 knockout mice showed remarkable impact of P-gp on oral bioavailability, disposition and tissue distribution of many drugs (van Asperen et al., 1997; Marchetti et al., 2008). In the case of cytotoxic drugs, this efflux activity leads to the enhanced cell survival. Expression of P-gp in epithelial cells of various organs provides a protective barrier against the entry of xenobiotics and prevents the accumulation of toxic substances.

SQV is demonstrated as a high-affinity substrate for P-gp. In comparison with other major secretary transporters like MRP2 located in rat jejunum, P-gp displays a dominating role on intestinal SQV absorption (Usansky et al., 2008). Transepithelial permeation of SQV across gut wall into systemic circulation is mainly restricted by P-gp, and consequently a larger fraction of SQV is available for pre-systemic biotransformation in GI tract.

*Multidrug resistance-associated protein 2 (MRP2):*

Human ABC sub-family C (ABCC) includes 12 members, in which MRP1-6 efflux proteins are known to be involved in the efflux of many therapeutic agents across lipid cellular membranes (Krishnamachary and Center, 1993; Zaman et al., 1994; Hulot et al., 2005; Letourneau et al., 2005; Gradhand and Kim, 2008; Paumi et al., 2009). MRP1-6 is divided into two sub-categories. MRP1, 2, 3, and 6 belong to the category of MRPs having an extra N-terminal domain and MRP4 and 5 belong to a category without one. MRP2 (190 kDa) is the second member of ABCC efflux pumps cloned from rat and human tissues (Buchler et al., 1996). In comparison to P-gp, MRP2 consists of 1545 amino acids and has an additional amino-proximal membrane-spanning domain represented by an extension of approximately 200 amino acids (Figure 7) (Tusnady et al., 1997; Leslie et al., 2005).

MRP2 is located on the apical membrane of various polarized cells and involved in the secretion of endogenous and xenobiotic substances from cells in the terminal phase of detoxification (Konig et al., 1999). Hence in comparison with other efflux pumps P-gp and BCRP, MRP2 is the optimal transporter to eliminate toxins and carcinogens that conjugated with various GSH, glucuronate, or sulfate from intestinal epithelial cells into the intestinal lumen (Nies and Keppler, 2007).

Results of cytotoxicity and transport studies by Williams *et al* indicated that SQV is transported by both hMRP1 and hMRP2 as well as hP-gp (Williams et al., 2002). Moreover, the rank order of apparent permeabilities of SQV on various MDR-transfected MDCKII cell models is P-gp > MRP2 >> MRP1. Apical expression of efflux pump proteins P-gp and MRP2 on intestine may lead to the poor oral bioavailability of SQV.

Studies on administration of PIs across the blood-cerebrospinal fluid and the BBB also demonstrated that MRP2 as well as P-gp contributes to drug-permeability barriers into and out of the central nervous system (Rao et al., 1999).

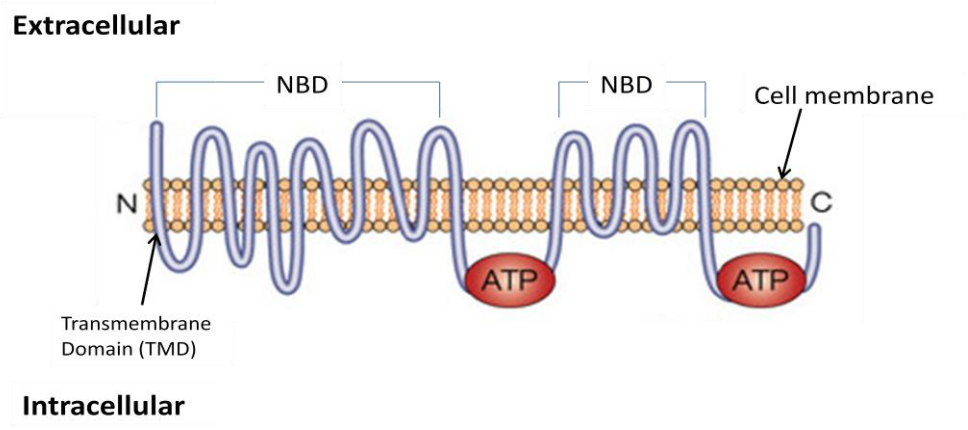


Figure 7. Topological structure of MRP2

*Breast cancer resistance protein (BCRP):*

Unlike P-gp and MRPs, BCRP is a 72 kDa half-transporter and needs to form multimers to be functional (Gradhand and Kim, 2008; Sharom, 2008; Pal et al., 2011). It consists of a single hydrophobic membrane spanning domain predicted to contain 6 TMD helices preceded by a single NBD (Figure 8) (Leslie et al., 2005).

BCRP is highly expressed in the epithelial cells of the intestine, liver bile canaliculi, human placenta syncytiotrophoblast, lobules of the mammary gland and renal tubules, as well as the endothelial cells of capillaries at the BBB and placenta (Doyle et al., 1998; Maliepaard et al., 2001; Cooray et al., 2002). Functions of BCRP include regulation of intestinal absorption, biliary and renal secretion of substrates as well as protection of brain from various xenobiotics and toxins. It influences the disposition of structurally

unrelated compounds, typically both hydrophobic and hydrophilic conjugated with organic anions (particularly the sulfates) (Doyle and Ross, 2003; Mao and Unadkat, 2005), from different therapeutic classes throughout the body due to its broad substrate specificity. The substrates of BCRP include anti-hypertensive, anti-diabetics and chemotherapeutic agents, antibiotics, and numerous diverse drugs like glyburide, nitrofurantoin, dipyridamole, cimetidine and leflunomide (Jani et al., 2009; Beery et al., 2012). The overlap in substrate specificity between BCRP and P-gp increases the barrier function of the efflux transporters (Kodaira et al., 2010). BCRP also shares substrates with MRP2 but with different affinity. Unlike MRP2 that transports most of glutathione, sulfate and glucuronate conjugates, BCRP can efflux out more sulfate than glucuronide conjugates (Mao and Unadkat, 2005; Nies and Keppler, 2007).

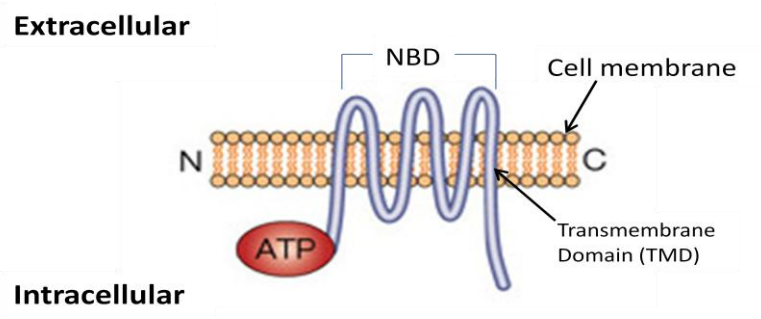


Figure 8. Topological structure of BCRP

Low Resistance to Metabolic Enzymes

As we mentioned above, drug-metabolizing enzymes are highly expressed in both liver and intestine mucosa. Poor pharmacokinetics of orally administered SQV is often attributed to rapid and extensive first-pass metabolism in both small intestine and liver (Fitzsimmons and Collins, 1997). CYP3A has been identified as the predominant

subfamily of hepatic and intestinal CYP enzymes that is responsible for oxidative biotransformation of more than 50% of drugs in humans and rats (Gomez et al., 1995; Backman et al., 1996). SQV is metabolized primarily by CYP3A4 with $K_m$ values of 0.3-0.5 μM to mono- and di- hydroxylated metabolites with negligible antiviral activity (Faesch, 1991; Fitzsimmons and Collins, 1997; Ernest et al., 2005). It inhibits CYP3A4-dependent biotransformation of terfenadine to its inactive metabolites with a $K_i$ of 0.7 μM in human small-intestinal microsomes, suggesting that SQV can be metabolized by human intestinal CYP3A4 (Fitzsimmons and Collins, 1997). Another isoform CYP3A5 also contributes metabolism of SQV in humans. After oral administration of single-dose SQV soft gel capsules (1200 mg) to healthy volunteers, median value of $AUC_{0-24h}$ for SQV has been reported to be 34% lower in the individuals with functional CYP3A5 alleles than that among those without functional alleles (Josephson et al., 2007). SQV also shows moderate affinity to CYP2C9 and CYP2D6. It inhibited CYP2C9 activities in human liver microsomes with an $IC_{50}$ of 53.9 ± 9.9 μM (Eagling et al., 1997). While the results of inhibitory studies of desipramine hydroxylation, an index reaction used to assess human CYP2D6 activity, indicate that SQV can competitively inhibit this metabolizing enzyme ($K_i$ =24.0 ± 1.5 μM) (von Moltke et al., 1998).

High Plasma Protein Binding

Drug in plasma is in a state of equilibrium between unbound drug and protein bound drug. The ratio of unbound to bound drug is generally determined by drug and protein concentrations and binding constants. Therefore protein binding in plasma is one of the most important characteristics for the evaluation of drug disposition in human bodies,

because only the free drug fraction is useful in establishing the actual concentration to elicit its pharmacological action and achieve the maximum therapeutic effects. HIV PIs exhibit moderate to high affinity to plasma proteins, especially to α1-acid glycoprotein (AAG), an acute phase plasma α-globulin glycoprotein (Acosta et al., 2000). SQV is highly bound to plasma proteins, and shows more than 98% plasma protein bound in humans (Flexner, 1998). It suggests that only 2% of total amount of SQV in plasma is free and able to show the potent antiretroviral effects *in vivo*. Moreover, protein binding in plasma must be taken into consideration when using *in vitro* data to estimate the *in vivo* pharmacokinetic or pharmacodynamic parameters like $IC_{90}$. The *in vivo* $IC_{90}$ of SQV would be 50 times higher than that observed *in vitro* (determined in the absence of any plasma proteins) due to its 98% protein bound.

Targeted Prodrug Modification – Way to Improve Saquinavir Oral Bioavailability

Optimizing the oral administration of drugs with narrow therapeutic index is critically important, especially for chronically ill patients requiring long-term treatment. SQV is one of such agents. We have discussed that SQV exhibits high affinity for both CYP enzymes and efflux transport pumps, as well as poor solubility and high plasma protein binding. Absorption, distribution, and disposition of SQV in human body are significantly influenced by the combined effects of these unfavorable factors.

In order to overcome these physicochemical and biological barriers, various strategies have been employed to enhance SQV absorption in intestine and brain. Nano-sized formulations like nanoparticles (Shah and Amiji, 2006; Kuo and Yu, 2011), nanoemulsions (Vyas et al., 2008) and nanosuspensions (Dodiya et al., 2011) constitute

one of such strategies. Even through these nanoparticulated carriers exhibit some enhancement in SQV oral absorption or BBB penetration, the poor stability and short circulating life span within the body dramatically limit the application of these formulations. Other strategies to increase oral bioavailability of SQV include co-administration of absorption enhancers like DeltaG, the biologically active fragment of Zonula occludens toxin (Zot) (Salama et al., 2005). It reversibly opens the tight junctions present in small intestine and enhances SQV oral absorption in rats. However, cellular toxicities have, for the most part, limited their use.

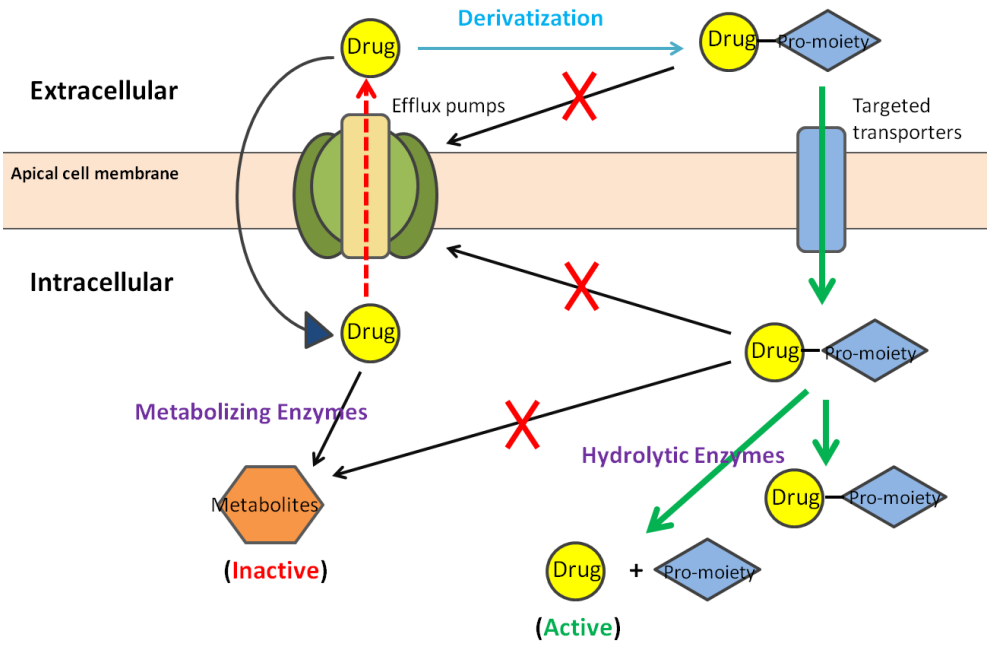


Figure 9. Transporter-targeted prodrug strategy

Transporter-targeted prodrug strategy, prodrugs targeting towards transporters expressed on epithelial cell membranes, seems to provide a good resolution to improve

oral bioavailability of SQV (Figure 9). Various nutrient transporters and receptors are present on the membrane surface of epithelial cells. The drug conjugating with a specific pro-moiety which is a substrate for these membrane transporters/receptors can be recognized and facilitated across epithelial cell membrane, subsequently these derivatives may permeate the intracellular environment and reach the systemic circulation. Moreover, modification of drug molecular structure may evade the recognition by efflux pumps or metabolizing enzymes. In addition, solubility of drug molecules may also be enhanced due to the conjugation of polar pro-moiety to drug. After translocation across cellular epithelial membrane, the pro-moiety of intact compounds can be cleaved by hydrolytic enzymes present in systemic circulation or targeting sites to release the active drug. Therefore absorption of poorly permeating therapeutic agents can be enhanced by targeted prodrug modifications.

**Peptide Transport System**

Small intestine has been considered as the major site for nutrients uptake into the body. Generally the proteins are hydrolyzed into di- or tri- peptides (80%) and free amino acids (20%) by proteases located in the gut lumen, and then transported into enterocytes under the facilitation of certain transporters expressed on the apical membrane of intestinal epithelial cells (Adibi and Mercer, 1973). Proton-coupled oligopeptide transporter (POT) is one of such influx transport systems. POT transporters are integral plasma membrane proteins. They are driven by inwardly-directed proton concentration gradient and negative membrane potential across the biological membrane. Wide spectrum of di- and tri-peptides as well as a number of peptidomimetics can be

recognized and transported across epithelial membrane by POTs. Up to date, four members of POT family, peptide transporter 1 (PepT1, SLC15A1), peptide transporter 2 (PepT2, SLC15A2), peptide/histidine transporter 1 (PHT1, SLCA4) and peptide/histidine transporter 2 (PHT2, SLCA3), have been identified in mammals. PepT1 and PepT2 have attracted more attention due to their high expression in various epithelia, broad substrate specificity, as well as high affinity and transporter capacity (Rubio-Aliaga and Daniel, 2008).

PepT1, first isolated and cloned from rabbit intestine (Fei et al., 1994), is a low-affinity ($K_m$ > 0.5 mM) and high-capacity transporter with the molecular mass predicted to be about 75 KDa (Saito et al., 1995; Brandsch et al., 2008). It is highly expressed in the apical membrane of epithelial cells of intestine, kidney, pancreas, extrahepatic bile duct and liver (Knutter et al., 2002; Daniel and Kottra, 2004; Biegel et al., 2006; Brandsch et al., 2008). PepT1 has been considered to be the primary influx transporter that attributes to intestinal absorption of most small peptides and peptidomimetic compounds with different conformation, size, polarity and charges. PepT2, a high-affinity ($K_m$ < 0.1 mM) and low-capacity nutrient transporter (Luckner and Brandsch, 2005), is the next identified peptide transporter isolated from human kidney in 1995 (Liu et al., 1995). PepT2 (~107 KDa) is expressed in a variety of tissues including kidney, lung, brain, mammary gland and testis (Boll et al., 1996; Lu and Klaassen, 2006; Brandsch et al., 2008). The general function of PepT2 is to remove small peptides from extracellular fluids. Typically PepT2 located in kidney reabsorbs amino acids in peptide-bound form from glomerular filtrate to avoid the loss of amino acid nitrogen from urine.

Both PepT1 and PepT2 exhibit wide substrate specificity. Besides di- and tri-peptides, numerous peptidomimetics including β-lactam antibiotics, angiotensin-converting-enzyme (ACE) inhibitors, renin inhibitors, thrombin inhibitors, anticancer drugs like bestatin, and antiviral prodrugs like valacyclovir can be delivered by the facilitation of peptide transporters (Yang et al., 1999). Therapeutic efficacy of these drugs after oral administration is determined not only by their efficient intestinal absorption, but also by their half lives in systemic circulation. Intestinal PepT1 acts as vehicle for their effective oral absorption, and rental PepT2 reabsorbs these compounds to maintain their half lives in body. Therefore peptide transport system plays an important role in drug absorption, distribution and disposition. It is believed to be an ideal targeting transporter for prodrug design to achieve improved systemic bioavailability and optimized pharmacokinetic profiles.

**Peptide Prodrug Modification**

Recently peptide prodrug modification has been considered as a promising strategy to improve the therapeutic outcomes of drugs with poor bioavailability, such as SQV. Peptide prodrugs are designed by conjugating parent drug to small peptides like di- or tri-peptides. The newly formed "peptidomimetic prodrug" may be easily recognized as substrates by peptide transporters, which present on both apical and basolateral membranes of intestinal epithelial cells, and ferried across the epithelium into the systemic circulation (Figure 10) (Irie et al., 2004; Pieri et al., 2010). Structural modification may further reduce the interaction of the parent drug with efflux transporters and metabolizing enzymes. Therefore enhanced permeation could be achieved by the

cumulative effects of reducing secretion and increasing absorption. Moreover, physicochemical properties such as water solubility may be also improved based on the amino acid chosen for derivatizing the drug. It is reported that valine ester prodrugs of acyclovir and ganciclovir showed an increased solubility (Yang et al., 2001). Extensive research has been performed towards prodrug design by targeting peptide transporter to increase the bioavailability of various therapeutic reagents. *In vitro* permeability studies on *L*-valyl, *L*-leucyl, and *L*-phenylalanyl ester conjugates of SQV and indinavir demonstrated an increased translocation across Caco-2 cell monolayers (Rouquayrol et al., 2002). Valine-valine and glycine-valine prodrugs derived from SQV have also exhibited 4.6- and 1.8- fold enhanced absorption relative to parent drug in rat jejunum, respectively (Zappella et al., 2003).

After evasion these most dominating barriers which may lead to poor oral bioavailability, the hydrolysis of intact peptide prodrugs would be catalyzed by a large variety of hydrolases *i.e.* esterases and peptidases, then amino acid prodrugs and free parent drugs would be regenerated and further translocated into biological fluids or target tissues by amino acid transporters (Figure 10).

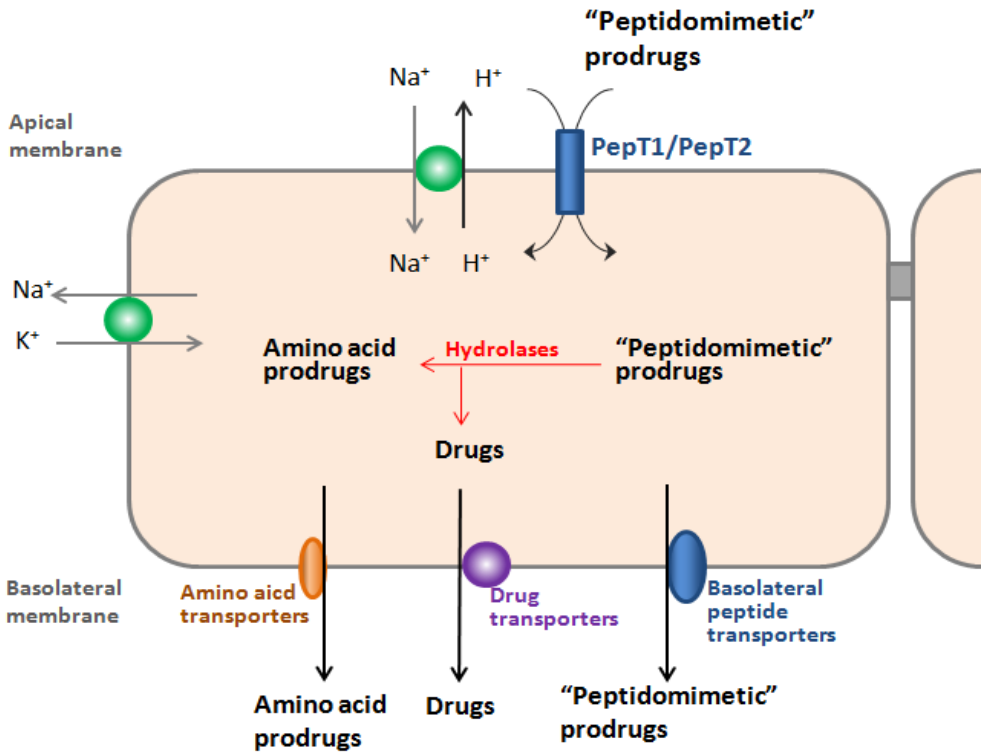


Figure 10. Cellular processes of peptide prodrug transport across intestinal epithelial cells

**Stereoselectivity**

Chiral technology was discovered in 1848, with the identification of two isomers of sodium ammonium tartrate by the mold *Penicillium glaucum*. However, the phenomenon of chirality was widely believed to play a major role in pharmaceutical industries until the 1950's (Nguyen et al., 2006). Currently chiral drugs have become a majority of newly introduced products in global market and is expected to reach 95% by 2020 (Nguyen et al., 2006). For many years, the racemic mixture drug products were justified by their lower production costs and lack of availability of chirally specific drug synthesis techniques. But recently single enantiomer drugs are showing a continuous growth worldwide and many of the top-selling drugs are marketed as single enantiomers.

The living body is a highly chiral environment because all proteins, enzymes, amino acids, carbohydrates, nucleosides as well as a number of alkaloids and hormones are chiral compounds. Although they have the same chemical structure, stereoisomeric drugs always exhibit different biological activities due to their differential 3-point fit at the target sites like transporters, receptors and enzymes (Lees et al., 2012). Therefore stereoisomers of drug molecules containing one or more chiral centers exhibit differing potencies for pharmacokinetic processes and pharmacological effects, also called "stereoselectivity", with respect to affinity for certain subtypes of receptor or enzymes, distribution, metabolism and excretion, as well as in antagonistic actions and their toxicological properties (Siccardi et al., 2003; Wang et al., 2010). Thalidomide is an anti-nausea and sedative drug that was believed to be safe and effective in the 1960's. However, many newborns suffered from severe birth defects were reported to be born to the women who had taken thalidomide during pregnancy. The later research found that one enantiomer of thalidomide, (R)-, was therapeutically effective whereas another isomer (S)- showed severe adverse effects (Eriksson et al., 2001; Smith, 2009).

Derivatives of a compound conjugating with different stereoisomeric pro-moieties may be also featured with various physicochemical and biological properties. Most amino acids currently applied in prodrug strategy are *L*-isomers (levorotatory). Major advantages to *L*-configurations include their natural occurrence in the body, and their optimal three-dimensional spatial arrangement of atoms which exhibit high affinity to transporters or receptors (Hutt and O'Grady, 1996; Sawada et al., 1999). However, most *L*-isomeric derivatives have limited chemical or enzymatic stability, while *D*-amino acid (dextrorotatory) conjugated prodrugs exhibit much better resistance to enzymatic

hydrolysis (Pochopin et al., 1994; Tamura et al., 1996b; Song et al., 2002). *L*-valine-*L*-valine has been reported to be degraded completely in 15 min in Caco-2 cell homogenate (1 mg/ml) at 37°C which is much faster than the other diastereomers (Tamura et al., 1996a). In contrast, *D*-amino acid prodrugs of dapsone exhibited much better resistance to enzymatic hydrolysis and showed a longer residence time *in vivo* (Pochopin et al., 1994). Half life of *L*-valine-*L*-valine-acyclovir in rat intestinal homogenates has been reported to be less than 0.08 h, whereas *L*-*D*- and *D*-*L*- conjugates showed much higher stability with the $t_{1/2}$ values of 0.49 h and 2.82 h, respectively (Talluri et al., 2008). Therefore, prodrug modification with different stereoisomeric amino acid or small peptide pro-moieties may serve as a promising strategy to provide an optimal medicinal treatment and a right therapeutic control for the patient.

# CHAPTER 3

# INFLUENCE OF EFFLUX PUMPS ON FUNCTIONAL ACTIVITIES OF PEPTIDE TRANSPORTERS IN MDR-TRANSFECTED MDCK CELL LINES

## Rationale

Madin-Darby canine kidney (MDCK) cell line has been widely employed for cell-based permeability screening model. There are two strains of MDCK cells, both of which are derived from the distal tubule or collecting duct of the nephron (Ojakian and Herzlinger, 1984). In comparison with MDCK strain I cells which are non-ciliated, the strain II cells are ciliated, columnar in shape, and have microvilli on their apical surface when grown on permeable supports (von Bonsdorff et al., 1985). MDCK cells express various endogenous influx transporters, including amino acid transporters (Boerner et al., 1986), organic cation transporters (Hantz et al., 2001) and peptide transporters (Putnam et al., 2002; Landowski et al., 2005) and efflux transporters like P-gp (Horio et al., 1989) and the multidrug resistance protein (MRP, *ABCC*) family (Flanagan et al., 2002). At present, wild-type MDCK strain II cells transfected with the human *MDR1*, *MRP2*, or *BCRP* genes are employed as quick assessment models to estimate *in vivo* permeability of new drug candidates, which are substrates, inducers, or inhibitors of these efflux pumps, across intestinal mucosa (Tang et al., 2002b; Tang et al., 2002a; Xiao et al., 2006; Agarwal et al., 2007a) or the blood-brain barriers (Gumbleton and Audus, 2001; Wang et al., 2005). However, a large number of these drug candidates are also substrates for influx transporters, and prodrug modification with peptide is a common practice to circumvent efflux. The assumption for drug screening using transfected cell models is that the function and expression of endogenous transporters in transfected cells are comparable

with parental cells. Accordingly a proper prediction for the *in vivo* drug absorption can be obtained from results of permeability assay conducted across these transfected cell models. But recently, gene expression of endogenous canine P-gp in MDCK cells has been reported to be significantly down-regulated after transfection with human *MDR1*. Transepithelial transport of vinblastine, a substrate for P-gp, was consequently underestimated when comparing the result obtained across human *MDR1*- transfected versus wild-type MDCK cells (Kuteykin-Teplyakov et al., 2010). Therefore we asked question, does transfection of efflux transporters affect the function of endogenous influx transporters too? If so, it might lead to significant bias in screening dual substrates for influx/efflux transporters, like "peptidomimetics" using these transfected cell lines.

In recent years, considerable research in targeted drug delivery indicate that peptide transporters are attractive targets for new drug discovery because they have broad substrate specificity and high capacity, especially for smaller peptides *i.e.* di and tripeptides (Ganapathy and Leibach, 1996; Steffansen et al., 2004). Also "peptidomimic" drugs can be recognized as substrates by the peptide transporter-mediated influx system and ferried across epithelial membrane into systemic circulation (Ganapathy et al., 1995; Wang et al., 2012). Apical peptide transporters in MDCK cells are $H^+$/peptide co-transporters, mainly peptide transporter-2 (PepT2, SLC15A2) (Sawada et al., 2001; Balimane et al., 2007), whereas basolateral peptide transporters are still unknown (Terada et al., 2000). PepT2, a high-affinity and low-capacity nutrient transporter, is expressed in a variety of tissues including kidney, lung, brain, mammary gland, and testis (Lu and Klaassen, 2006). The driving force for PepT2-mediated peptide transport is provided by an inwardly directed $H^+$ gradient and an inside-negative membrane potential. It plays a

key role in the uptake and transport of mammalian protein nutrients across biological membranes as well as another important $H^+$/peptide cotransporter PepT1 (SLC15A1). Thus several publications have demonstrated the application of intact or transfected MDCK cell models to characterize permeability and absorption of substrates for peptide transporters (Agarwal et al., 2007b; Jain et al., 2008; Ouyang et al., 2009). However, no previous work has been reported about the alteration of endogenous peptide transporter system expressed in the MDCK cells, especially on apical membrane, after transfection with different human efflux protein genes.

Functional characterization of peptide transporters was evaluated in various MDCKII cell lines in this chapter. Uptake and transport of [$^3$H]Gly-Sar were conducted on MDCKII-MDR1, MDCKII-MRP2, and MDCKII-BCRP cells as well as MDCKII wild-type cells. Real-time PCR and Western blot analyses were also performed to investigate mRNA and protein levels of both exogenous efflux pumps and endogenous peptide transporters respectively. The aim of this work is to determine whether the function of peptide transporters is compromised by the overexpressed efflux transporter in transfected MDCKII cell lines or not. This study may provide a more accurate assessment for these *in vitro* models to screen the compounds mediated by peptide transporter/efflux pumps in drug discovery.

## Materials and Methods

### Materials

Transfected MDCKII cells overexpressing human MDR1 (MDCKII-MDR1, passage 3-30), human MRP2 (MDCKII-MRP2, passage 3-30), human BCRP (MDCKII-BCRP,

passage 3-30), and wild-type MDCK cells (MDCKII-wt) were generously provided by Dr. P. Borst and Dr. A. Schinkel (The Netherlands Cancer Institute, Amsterdam, Netherland), respectively. [$^{3}$H]Glycylsarcosine ([$^{3}$H]Gly-Sar, 4 Ci/mmol), and [$^{14}$C]Mannitol (58.8 Ci/mmol) were purchased from Moravek Biochemicals (Brea, CA). Dulbecco's modified Eagle's Medium (DMEM), TrypLE™ Express Stable Trypsin Replacement, and Trizol-LS® reagent were obtained from Invitrogen (Carlsbad, CA). Fetal bovine serum (FBS) was purchased from Atlanta Biologicals (Lawenceville, GA). M-MLV Reverse Transcriptase, Random Hexamers, and M-MLV RT 5× Reaction Buffer were purchased from Promega (Madison, WI). Light Cycler® 480 SYBR Green 1 master kit was obtained from Roche Applied Science (Foster City, CA). ). NuPAGE® Novex 4-12% Bis-Tris Gels and MagicMark™ XP Western Protein Standard (20-220 kDa) were obtained from Invitrogen (Carlsband, CA). Polyclonal canine PepT1 and canine PepT2 primary antibodies were purchased from Biorbyt Ltd. (Cambridge, Cambridgeshire, UK). BioRad protein estimation kit was purchased from BioRad (Hercules, CA). BCA protein assay kit was obtained from Thermo Scientific (Rockford, IL). Fosinopril and scintillation cocktail reagent was obtained from Fisher Scientific Inc (Fair Lawn, NJ). Glycyl-*L*-proline (Gly-Pro) was purchased from TCI America (Portland, OR). Glycylsarcosine (Gly-Sar), cefadroxil, Triton X-100, hydroxyl ethyl piperazine ethane sulfonic acid (HEPES), d-glucose and all other chemicals were obtained from Sigma Chemical Co (St. Louis, MO). All chemicals were products of special reagent grade and used as such. Transwell® inserts and 12-well tissue culture plates were purchased from Corning Costar Corp (Cambridge, MA).

**Cell Culture**

Wild-type and transfected MDCKII cells were seeded at a density of 40,000 cells/$cm^2$ in 75 $cm^2$ cell culture flasks and maintained in DMEM containing 10% heat-inactivated FBS, 20 mM HEPES, 29 mM sodium bicarbonate, 100 units/ml penicillin, and 100 μg/ml streptomycin. Medium was replaced every other day. Cells were harvested and passaged at 70% – 80% confluency using TrypLE™ Express Stable Trypsin Replacement at 5-7 days postseeding, and plated at $7 \times 10^4$ cells /$cm^2$ on 12-well tissue culture plates for apical uptake studies, and $2 \times 10^5$ cells /$cm^2$ on 12-well Transwell® inserts (diameter 12 mm, pore size 0.4 μm) for basolateral uptake and transport studies. Medium was changed every alternate day.

**Uptake Studies**

Cells were washed twice with 2 ml Dulbecco's phosphate-buffered saline (DPBS, pH 7.4) before the experiments. Uptake was initiated by adding 1 ml DPBS with 0.5 μCi/ml of [$^3$H]Gly-Sar into the wells. Incubation was conducted at 37 °C or 4 °C for 15 min. The tracer solution was aspirated and cells were rinsed three times with ice-cold stop solution (200 mM KCl and 2 mM HEPES) to determine drug uptake. Then the cells were lysed by adding 1 ml of 0.3 N NaOH containing 0.1% Triton-X 100 solution to each well and left overnight at room temperature. Aliquots from each well were transferred to scintillation vials containing 3 ml of scintillation cocktail. Cellular radioactivity was quantified using a scintillation counter (Model LS-6500; Beckman Counter, Fullerton, CA) and then was normalized by amount of protein measured using BioRad protein estimation kit in each well.

**Growth, Temperature and pH Dependent Uptake**

Uptake of [$^3$H]Gly-Sar (0.5 μCi/ml) was conducted at 37 °C for different time in culture (3 to 8 days) to determine the optimum culture period for uptake studies. Temperature and pH dependent uptake of [$^3$H]Gly-Sar in various MDCK cell lines at low cell-passage was evaluated at 4 ℃ and 37 ℃, respectively. During final calculation of [$^3$H]Gly-Sar uptake at 37°C, the passive diffusion component (i.e. at 4°C) was subtracted. To study pH dependency of Gly-Sar uptake, incubation media DPBS with different pHs from 4.0 to 7.4 were prepared, and permeant solutions (0.5 μCi/ml [$^3$H]Gly-Sar) were made accordingly. Cells were pre-incubated with DPBS (pH7.4) for 20 min before adding permeant solutions with various pHs.

**Concentration Dependent Uptake**

[$^3$H]Gly-Sar solutions with various concentrations (5-250 μM) of unlabeled Gly-Sar were used in this study to determine concentration dependent Gly-Sar cellular accumulation in both wild-type and transfected MDCK cell lines. Uptake was carried out at 4 ℃ and 37 ℃, respectively. Then the data was fitted to a Michaelis-Menten equation as shown in "Data Analysis" section to determine the kinetic parameters of peptide transporter-mediated specific Gly-Sar uptake.

**Passage Dependent Uptake**

In order to illustrate whether various transfected MDCK cell lines exhibit passage dependency for Gly-Sar uptake, concentration dependent studies at both 4 ℃ and 37 ℃ were conducted on MDCKII-MDR1, MDCKII-MRP2, and MDCKII-BCRP cells with

different passage number (3-25). Then the uptake kinetic parameter *transport efficiency* for peptide transporters-mediated Gly-Sar uptake was estimated using Michaelis-Menten equation.

**Inhibitory Gly-Sar Uptake**

To determine the substrate specificity, apical [$^{3}$H]Gly-Sar (0.5 µCi/ml) in the absence or presence of peptide transporter inhibitors, fosinopril (100 µM), cefadroxil (20 mM) and Gly-Pro (20 mM), was evaluated in various MDCKII cell lines with low (<6) or high (>25) cell-passages.

**Transport Studies**

Transepithelial transport of Gly-Sar was evaluated across MDCKII cell monolayers (cell-passage number < 6) grown on Transwell® inserts. Medium was aspirated before experiments and cell monolayers were washed twice with DPBS (pH 7.4).Working volumes of the apical (AP) and basolateral (BL) compartments were 0.5 and 1.5 ml, respectively. The monolayer integrity was evaluated by measuring transepithelial electrical resistance (TEER) values using volt–ohm meter (EVOM-G, World Precision Instruments, Sarasota, FL). Only the monolayers with TEER values of about 600 ±60 ohm cm$^{2}$ was used in this study. Transport was initiated when 0.5 µCi/ml [$^{3}$H]Gly-Sar or 0.25 µCi/ml of [$^{14}$C]Mannitol in DPBS was added in donor chambers and only fresh DPBS in receiving chambers. The pH of incubation media varied from 4.0 to 7.4 in AP chambers only, but remained consistent in BL chambers to pH 7.4. Aliquots (200 µl) were withdrawn from receiving chambers at predetermined time intervals over a period

of 60 min and replaced with same volume of fresh DPBS to maintain sink conditions. Samples were analyzed using a liquid scintillation counter described in uptake studies. At the end of experiments, the integrity of monolayers was checked by measuring TEER values. Cell monolayers with less than 10% of initial TEER values dropped was considered as integrity unchanged. Specific Gly-Sar transport across both parental and transfected MDCKII cell lines was calculated by subtracting nonspecific transport (passive diffusion) estimated from [$^{14}$C]Mannitol from [$^{3}$H]Gly-Sar transport.

**Tight Junction Determination**

To evaluate the intercellular tight junctions of different MDCKII cell lines, transport of [$^{14}$C]Mannitol (0.125 μCi/ml) in DPBS (pH 7.4) was performed across MDCK cell monolayers for up to 60 min, as outlined above.

**Real-time PCR Assay**

Total RNA from different MDCK cells was isolated using Trizol reagent according to the manufacturer's protocol. Concentration and purity of RNA were estimated using spectrophotometer at 260 and 280 nm. Total RNA (1.5 μg) was reverse transcribed to cDNA using random hexamers and M-MLV Reverse Transcriptase Reagent. After the first strand cDNA synthesis, 100 ng of cDNA was amplified by real-time PCR using LightCycler® 480 SYBR Green-1 Master mix on an ABI Prism 5700 Sequence Detection System (PE Applied Biosystems, Foster City, CA) to evaluate the gene expression of h*MDR1* (human), h*MRP2* (human), h*BCRP* (human), c*PepT1* (canine), and c*PepT2* (canine). Sequences of primers used in this study are summarized in Table 2.

GAPDH gene was used as endogenous reference to normalize target gene mRNAs in samples. Comparative threshold method was used to calculate the relative amount of mRNA in comparison with control (cells with lowest passage number).

Table 2. PCR primers used in real-time RT-PCR assay of transporter expression.

| General names | Species | Primer directions | Primer sequences |
|---|---|---|---|
| PepT1 | Canine | Forward | 5'-GCTTGTTACCCACTGGCATT-3' |
| | | Reverse | 5'-GCAAAACCAATGCACTTGAC-3' |
| PepT2 | Human & canine | Forward | 5'-CAGCTTTTGGTGGAGACCAG-3' |
| | | Reverse | 5'-AAATCAAGCTCCCTGCATTG-3' |
| MDR1 | Human | Forward | 5'-GAAGCCAGAACATTCCTCCTGGAA-3' |
| | | Reverse | 5'-AGCCGCTACTCGAATGAGCTC-3' |
| MRP2 | Human | Forward | 5'-GGTCATCCTTTACGGAGAACATCA-3' |
| | | Reverse | 5'-GGACTGCGTCTGGAACGAAG-3' |
| BCRP | Human | Forward | 5'-CCGCCACTCCCACTGAGATT-3' |
| | | Reverse | 5'-CTCGGAGGCAGCGCTTTAAC-3' |

**Western Blot Assay**

Confluent cells grown on 75 $cm^2$ cell culture flask were washed twice with ice-cold PBS and lysed on ice in RIPA buffer containing freshly added protease inhibitor cocktail. Protein lysate was collected by centrifugation at 15,000 ×g, 4°C for 10 minutes and the total protein content was determined using BCA protein assay kit. Subsequently an equal amount of total protein (20 μg) was loaded and separated on ready-made Novex 4-12% Bis-Tris Gels. Proteins then were transferred to a polyvinylidene fluoride (PVDF) membrane, blocked with 5% non-fat dry milk and 1% BSA for non-specific binding and probed with primary antibodies specific to canine PepT1 and PepT2, respectively. Following three 5-minute washes in TBST (Tris buffered saline + 0.1% Tween 20), blots

were probed with secondary antibody in TBST (1:20,000 anti-rabbit IgG-HRP) and visualized by Fujifilm LAS 4000 imaging system (FUJIFILM Medical Systems USA, Inc. Stamford, CT). The images of immunoreactive staining were measured and analyzed by ImageJ 1.46r software.

**Data and Statistical Analysis**

Affinity and capacity of Gly-Sar to peptide transporters were fit to Michaelis-Menten equation by nonlinear regression to determine the kinetic parameters $K_m$ and $V_{max}$. Data modeling was performed using KaleidaGraph (Synergy Software). *Transport efficiency* of peptide transporters was subsequently represented by dividing $V_{max}$ by $K_m$.

$$V = \frac{V_{max} \times [S]}{K_m + [S]}$$

Where $V$ is the total rate of Gly-Sar uptake, $V_{max}$ is the maximum uptake rate for transporter-mediated process, $K_m$ (Michaelis-Menten constant) is the concentration at half-saturation, and [$S$] is the Gly-Sar concentration.

Apparent permeability coefficients $P_{app}$ (cm/s) were calculated by linear regression analysis on the time course plot of amount of drugs transported across cell monolayers.

$$P_{app} = \frac{TR_{cum}/dt}{C_0 \times A}$$

Where $TR_{cum}/dt$ is the flux rate of [$^3$H]Gly-Sar or [$^{14}$C]Mannitol obtained from the slope of transport profile. $A$ is the surface area of cell monolayers. $C_0$ is initial concentration of Gly-Sar/mannitol in the donor chambers.

All experiments were conducted at least in triplicate and repeated independently three or four times. The results were expressed as mean ± SD. One-way analysis of

variance (ANOVA) followed by Tukey post hoc test was performed to test for statistically significant differences. Statistical analysis and data fitting were performed using PASW Statistics 17.0 (SPSS Inc., Chicago, IL). Difference between mean values was considered statistically significant at $p < 0.05$ and very statistically significant at $p < 0.01$.

## Results

### Tight Junction Determination of MDCKII Cell Lines

The change of tight junction of MDCK cells after transfection with various human efflux genes was evaluated by determining AP-BL mannitol permeability across different cell lines. Results in Figure 11 indicate that [$^{14}$C]Mannitol permeability across wild-type MDCK cells significantly reduced from $(4.21 \pm 0.05) \times 10^{-5}$ cm/s to $(1.84 \pm 0.09) \times 10^{-5}$ cm/s, $(2.18 \pm 0.22) \times 10^{-5}$ cm/s, and $(1.07 \pm 0.12) \times 10^{-5}$ cm/s after transfection with human *MDR1*, *MRP2* and *BCRP* genes, respectively.

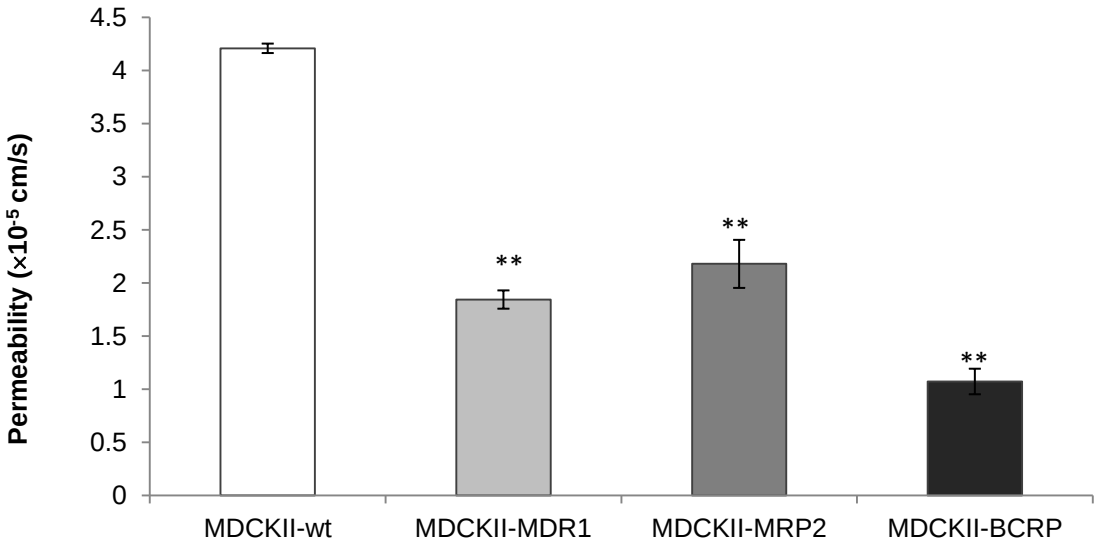


Figure 11. AP-BL permeability of [$^{14}$C]Mannitol (0.125 μCi/ml) across various MDCKII cell lines at pH 7.4.

Each point represents mean ± SD (n=4). ** $P < 0.01$ compared with MDCKII-wt cells.

**Growth Dependence of Gly-Sar Uptake in MDCKII Cell Lines**

Results in Figure 12 demonstrate growth dependent Gly-Sar uptake by apical peptide transporters in different MDCKII cell lines through 3-8 days of culture period. The most [$^{3}$H]Gly-Sar uptake was observed after 4-5 days post seeding in MDCKII-wt, MDCKII-MRP2 and MDCKII-BCRP cell lines. The transfected MDCKII-MDR1 cell line did not show statistically significant different in growth dependent Gly-Sar uptake study. Therefore all subsequent experiments were conducted on the 5th day of seeding to normalize and compare results. Apical uptake of [$^{3}$H]Gly-Sar was diminished significantly in all transfected MDCKII cell lines compared to wild-type cells.

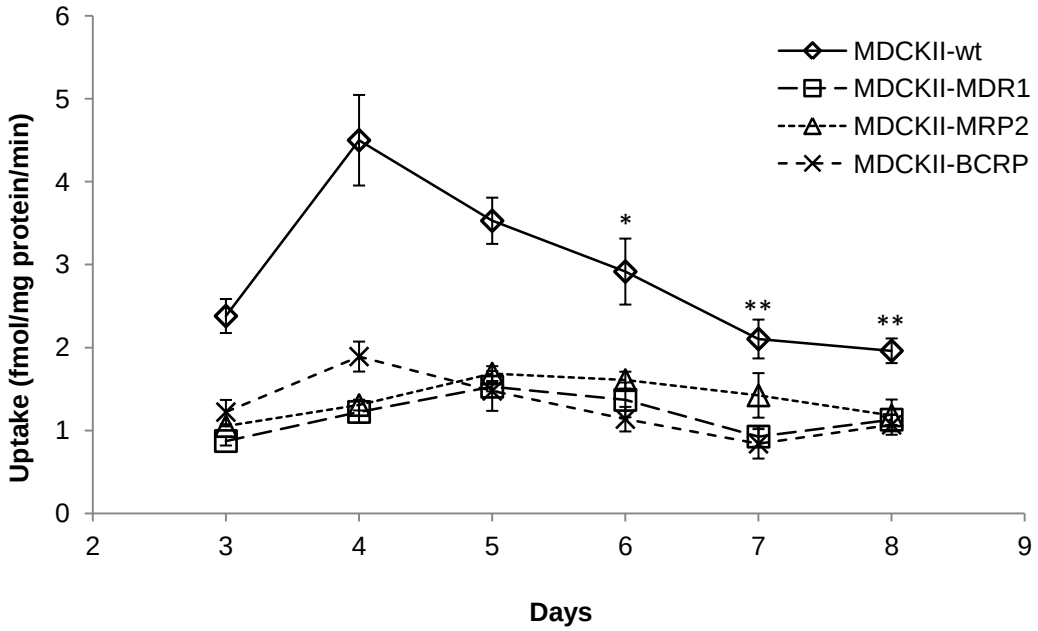


Figure 12. Growth dependent [$^3$H]Gly-Sar (0.5 µCi/ml) uptake at pH 7.4 for 15 min in various MDCKII cell lines.

Each point represents mean ± SD (n=4). * $P < 0.05$ and ** $P < 0.01$ compared with uptake of same cell line at day 4.

**Temperature Dependence of Gly-Sar Uptake in MDCKII Cell Lines**

Results of temperature dependent Gly-Sar uptake by apical peptide transporters in different MDCKII cell lines are described in Figure 13. Around 3- to 5- fold higher [$^3$H]Gly-Sar uptake was obtained in MDCKII-wt cells in comparison with transfected cells at 37°C. Whereas the Gly-Sar cellular accumulation at 4°C, which was mainly achieved via nonspecific uptake by transcellular passive diffusion, exhibited similar extent in all four MDCKII cell lines. Subsequently, apical peptide transporters-mediated specific [$^3$H]Gly-Sar uptakes, calculated by subtracting nonspecific cellular accumulation at 4 °C from total cellular uptake at 37 °C, were found to be 3.17 ± 0.33, 0.62 ± 0.14,

0.45 ± 0.06, and 0.64 ± 0.12 fmol/mg protein/min in MDCKII-wt, MDCKII-MDR1, MDCKII-MRP2, and MDCKII-BCRP cells, respectively.

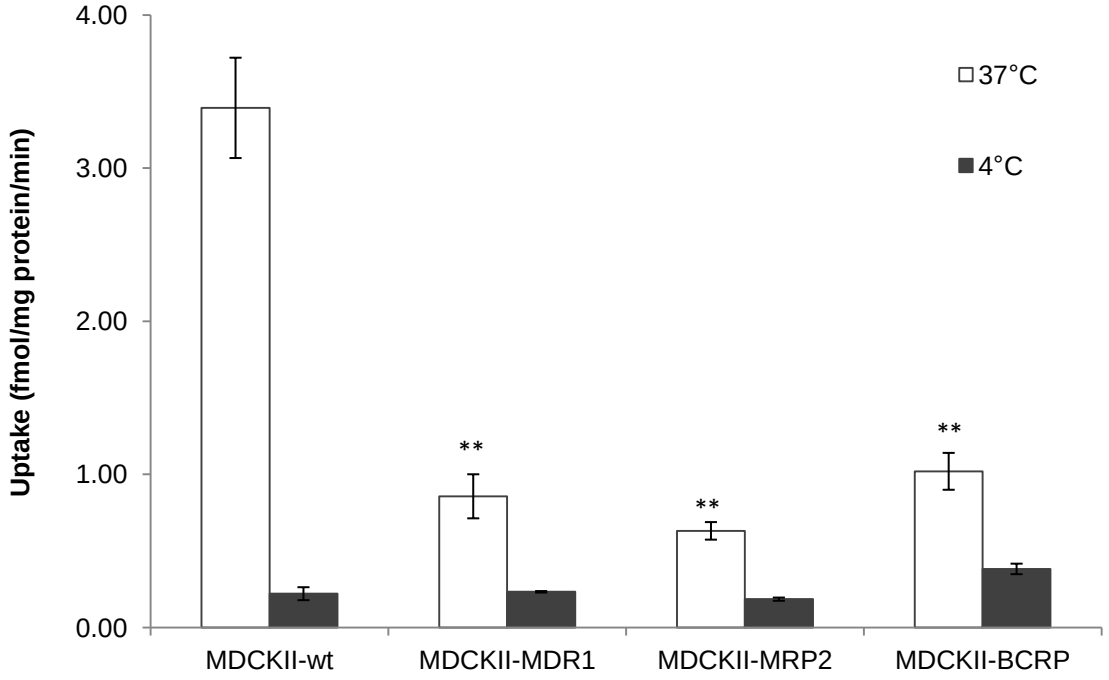


Figure 13. Temperature dependent [$^3$H]Gly-Sar (0.5 μCi/ml) uptake at pH 7.4 for 15 min in various MDCKII cell lines.

Each bar represents mean ± SD (n=4). ** $P < 0.01$ compared with MDCKII-wt cells at 37°C.

**pH Dependence of Gly-Sar Uptake in MDCKII Cell Lines**

Peptide transporter-mediated apical [$^3$H]Gly-Sar uptake in wild-type and transfected MDCKII cell lines was determined by subtracting nonspecific cellular accumulation at 4°C from total cellular uptake at 37°C. Results were compared at different extracellular

pH and summarized in Figure 14. Uptake in wild-type cells were 3- to 5- fold higher than that in transfected MDCKII cells at all pHs determined. The specific Gly-Sar uptake by apical peptide transporters in MDCKII-wt cells showed gradient enhancement when extracellular pH increased from 4.0 to 6.0, then decreased when environmental pH keeps increasing to 7.4. Similar trends were observed for MDCKII-MDR1, MDCKII-MRP2, and MDCKII-BCRP cells. The maximal apical Gly-Sar uptake was obtained at pH 6.0 in all MDCKII cell lines.

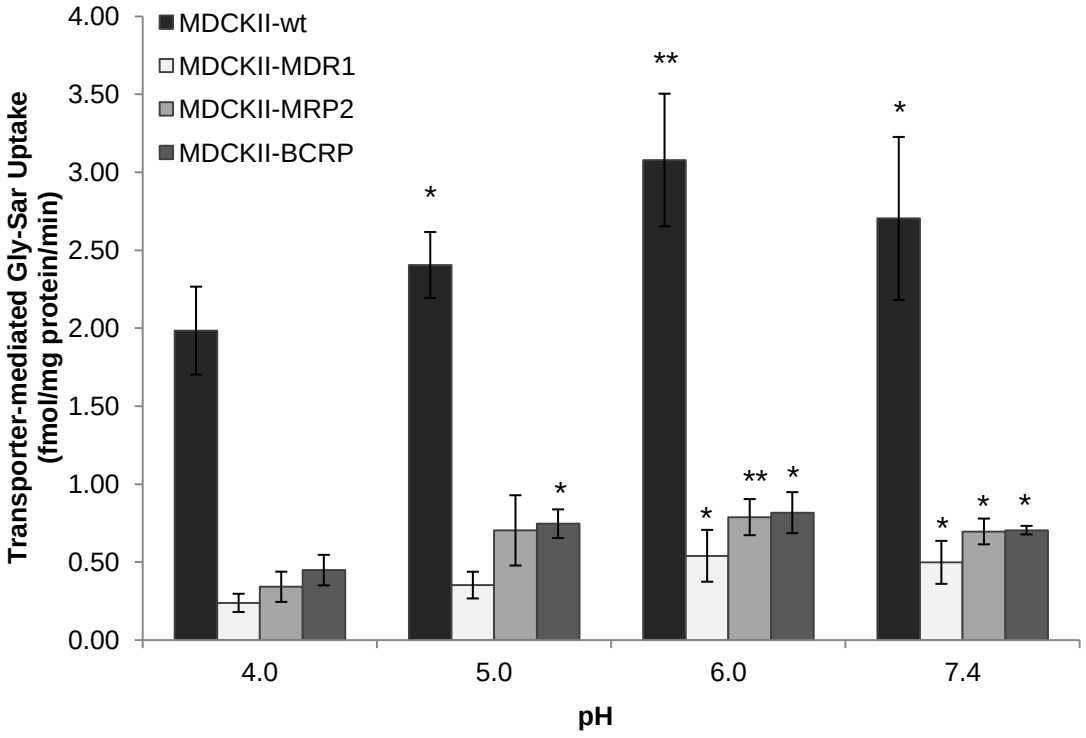


Figure 14. The pH dependent specific [$^3$H]Gly-Sar (0.5 μCi/ml) uptake by apical peptide transporters for 15 min in various MDCKII cell lines.

Each point represents mean ± SD (n=4). * $P < 0.05$ and ** $P < 0.01$ compared with same cell line at pH 4.0.

**Concentration Dependence of Gly-Sar Uptake in MDCKII Cell Lines**

Concentration dependent uptake of [$^3$H]Gly-Sar was carried out at both 37°C and 4°C to evaluate the uptake kinetics of Gly-Sar by apical peptide transporters in different MDCKII cell lines. Concentration dependence of apical peptide transporter-mediated specific Gly-Sar uptake was calculated by subtracting nonspecific uptake estimated at 4°C from total uptake determined at 37°C (Figure 15). Uptake kinetic parameters including apparent $K_m$, $V_{max}$, and *transport efficiency* ($V_{max}$ / $K_m$) are summarized in Table 3. The value of $V_{max}$ for apical peptide transporters in MDCKII-wt cells was 10.76 ± 1.68 fmol/mg protein/min. After transfection with human *MDR1*, *MRP2*, and *BCRP* genes, it decreased to 1.30 ± 0.36, 4.62 ± 0.76, and 4.50 ± 0.83 fmol/mg protein/min respectively. *Transport efficiency* values, which represent the amount of Gly-Sar translocated by unit peptide transporters in unit time, were estimated to 0.180 ± 0.009, 0.045 ± 0.010, 0.055 ± 0.011, and 0.074 ± 0.016 nl/mg protein/min for apical Gly-Sar uptake in MDCKII-wt, MDCKII-MDR1, MDCKII-MRP2, and MDCKII-BCRP cell lines, respectively. It indicates that *transport efficiency* for apical peptide uptake was also diminished in all transfected MDCKII cell lines.

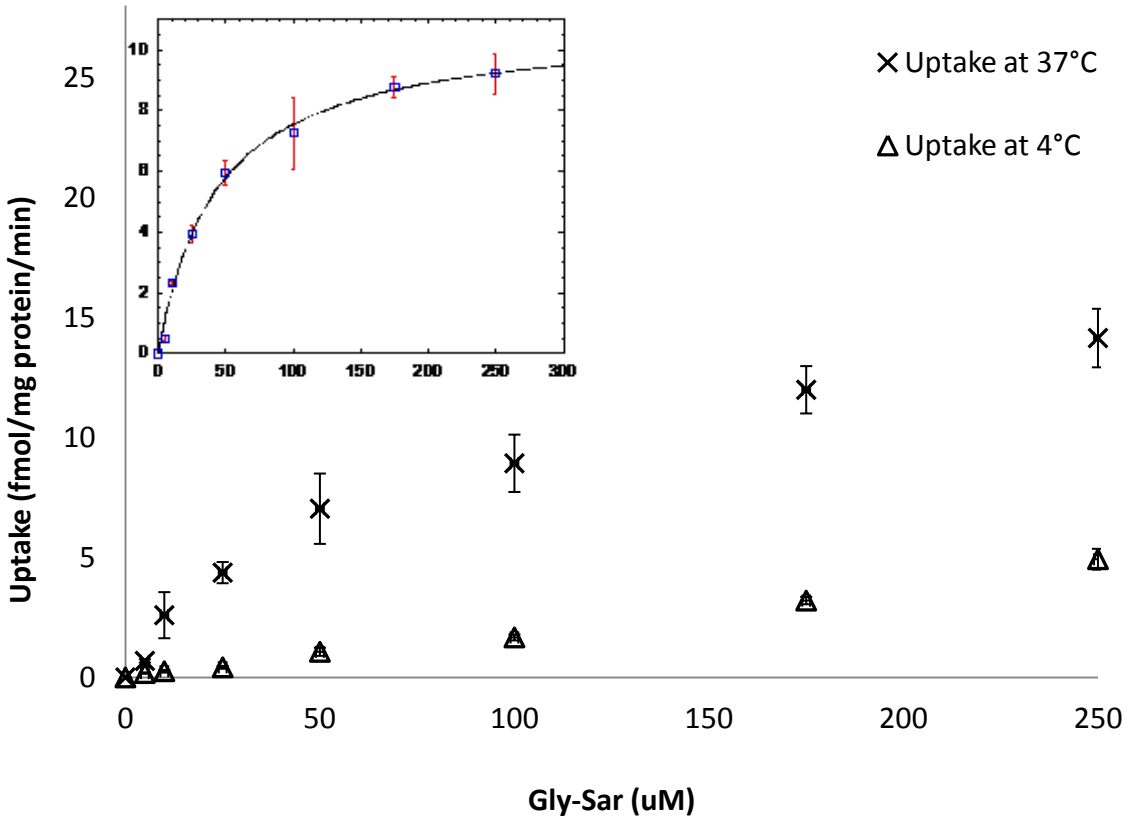


Figure 15. Concentration dependence of [$^3$H]Gly-Sar uptake by apical peptide transporters for 15 min in MDCKII-wt cells at 37°C and 4°C respectively.

Insert: Concentration dependence of apical peptide transporter-mediated specific Gly-Sar uptake in MDCKII-wt cells. Data (□) were calculated by subtracting nonspecific uptake estimated at 4°C (Δ) from total uptake at 37°C (×). Solid line represents the calculated fit of the data to Michaelis-Menten equation. Each point represents mean ± SD (n=3).

Table 3. Kinetic parameters for Gly-Sar uptake mediated by apical or basolateral peptide transporters in various MDCKII cell lines.

| | Apical uptake | | | | Basolateral uptake | | | |
|---|---|---|---|---|---|---|---|---|
| | MDCKII-wt | MDCKII-MDR1 | MDCKII-MRP2 | MDCKII-BCRP | MDCKII-wt | MDCKII-MDR1 | MDCKII-MRP2 | MDCKII-BCRP |
| $K_m$ (μM) | 59.69 ± 1.10 | 29.13 ± 3.29 | 84.75 ± 18.59 | 60.67 ± 8.56 | 13.71 ± 2.22 | 50.87 ± 7.86 | 64.56 ± 4.09 | 46.15 ± 2.26 |
| $V_{max}$ (fmol/mg protein/min) | 10.76 ± 1.68 | 1.30 ± 0.36 | 4.62 ± 0.76 | 4.50 ± 0.83 | 4.45 ± 0.04 | 8.52 ± 0.81 | 8.03 ± 1.78 | 13.07 ± 2.61 |
| $V_{max}/K_m$ (nl/mg protein/min) | 0.180 ± 0.009 | 0.045 ± 0.010** | 0.055 ± 0.011** | 0.074 ± 0.016** | 0.324 ± 0.050 | 0.167 ± 0.058 | 0.124 ± 0.016 | 0.283 ± 0.098 |

Uptake of [$^3$H]Gly-Sar were conducted in the presence of different concentrations of unlabeled Gly-Sar (0-250 μM) at 4°C and 37°C, respectively. Each value represents mean ± SD (n=3). ** $P < 0.01$ compared with apical uptake observed in MDCKII-wt cells.

**Passage Dependence of Gly-Sar *Transport Efficiency* in MDCKII Cell Lines**

Since the expression of transfected efflux transporters varies with ascending passage number, *transport efficiency* of apical peptide transporters-mediated specific [$^3$H]Gly-Sar uptake was investigated in various MDCKII cell lines with different passage number. Figure 16 A-C illustrate that in comparison to wild-type cells with the value of 0.180 ± 0.009 nl/mg protein/min, *transport efficiency* of [$^3$H]Gly-Sar uptake mediated by apical peptide transporters was reduced to different extents after transfection. Lowest *transport efficiency* values were observed at lowest cell passage. With passage number increasing, an increment on the *transport efficiency* for Gly-Sar uptake was achieved for all transfected cell lines. Finally apical peptide transporters showed relatively invariable *transport efficiency* values at higher cell passage. At passage 25, these values were obtained to be around 0.10 nl/mg protein/min for MDCKII-MDR1 cells, 0.12 nl/mg protein/min for MDCKII-MRP2 cells, and 0.15 nl/mg protein/min for MDCKII-BCRP cells, respectively.

**A**

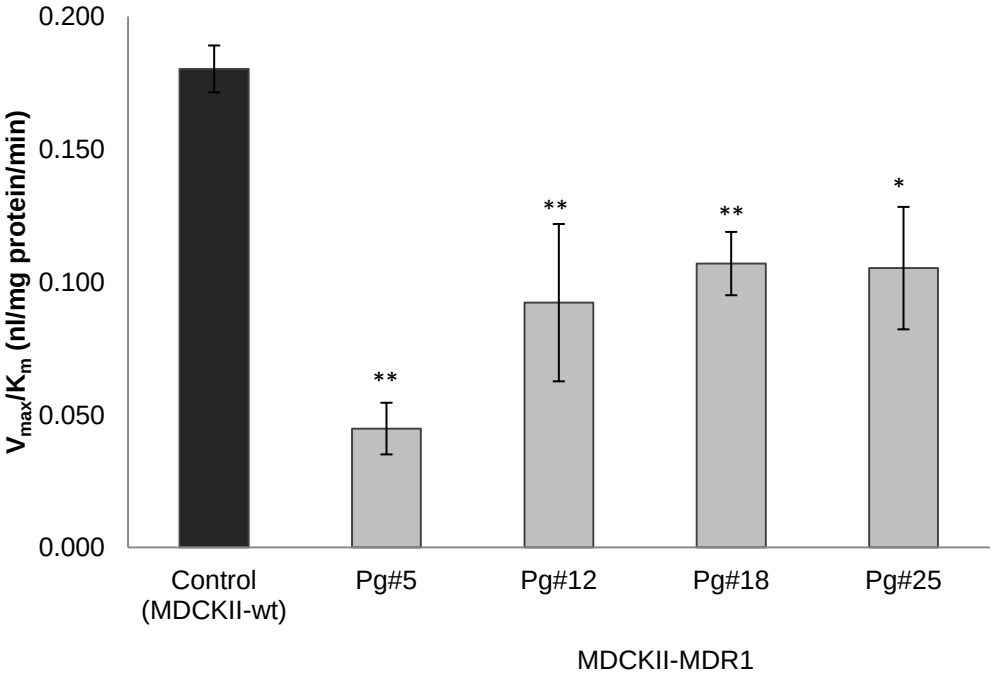
0.200
0.150
0.100
0.050
0.000
$V_{max}/K_m$ (nl/mg protein/min)
**
**
**
*
Control (MDCKII-wt)
Pg#5
Pg#12
Pg#18
Pg#25
MDCKII-MDR1

**B**

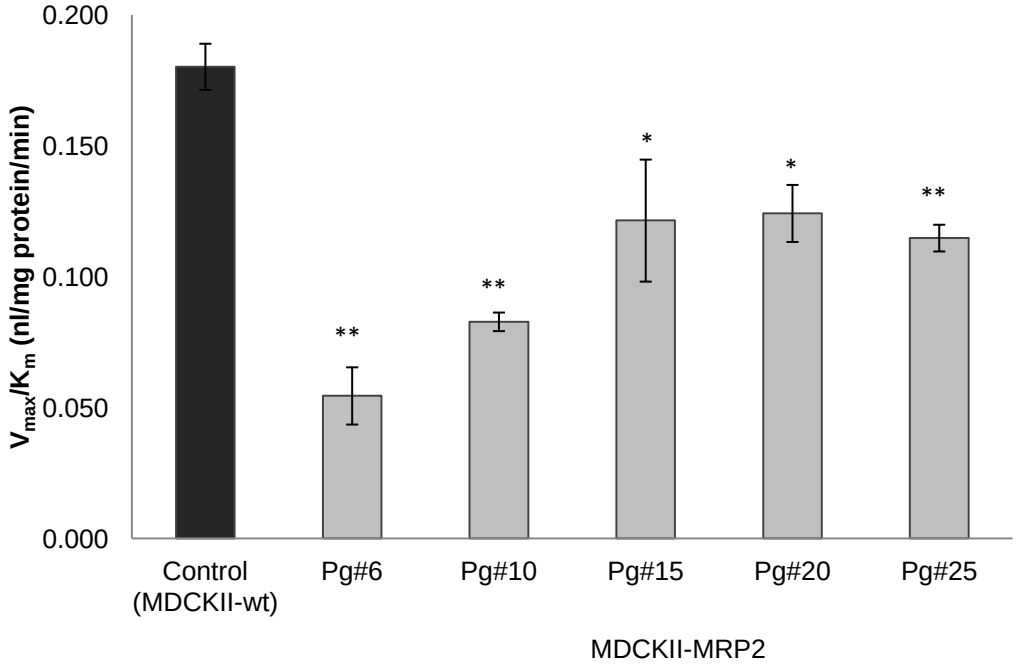
0.200
0.150
0.100
0.050
0.000
$V_{max}/K_m$ (nl/mg protein/min)
**
**
*
*
**
Control (MDCKII-wt)
Pg#6
Pg#10
Pg#15
Pg#20
Pg#25
MDCKII-MRP2

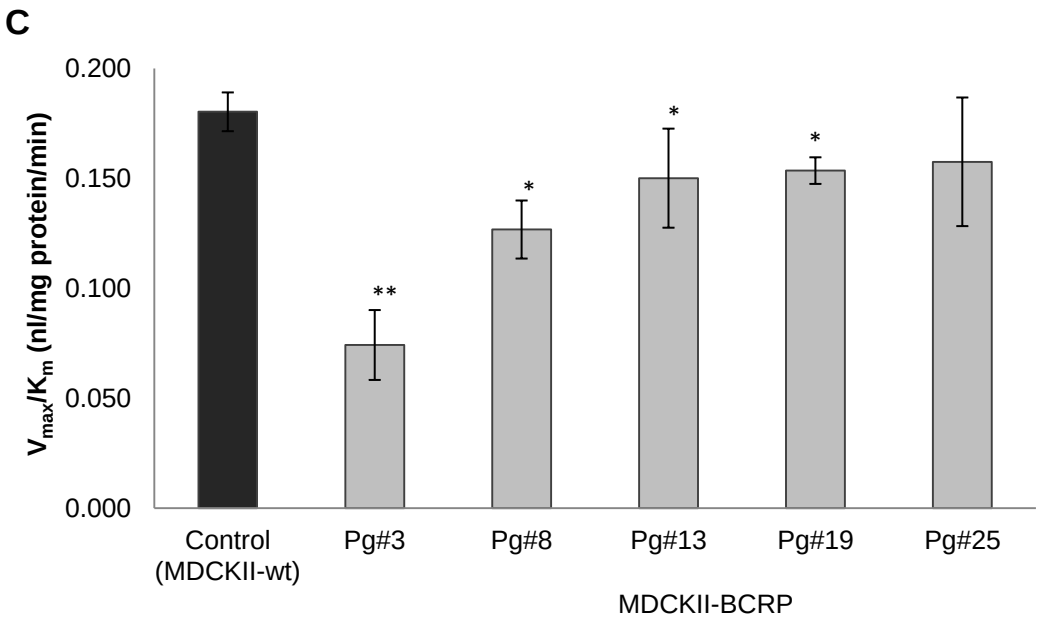


Figure 16. Estimation of transport efficiency ($V_{max}/K_m$) for specific [$^3$H]Gly-Sar uptake by apical peptide transporters in various transfected MDCKII cell lines with different passage number.

Uptake of [$^3$H]Gly-Sar were conducted in the presence of different concentrations of unlabeled Gly-Sar (0-250 μM) at 4°C and 37°C, respectively. A, MDCKII-MDR1 cells; B, MDCKII-MRP2 cells; C, MDCKII-BCRP cells. Each bar represents mean ± SD (n=3). * $P < 0.05$ and ** $P < 0.01$ compared with control.

**Effects of Peptide Transporter Inhibitors on Apical Gly-Sar Uptake in MDCKII Cell Lines**

Competitive inhibition studies were conducted on MDCKII cell lines in the presence of both PepT1 and PepT2 inhibitors to evaluate the substrate specificity. Results in Figure 17 indicate that all the observed inhibitors showed significantly reduced apical Gly-Sar uptake compared to control, in which both PepT2 inhibitors fosinopril (100 μM) and

cefadroxil (20 mM) exhibited more remarkable inhibitory effects than PepT1 inhibitor Gly-Pro (20 mM) in all four MDCKII cell lines. Moreover, transfected cell lines with low cell passage (lower than passage number 6) exhibited less Gly-Sar uptake than high cell passage (higher than passage number 25). In comparison with MDCKII-wt cells, all transfected MDCKII cell lines showed reduced apical cellular accumulation of Gly-Sar, no matter of the cell passages.

**pH Dependent Transcellular Permeability of Gly-Sar in MDCKII Cell Lines**

Transporter-mediated specific Gly-Sar transport across both parental and transfected cell monolayers of MDCKII cell lines was estimated by subtracting nonspecific transport (passive diffusion) of [$^{14}$C]Mannitol from [$^{3}$H]Gly-Sar transport. Results for both AP-BL and BL-AP permeability values are summarized in Table 4. Gly-Sar transport mediated by peptide transporters on AP to BL direction showed significantly higher permeability in MDCKII-wt cells than transfected cells at all pHs examined. Additionally, AP-BL Gly-Sar transport on all MDCKII cells exhibited gradual enhancement when apical pH increased from 4.0 to 7.4, and reached maximal at pH 7.4. However, apparent permeability values of BL-AP Gly-Sar transport across transfected cell monolayers were similar or greater than that on wild-type cells at all pHs observed. Furthermore, no obvious relationship between apical pH and BL-AP transcellular Gly-Sar permeability could be obtained on all MDCKII cells in this study.

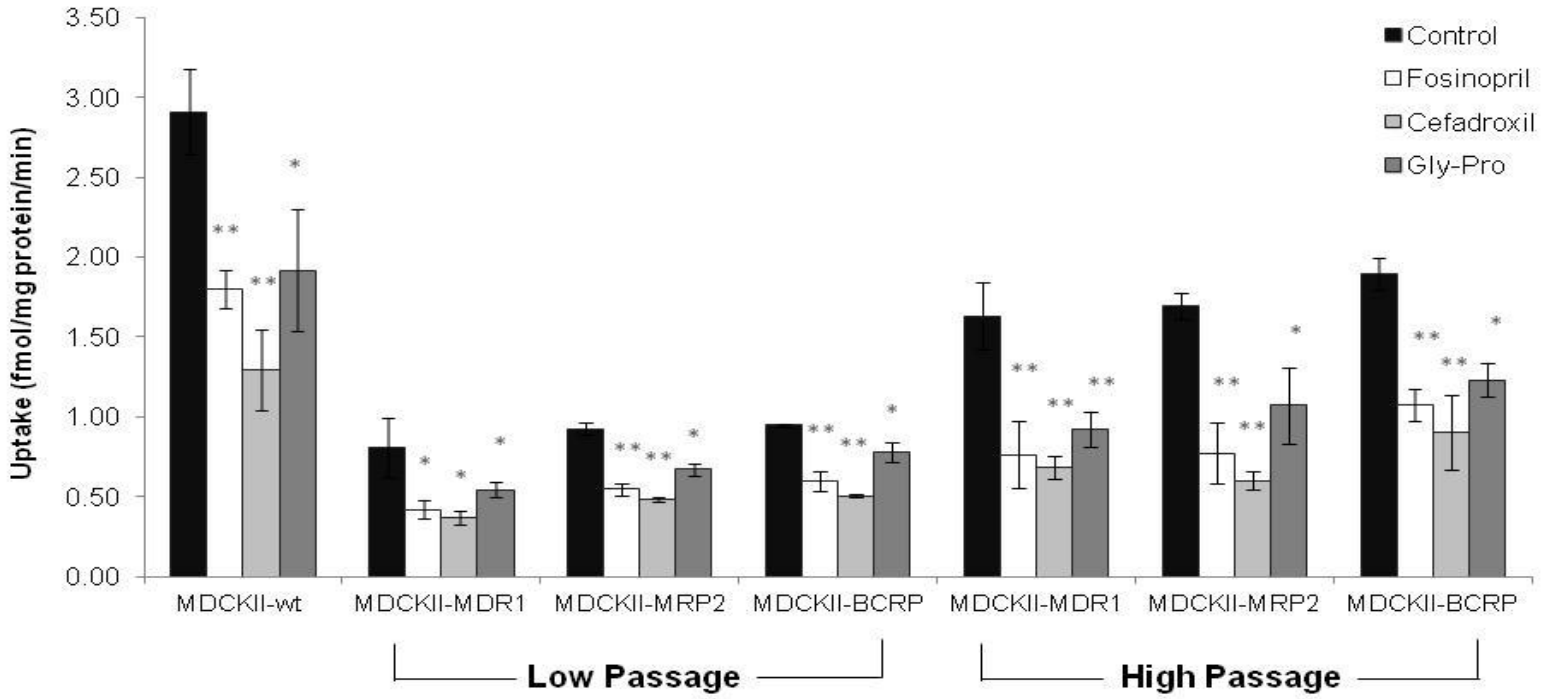


Figure 17. Apical uptake of [$^3$H]Gly-Sar (0.5 μCi/ml) in the absence (control) or presence of peptide transporter inhibitors, fosinopril (100 μM), cefadroxil (20 mM) and glycyl-*L*-proline (Gly-Pro, 20 mM) at pH 7.4, 37°C for 15 min in various MDCKII cell lines with different cell passages.

Low Passage: passage number is less than 6; High Passage: passage number is more than 25. Each data point represents mean ± SD (n=3). * $P < 0.05$ and ** $P < 0.01$ compared with control.

Table 4. pH dependent transporter-mediated Gly-Sar transport on both AP-BL and BL-AP directions across various MDCKII cell monolayers.

| pH in AP chamber | AP-BL Permeability ($\times 10^{-6}$ cm/s) | | | | BL-AP Permeability ($\times 10^{-6}$ cm/s) | | | |
|---|---|---|---|---|---|---|---|---|
| | MDCKII-wt | MDCKII-MDR1 | MDCKII-MRP2 | MDCKII-BCRP | MDCKII-wt | MDCKII-MDR1 | MDCKII-MRP2 | MDCKII-BCRP |
| 4.0 | 13.1 ±1.4 | 6.0 ±0.4 [a] | 8.6 ±1.1 [a] | 7.1 ±0.3 [a] | 9.4 ±0.4 | 10.1 ±1.3 | 8.5 ±0.6 | 10.9 ±0.7 |
| 5.0 | 14.9 ±2.8 | 6.4 ±0.5 [a,b] | 9.9 ±0.8 [a] | 7.6 ±1.2 [a,c] | 6.6 ±0.6 | 7.6 ±0.8 | 6.3 ±0.4 | 6.5 ±0.7 |
| 6.0 | 22.2 ±1.9 | 8.0 ±0.4 [a] | 10.6 ±0.1 [a] | 10.7 ±0.7 [a] | 6.0 ±01.0 | 8.2 ±0.5 | 7.5 ±0.5 | 7.2 ±0.9 |
| 7.4 | 36.7 ±0.2 | 11.7 ±0.6 [a,b,d] | 17.7 ±1.4 [a] | 18.6 ±1.9 [a] | 8.0 ±0.9 | 12.9 ±1.3 | 15.7 ±0.6 | 15.6 ±0.1 |

The pH of incubation media varied from 4.0 to 7.4 in apical (AP) chambers, and remained consistent in basolateral (BL) chambers to pH 7.4. Each value represents mean ± SD (n=4). Statistical analysis was performed to evaluate the difference of AP-BL permeability at each pH within MDCKII cell lines. [a] $P < 0.01$ compared with MDCKII-wt cells, [b] $P < 0.01$ and [c] $P < 0.05$ compared with MDCKII-MRP2 cells, and [d] $P < 0.05$ compared with MDCKII-BCRP cells, respectively.

**Real-time PCR Assay**

Levels of mRNA for both endogenous peptide transporters (cPepT1 and cPepT2) and transfected human efflux transporters (hP-gp, hMRP2, and hBCRP) expressed on various MDCKII cell lines were determined using real-time PCR. The relative amount of mRNA expression at different passage number was illustrated in Figure 18. All three transfected MDCKII cell lines showed remarkably diminished efflux genes expression with ascending cell passage, and conversely enhanced peptide genes expression was observed on corresponding cell passages from low (passage number 4-8) to high (passage number 30). The relative fold of h*MDR1* (transfected) gene expression was reduced from 1.00 ± 0.23 (passage number 5) to 0.03 ± 0.01 (passage number 30) in MDCKII-MDR1 cells. In contrast, endogenous influx c*PepT1* and c*PepT2* gene expression was enhanced from 1.00 ± 0.22 fold and 1.00 ± 0.09 fold at passage 5 to 1.64 ± 0.47 fold and 3.27 ± 1.38 fold at passage 30, respectively (Figure 18A). Similar trend was also obtained in h*MRP2*- and h*BCRP*- transfected cell lines. Corresponding data in MDCKII-MRP2 cells at passage 30 was found to be 0.37 ± 0.19, 1.88 ± 0.13, and 4.66 ± 1.44, for h*MRP2*, c*PepT1*, and c*PepT2*, respectively (Figure 18B), and in MDCKII-BCRP cells (passage 30) was 0.29 ± 0.07, 1.77 ± 0.56, and 6.15 ± 1.95 for h*BCRP*, c*PepT1*, and c*PepT2*, respectively (Figure 18C).

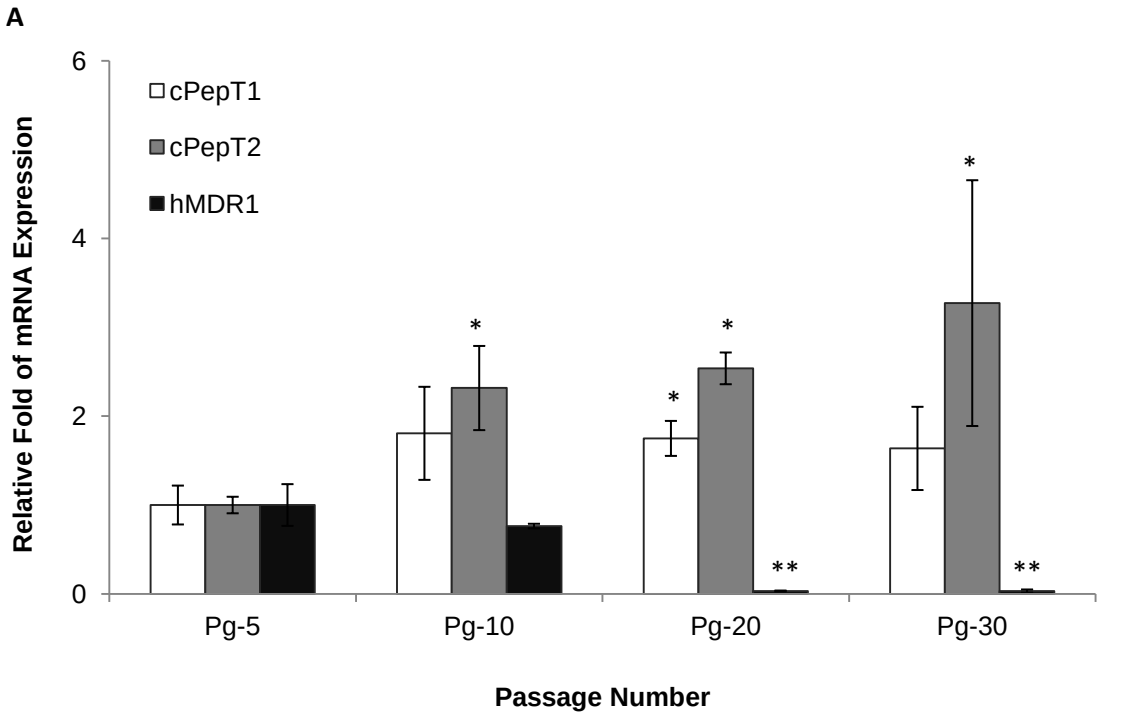
A
Relative Fold of mRNA Expression
6
4
2
0
cPepT1
cPepT2
hMDR1
*
*
*
*
**
*
**
Pg-5
Pg-10
Pg-20
Pg-30
Passage Number

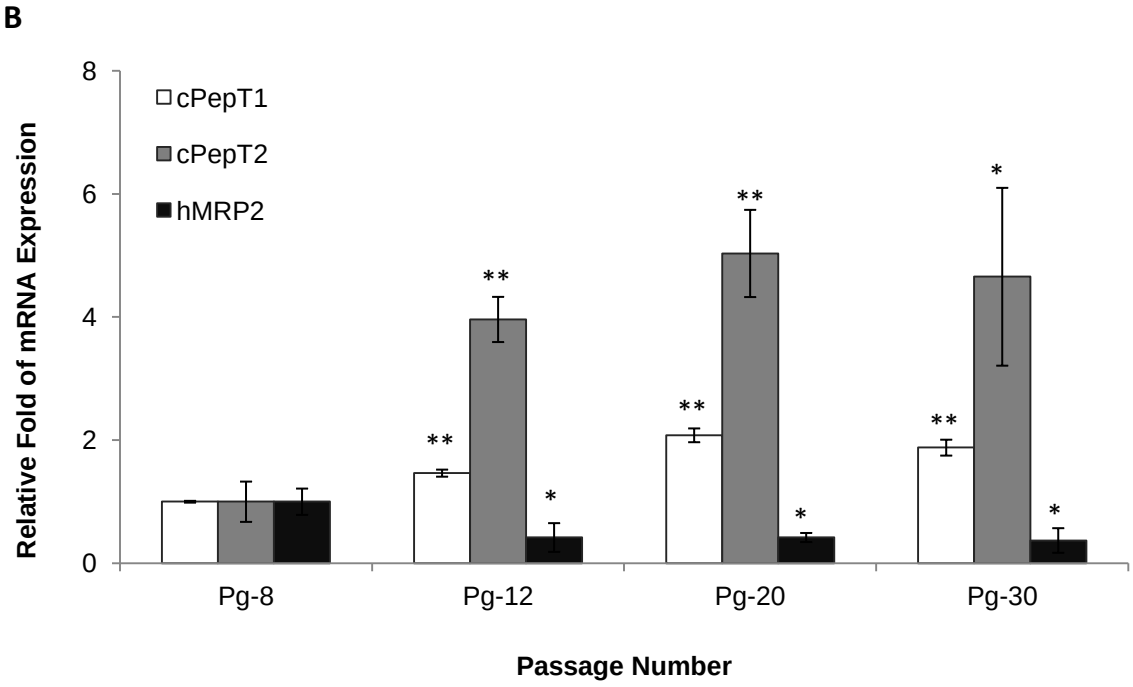
B
Relative Fold of mRNA Expression
8
6
4
2
0
cPepT1
cPepT2
hMRP2
**
**
*
**
**
*
**
*
*
Pg-8
Pg-12
Pg-20
Pg-30
Passage Number

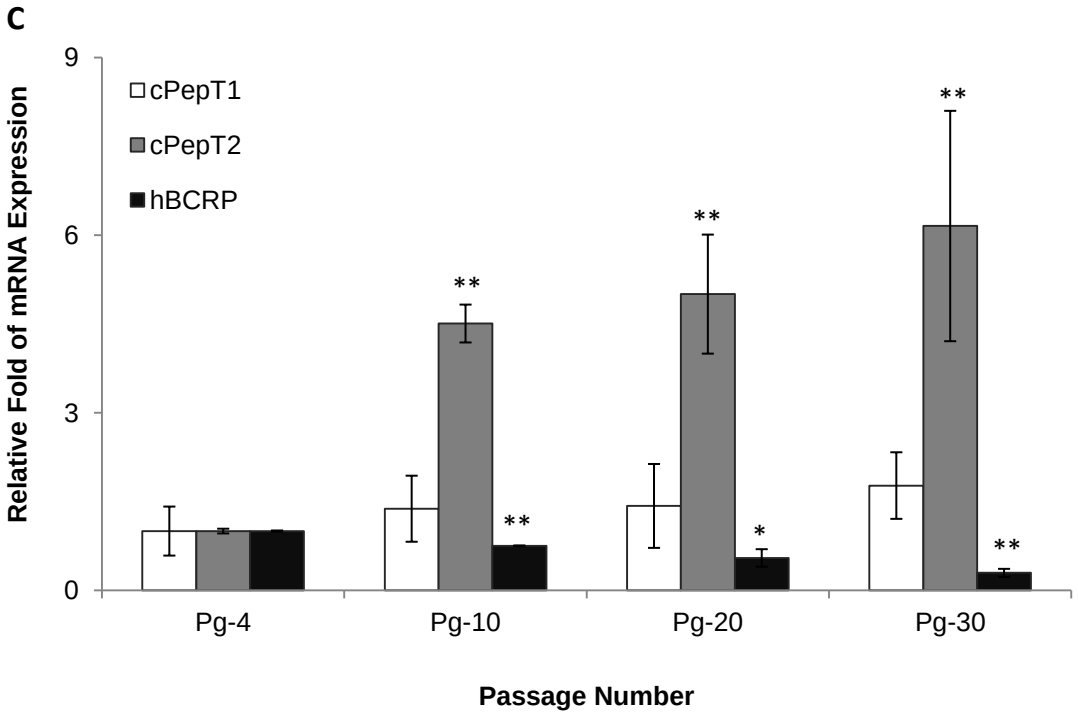


Figure 18. Determination of mRNA levels of endogenous influx transporters, canine PepT1 (cPepT1) and canine PepT2 (cPepT2), and exogenous efflux transporters, human P-gp (hMDR1), human MRP2 (hMRP2) and human BCRP (hBCRP) in various transfected MDCKII cell lines with different passage number using real-time PCR.
A, MDCKII-MDR1 cells; B, MDCKII-MRP2 cells; C, MDCKII-BCRP cells. Each bar represents mean ± SD (n=3). * $P < 0.05$ and ** $P < 0.01$ compared with the lowest cell passage.

**Expression of endogenous PepT1 and PepT2 in MDCKII cells**

In order to evaluate protein levels of endogenous PepT1 and PepT2 in MDCKII cells after transfection with different human efflux genes, Western blot analysis was performed using polyclonal primary antibodies specific to PepT1 (78 kDa) and PepT2 (81 kDa) in the present study. Results in Figure 19 showed that expression of endogenous (canine)

PepT2 in MDCKII-wt cells is much higher than PepT1. Moreover, Figure 20 illustrates that MDCKII-MDR1, MDCKII-MRP2, and MDCKII-BCRP cells expressed significantly less amounts of cPepT2 protein (lane 3-8) as compared to the MDCKII-wt cells (lane 1-2). Furthermore, PepT2 expression was observed to be enhanced at higher cell-passages for all transfected MDCKII cells (Figure 20B). However, this passage-dependent phenomenon can not be observed for cPepT1 expression (Figure 21).

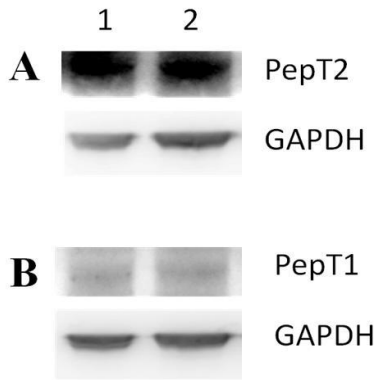


Figure 19. Determination of protein levels of endogenous canine PepT2 (A) and canine PepT1 (B) in wild-type MDCKII cell line by western blot assay.

Lane 1, MDCKII-wt (Pg-14); lane 2, MDCKII-wt (Pg-30);

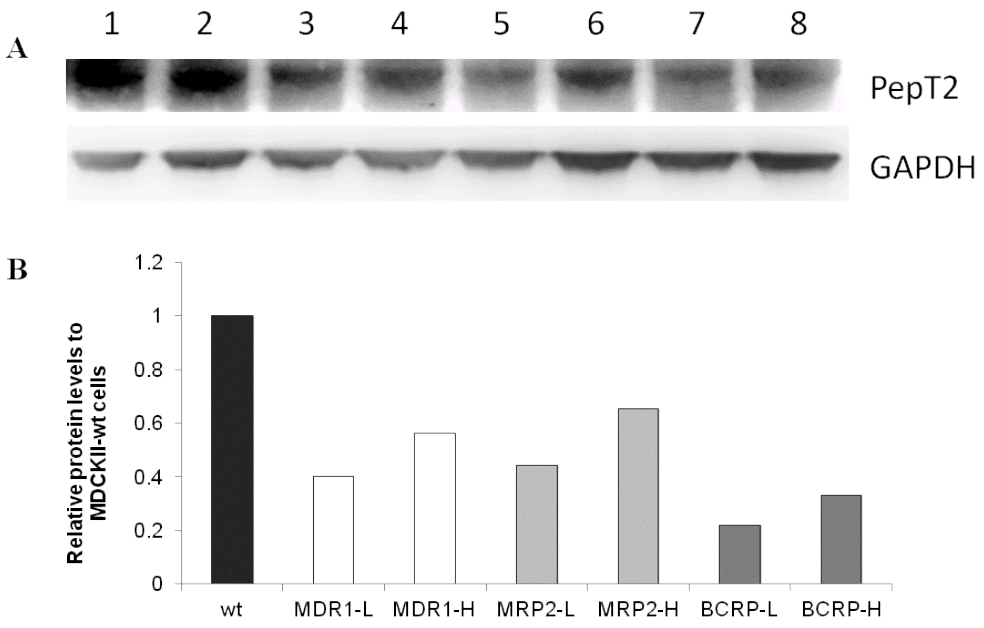


Figure 20. Determination of protein levels of endogenous (canine) PepT2 in wild-type and transfected MDCKII cell lines by western blot assay (A) and comparative canine PepT2 levels in MDCK cells after human *MDR* genes transfection (B).

Lane **1**, MDCKII-wt (Pg-14); lane **2**, MDCKII-wt (Pg-30); lane **3**, MDR1-L (Pg-5); lane **4**, MDR1-H (Pg-30); lane **5**, MRP2-L (Pg-8); lane **6**, MRP2-H (Pg-30); lane **7**, BCRP-L (Pg-4); lane **8**, BCRP-H (Pg-30).

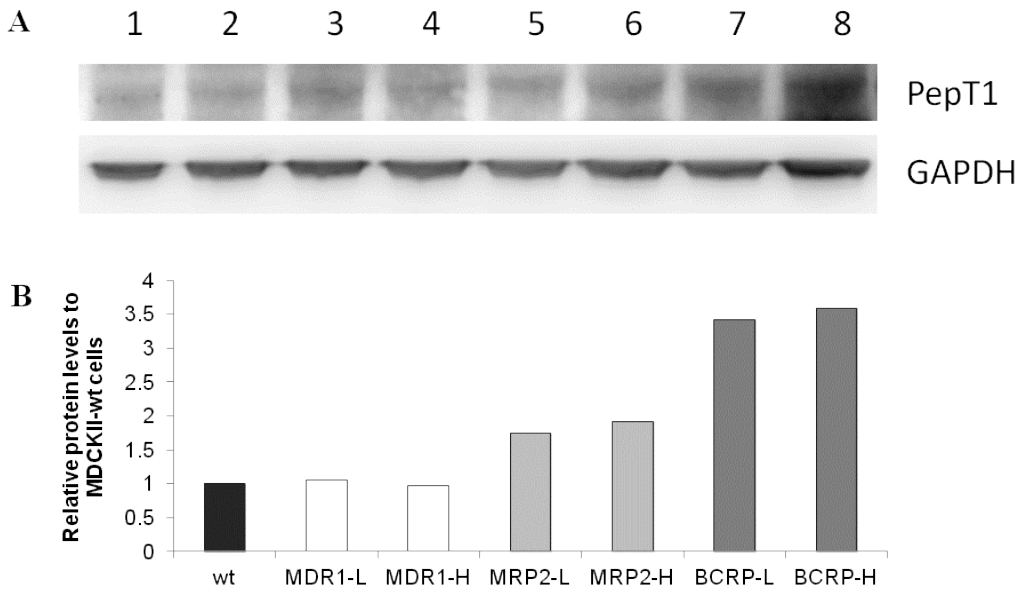


Figure 21. Determination of protein levels of endogenous (canine) PepT1 in wild-type and transfected MDCKII cell lines by western blot assay (A) and comparative canine PepT1 levels in MDCK cells after human *MDR* genes transfection (B).

Lane **1**, MDCKII-wt (Pg-14); lane **2**, MDCKII-wt (Pg-30); lane **3**, MDR1-L (Pg-5); lane **4**, MDR1-H (Pg-30); lane **5**, MRP2-L (Pg-8); lane **6**, MRP2-H (Pg-30); lane **7**, BCRP-L (Pg-4); lane **8**, BCRP-H (Pg-30).

## Discussion

MDCK cells have been wildly used as an alternative *in vitro* model to Caco-2 cells which exhibit good correlation with human intestinal mucosa (Irvine et al., 1999; Volpe, 2008). In comparison with Caco-2 cells, MDCK cells have shown common epithelial characteristics and much shorter culture time (5 days for MDCK *vs*. 21 days for Caco-2). Therefore it has been accepted as an attractive tool for predicting absorption of new drug candidates in drug discovery stage. Especially MDCK strain II cells transfected with

different human efflux genes, have been utilized to screen efflux-mediated drug transport (Tang et al., 2002b; Tang et al., 2002a; Wang et al., 2005). However, some functions and biological characteristics of cells might change due to transfection. Our studies demonstrate that [$^{14}$C]Mannitol transport, an indicator of paracellular permeability, was greatly reduced in *MDR1*, *MRP2*, and *BCRP*-transfected MDCKII cells on apical to basolateral direction in comparison with wild-type cells (Figure 11), suggesting an enhanced barrier function after transfection. Enhanced tight junctions in transfected MDCKII cells indicate that the function of endogenous active transporters may also be altered. Thus a potential imperfect permeability result may be obtained in transcellular transport of substrates determined on transfected cells when compared with wild-type cells.

MDCK cells express endogenous canine peptide transporters on both apical and basolateral membranes, whereas all the transfected exogenous efflux genes are expressed apically (Tang et al., 2002b; Tang et al., 2002a; An and Morris, 2010). Figure 12 displayed apical uptake of [$^{3}$H]Gly-Sar, a typical substrate for peptide transporters, in various MDCKII cell lines at different days of culture. A remarkably different Gly-Sar cellular accumulation was obtained between wild-type and transfected cells. Total uptake of [$^{3}$H]Gly-Sar at 37°C, via the routes of both passive diffusion and peptide transporter-mediated influx, was much lower in human P-gp, MRP2, and BCRP-overexpressed MDCKII cell lines. These results have been further confirmed by temperature dependence study (Figure 13). It has been reported that passive uptake of dipeptides (non-peptide transporter mediated) can be estimated by measuring uptake at cold temperature, and "transporter-mediated" component can be calculated by subtracting

passive uptake component observed at 4°C from the total uptake measured at 37°C (Scow et al., 2011). Significant temperature dependent peptide uptake was observed in all four MDCKII cell lines. Uptake of [$^{3}$H]Gly-Sar was much higher at 37°C than that at 4°C, suggesting that the active transporter-mediated transport was involved in cellular uptake of Gly-Sar. Additionally, apical Gly-Sar influx via specific transporters in MDCKII-wt cells was 5- to 7- fold higher than that in MDCKII-MDR1, MDCKII-MRP2, and MDCKII-BCRP cells, indicating a reduced function of apical endogenous peptide transporters after transfection with exogenous efflux genes. This observation suggests that transfection of foreign gene(s) may affect the function of endogenous gene.

$H^{+}$/peptide co-transporters (PepT1 and PepT2) are generally believed to be functionally expressed at apical membranes of MDCK wild-type cells (Sawada et al., 2001). It suggests that uptake of small peptides from apical side of MDCK cells can be stimulated by an inwardly directed $H^{+}$ gradient. However, it has also been reported that the binding affinity for charged peptides to peptide transporters can change when extracellular pH altered (Daniel and Kottra, 2004). The neutral substrates like Gly-Sar at brush border or urinary pH (6.0 to 6.5) were observed to be preferred substrates for PepT1 and PepT2 (Terada et al., 2000; Pan et al., 2001). Specific peptide transporter-mediated Gly-Sar uptake was found to be a "bell-shape" and reached greatest at pH 6.0–6.5 when Terada *et al* tested apical [$^{14}$C]Gly-Sar uptake in MDCK cells with changing environmental pH from 5.0 to 7.5 (Terada et al., 2000). In the present study, apical transporter-mediated specific [$^{3}$H]Gly-Sar uptake in MDCKII-wt cells was also observed to be maximal at extracellular pH 6.0 (Figure 14). The pH profiles of uptake in human efflux genes-transfected cell lines appeared to be similar as MDCKII-wt cells, but the

uptake in these transfected cells was much lower. The most probable explanation is that characteristic of peptide transporters in the transfected cell lines possibly remains unchanged, but its expression level was possibly too low to facilitate a significant pH-dependent difference in Gly-Sar uptake.

In order to recognize its functional properties, concentration dependence of apical and basolateral peptide transporters-mediated specific Gly-Sar uptake was evaluated in various MDCKII cell lines. It was observed that mean values of apparent $K_m$ from apical side of both wild-type and transfected MDCKII cells varied in the range of 30 – 85 μM. According to the classification of substrates/inhibitors suggested by previous research (Luckner and Brandsch, 2005; Biegel et al., 2006), this result clearly demonstrates that apical peptide transporters exhibit the significant PepT2 characters of high-affinity ($K_m$ < 0.1 mM) for Gly-Sar uptake. The corresponding $V_{max}$ values were tremendously diminished to about 12%, 43% and 42% of that in wild-type cells after transfection with h*MDR1*, h*MRP2*, and h*BCRP* efflux genes, respectively. It indicates that the capacity of apical peptide transporters markedly declined. However, $V_{max}$ values obtained from different laboratories are usually diverse, since its determination can be affected by different methodology and calculations applied by different investigators. In our current investigation, $V_{max}$ values obtained after subtraction of passive diffusion values. Thus determination of *transport efficiency* (the ratio of $V_{max}$ to $K_m$) provides a more reliable way to investigate transporter function (Jedlitschky et al., 1996; Zhou et al., 2010). *Transport efficiency* values for apical peptide transporters summarized in Table 3 exhibit a significant decrease to around 25% (MDCKII-MDR1), 30% (MDCKII-MRP2), and 41% (MDCKII-BCRP) of that in wild-type cells. In contrast, basolateral peptide transporters

in transfected cell lines showed an increased rate for Gly-Sar translocation with higher $V_{max}$ values. These results again confirm our hypothesis that alien gene(s) in apical membrane can influence the function of endogenous transporters.

To further investigate the properties of peptide transporter system expressed on apical membrane of MDCKII cell lines after transfection, inhibitory uptake of [$^3$H]Gly-Sar was carried out in the presence of various peptide transporter inhibitors. Gly-Pro showed markedly competitive inhibition for Gly-Sar uptake and was reported as a selected PepT1 inhibitor (Giacomini et al., 2010; Omkvist et al., 2010). Angiotensin-converting enzyme (ACE) inhibitor fosinopril and aminocephalosporin antibiotic agent cefadroxil have been considered as powerful PepT2 inhibitors due to their high affinity for binding to PepT2 (Giacomini et al.; Ocheltree et al., 2004; Knutter et al., 2008). In the current study, 20 mM Gly-Pro exhibited a less reduction in [$^3$H]Gly-Sar uptake than 20 mM cefadroxil and 100 µM fosinopril in MDCKII-wt cells indicating less PepT1 than PepT2 expressions on the apical membrane of MDCK cells and similar substrate specificity was observed in transfected cell lines (Figure 17). These findings provide further evidence that the type of apical peptide transporter system remained unaltered after transfection with exogenous efflux genes, but reduced capacity of influx transporter due to less expression resulting in decreased Gly-Sar uptake compared to wild-type cells.

Functional activities of peptide transporters in MDCK cell lines influences significantly on transepithelial transport of [$^3$H]Gly-Sar across cell monolayers. Previous studies have reported that apical peptide transporter present in MDCKII cells, primarily $H^+$/peptide co-transporter system, is responsible to the luminal uptake into the cells, whereas the basolateral peptide transporter system, a novel peptide transporter which

does not appear pH-dependent, is involved in the cellular re-absorption of small peptides from peritubular capillaries (Terada et al., 2000; Sawada et al., 2001). Therefore transcellular transport of Gly-Sar from donor chamber to receiver chamber should be contributed by influx activities mediated by both apical and basolateral peptide transporters. As demonstrated by the present transport data in Table 4, MDCKII-wt cells displayed a significantly higher AP-BL permeability and a similar or slightly lower BL-AP permeability of [$^3$H]Gly-Sar over that in transfected cell lines at all pHs. These findings further confirm the reduced transport efficiencies, particularly the apical endogenous peptide transporters that we reported previously (Agarwal et al., 2007a). Moreover, such inefficiency in apical peptide transporters might be more significant than that in basolateral peptide transporters, as the difference of Gly-Sar transport between wild-type versus transfected cell lines on AP-BL direction seems to be much more than that on BL-AP direction. All human efflux transporter genes are transfected on apical membrane of MDCK cells, thus function of apical peptide transporters has attracted more attention in the present study. We assumed that the transfection of human *MDR1*, *MRP2*, and *BCRP* genes localized in the apical membrane of cells may affect the function of peptide transporters. Overexpression of efflux transporters at the apical cell membrane and their overriding activities may cause differential functional activities and inefficiency of endogenous peptide transporters in transfected MDCKII cell lines.

Expression levels of transfected genes are cell-passage-dependent, since transfected cells may lose the cDNA with ascending passage number. Previous research has reported that higher passaged MDCK-MDR1 cells showed lower levels of transfected human *MDR1* gene expression than lower passaged cells (Tang et al., 2002b). Thus cell-passage-

dependent effects on the determination of *transport efficiency* of apical peptide transporters were investigated in various MDR genes-transfected MDCKII cell lines. All transfected cell lines demonstrated markedly reduced translocation efficiency for Gly-Sar apical uptake (Figure 16). Interestingly, this functional inefficiency was found to be clearly passage-dependent, since disparity in transport efficiency between intact and transfected cells attenuated with increasing cell passage. Lower Gly-Sar transport efficiency in transfected cell lines is possibly associated with a corresponding lower expression level of peptide transporters, which might be the results of down-regulation by highly-expressed robust efflux genes. When expression of these robust transporters diminishes, the down-regulatory effect also ceases. This assumption is well substantiated by the results of mRNA determination using real-time RT-PCR assay and subsequent protein expression by Western blot analysis.

Expression of transfected human genes decreases quickly as cell passage increases (Figure 18). P-gp- overexpressed cells exhibited a faster diminishing than MRP2 and BCRP expression levels. This is possibly due to differential transfection stability with different genes. Conversely, expression of both peptide transporters PepT1 and PepT2 present on apical membrane of various transfected MDCK II cell lines has been raised progressively with apical Gly-Sar gradually enhanced uptake along with increasing cell passage in various transfected cells (Figure 16). Additionally, a more significant enhancement in c*PepT2* gene expression over c*PepT1* was obtained in all three transfected cell lines. Such inverse correlation between endogenous influx genes and transfected efflux genes suggests that highly active exogenous efflux transporters may influence the expression and function of endogenous peptide transporters. This

assumption has been further confirmed by the results of Western blot analysis (Figure 20). Whether this inverse relationship between alien gene and endogenous gene is an adaptation to maintain cellular concord or domination of MDR gene to protect the cells from toxicity is yet to be completely established.

Our study clearly demonstrates that transfected efflux robust genes dominate over endogenous influx transporters. The molecular mechanism of such interaction between transporters is yet to be elucidated. One explanation is that transfected exogenous genes may compete with the endogenous genes for binding sites on transcription factors or transcriptional coactivator and corepressor complexes. Recent studies have shown that transcription factors, Sp1 binding sites play a decisive role in the basal expression of *MDR1* (human), *MRP2* (rat), *BCRP* (human) and *PepT1* (human) (Cornwell and Smith, 1993; Kauffmann et al., 2001; Shimakura et al., 2006; Takakura et al., 2010; Zhang et al., 2012). Competition with highly-expressed exogenous genes might trigger the down-regulation of endogenous gene expression in these cells. Transfection of h*MDR1* in MDCKII cells can cause negative feedback and trigger down-regulation of endogenous *Mdr1* (Kuteykin-Teplyakov et al., 2010). This down-regulation of endogenous mRNA as well as protein expressions by exogenous gene transfection such as *hMDR1* vs. *Mdr1* has also been reported by the previous studies, which indicated a feedback-regulatory mechanism from endogenous gene/transcription factor to maintain cellular milieu (Lloyd et al., 1992). The fundamental difference of our work is that we have demonstrated the interplay between two unrelated genes i.e. *hMDR1/ hMRP2*/ *hBCRP* vs. *PepT* (canine) controlling efflux of xenobiotics and nutrients respectively which was unknown before.

The understanding of transporters crosstalk between divergent proteins is critical for developing new peptidomimetics.

# CHAPTER 4

# SYNTHESIS OF STEREOISOMERIC AMINO ACID AND DIPEPTIDE PRODRUGS OF SAQUINAVIR

## Rationale

Saquinavir (SQV) is the first HIV-protease inhibitor marketed for the treatment of AIDS in the United States. Although SQV has been reported for its potent activity against HIV, its therapeutic efficacy is limited in clinical application due to some undesirable properties like poor aqueous solubility as well as high affinity for efflux transporters and metabolic enzymes (Kim et al., 1998a; Plosker and Scott, 2003). In order to overcome these pharmaceutical and physicochemical barriers and improve absorption following oral administration, "transporter-targeted prodrugs" have been developed as an attractive strategy. In comparison with classical prodrugs, which represent a nonspecific chemical promoiety attached to the active parent drug by a covalent linker, targeted prodrugs approach is designed to target specific endogenous transporters to facilitate epithelial transport of these compounds (Han and Amidon, 2000; Yang et al., 2001; Rautio et al., 2008). Following the translocation across cellular membrane, the prodrug could be cleaved by hydrolytic enzymes specifically to regenerate the active parent drug.

Recent advances in transporter-targeted drug delivery indicated that peptide transporters, primarily expressed in the small intestine and kidney, are attractive targets for prodrug design because they have broad substrate specificity and high capacity, especially for smaller peptides *i.e.* di and tripeptides (Ganapathy and Leibach, 1996; Leibach and Ganapathy, 1996; Steffansen et al., 2004). On the basis of these findings, "peptidomimetic" prodrugs are designed by conjugating parent drug to small peptides.

Such prodrugs could be recognized easily by the peptide transporter-mediated influx system and ferried across the epithelial membrane (Ganapathy et al., 1995). Additionally, structure modification reduces the interaction of the parent drug with efflux transporters such as P-glycoprotein (P-gp) and multidrug resistance-associated protein (MRP). Therefore enhanced cellular permeation could be achieved by the cumulative effects of reducing secretion by efflux transporters and increasing absorption by influx transporters.

Several peptide prodrugs of PIs have been synthesized successfully. Valine-valine and glycine-valine prodrugs derived from SQV have also exhibited 4.6- and 1.8- fold enhanced absorption relative to parent drug in rat jejunum, respectively (Jain et al., 2007). Also it has been reported previously that different stereoisomers of chiral drug molecules possess different biological properties (Siccardi et al., 2003; Wang et al., 2010). These encouraging findings prompted us to extend the study of valine-valine-SQV with its stereoisomeric configuration.

In this chapter, four stereoisomeric dipeptide prodrugs derived from SQV including *L*-valine-*L*-valine-SQV (LLS), *L*-valine-*D*-valine-SQV (LDS), *D*-valine-*L*-valine-SQV (DLS) and *D*-valine-*D*-valine-SQV (DDS) and two amino acid prodrugs *L*-valine-SQV (LS) and *D*-valine-SQV (DS) were synthesized and purified, and their structures were identified using mass spectrography and $^{1}$H NMR. Furthermore, the quantitative dermination methods including HPLC and LC-MS/MS were developed in this chapter.

## Materials and Methods

### Materials

SQV mesylate salt was kindly donated by Hoffmann-La Roche. All chemicals and solvents were purchased from Sigma Chemical Co. (St. Louis, MO) or Fisher Scientific Co. (Pittsburgh, PA), and all chemicals were products of special reagent grade and used as such.

**Synthesis of SQV Prodrugs**

Stereoisomeric dipeptide prodrugs (valine-valine-SQV) were prepared from amino acid prodrugs (valine-SQV) following the published procedure with slightly modifications (Jain et al., 2005). The synthetic procedure of valine-valine-SQV is shown in Figure 22 and 23. All the reactions were performed under anhydrous condition and protected by nitrogen. All chemicals were dessicated before reaction and anhydrous solvents were used.

**Synthesis of Amino Acid Prodrugs of SQV**

Stereoisomeric valine-SQV was synthesized in two steps: Conjugating SQV with N-Boc-(*L*)-valine or N-Boc-(*D*)-valine, and then deprotection of amino protecting group N-Boc. 280 mg N-Boc-(*L*)-valine or N-Boc-(*D*)-valine (1.30 mmol) and 390 mg dicyclohexylcarbodiimide (DCC, 1.95 mmol) were dissolved into 5 ml of dichloromethane (DCM) and stirred for 1 h on ice-bath (mixture A). In another round bottom flask, several drops of dry triethylamine (TEA) was added to 500 mg SQV (0.65 mmol), then a proper amount of DCM with 240 mg dimethylamino pyridine (DMAP, 1.95 mmol) were added until all SQV dissolved after 10-minute stirring (mixture B). Mixture A was removed from ice bath, and mixture B was added dropwise into mixture

A at room temperature while continually stirring the mixture for 24 h. Reactions were monitored with Mass Spectra to ensure complete conversion of the starting compounds to intermediates SQV-(*L*)-val-Boc or SQV-(*D*)-val-Boc. The intermediates were purified using silica column chromatography (Silica gel 60 Geduran®, 40-63 μm) with hexane and ethyl acetate (3:7) as eluent. The deprotection of the N-Boc protecting group was achieved using 10 ml of DCM and trifluoroacetic acid (TFA) (1:1) at 0 ℃ for 2.5 h to get final *L*-val-SQV or *D*-val-SQV (mono-TFA salt). Crude products were purified by recrystallization using cold diethyl ether and dried in Speed Vac (SPD101B, Savant Instruments INC, Holbrook, NY) until the weight was constant. Synthesis process of DS is shown in Figure 22.

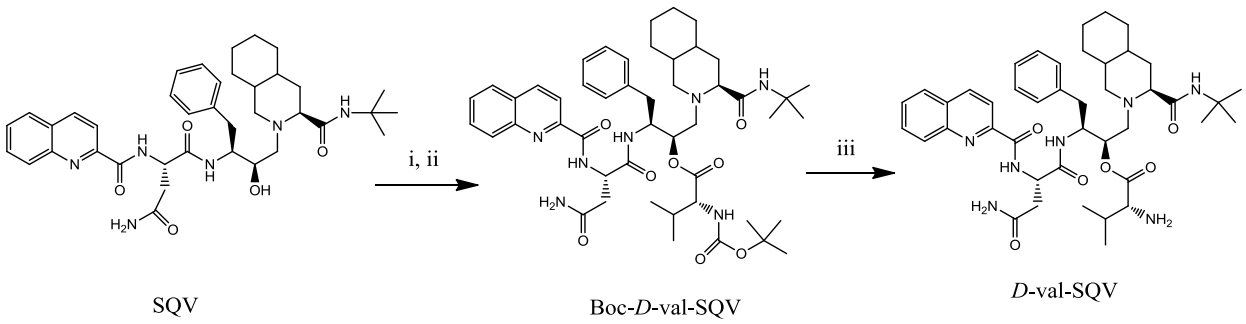


Figure 22. Synthesis process of *D*-valine-saquinavir (DS).

Reagents and conditions: (i) Boc-*D*-valine-OH, DCC, DCM, $N_2$, 0°C, 1 hour; (ii) TEA, DMAP, DCM, $N_2$, RT, 24 hours; (iii) TFA/ DCM (1:1), 0°C 2.5 hours.

**Synthesis of Dipeptide Prodrugs**

Dipeptide prodrugs were synthesized using the similar procedure described above. The starting material was 570 mg stereoisomeric valine-SQV conjugate (0.65 mmol),

which was treated with 2 ml of TEA instead of DMAP, and the reaction was conducted at room temperature for 24 h. Intermediates N-Boc-valine-valine-SQV were purified using silica gel 60 column with MeOH/DCM (3:97) as eluent. Synthesis process of LDS is shown in Figure 23.

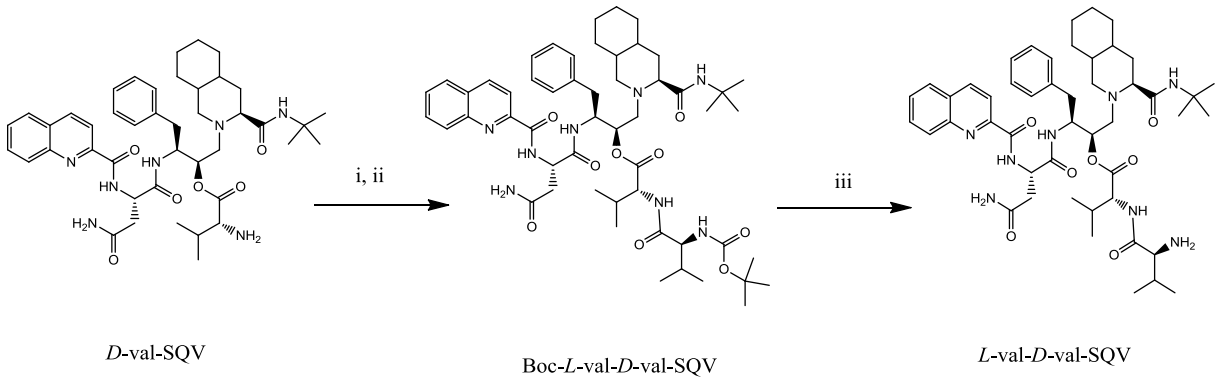


Figure 23. Synthesis process of *L*-valine-*D*-valine-saquinavir (LDS).

Reagents and conditions: (i) Boc-*L*-valine-OH, DCC, DCM, $N_2$, 0°C, 1 hour; (ii) , TEA, DCM, $N_2$, RT, 24 hours; (iii) TFA/ DCM (1:1), 2.5 hours.

**Identification of Prodrugs**

Structure and purity of reaction intermediates and final compounds were confirmed by Mass Spectrography and $^1$H NMR. $^1$H NMR was carried out using a Varian-400MHz NMR spectrometer.

**Quantitative Analysis**

HPLC

All samples, SQV and prodrugs, for *in vitro* studies were analyzed by HPLC chromatography with a reversed Luna C-8 column (250mm×4.6mm, 5 μm; Phenomenex, Torrance, CA). The HPLC system included HP 1050 pump, Waters dual wavelength absorbance UV detector, and an Alcott HPLC autosampler 718AL. Mobile phase was composed of acetonitrile/water/triethylamine (60:39:1, v/v/v), and pH in aqueous phase was adjusted to 6.50 with *o*- phosphoric acid. Detection wavelength was set to 240 nm, and flow rate of mobile phase was 1.0 ml/min.

LC-MS/MS

QTrap® LC-MS/MS mass spectrometer (Applied Biosystems, Foster City, CA) equipped with Agilent 1100 Series quaternary pump (Agilent G1311A), vacuum degasser (Agilent G1379A) and autosampler (Agilent G1367A, Agilent Technology Inc., Palo Alto, CA) was utilized to analyze SQV and prodrug samples. The detection was operated in multiple-reaction monitoring (MRM) mode. The precursor and the product ion generated for SQV, valine-SQV, and valine-valine-SQV are 671.4/570.3, 770.5/367.2, and 869.5/367.2, respectively. Samples were prepared using liquid-liquid extraction technique with ice-cold *tert*-butyl methyl ether. Verapamil (200 nM) was employed as an internal standard. Relative extraction efficiency for SQV and its prodrugs were around 70%. Samples reconstituted in distilled deionized water with 0.05% cremophor EL were loaded onto a Luna C-18 column (100×2.0 mm, 3 μm; Phenomenex Torrance, CA) and eluted with acetonitrile/water (40:60) in presence of 0.1% formic acid at a flow rate of 0.2 ml/min.

## Results

### Synthesis of SQV Stereoisomeric Prodrugs

The final amino acid and dipeptide prodrugs were obtained as white powder with a yield of 85% and 80%, respectively (calculated from SQV). Three-dimensional structures of obtained dipeptide and amino acid prodrugs are showed in Figure 24.

### Identification of Prodrugs

Structure and purity of reaction intermediates and final compounds were confirmed by Mass Spectrography (DS in Figure 25 and DLS in Figure 26) and $^{1}$H NMR.

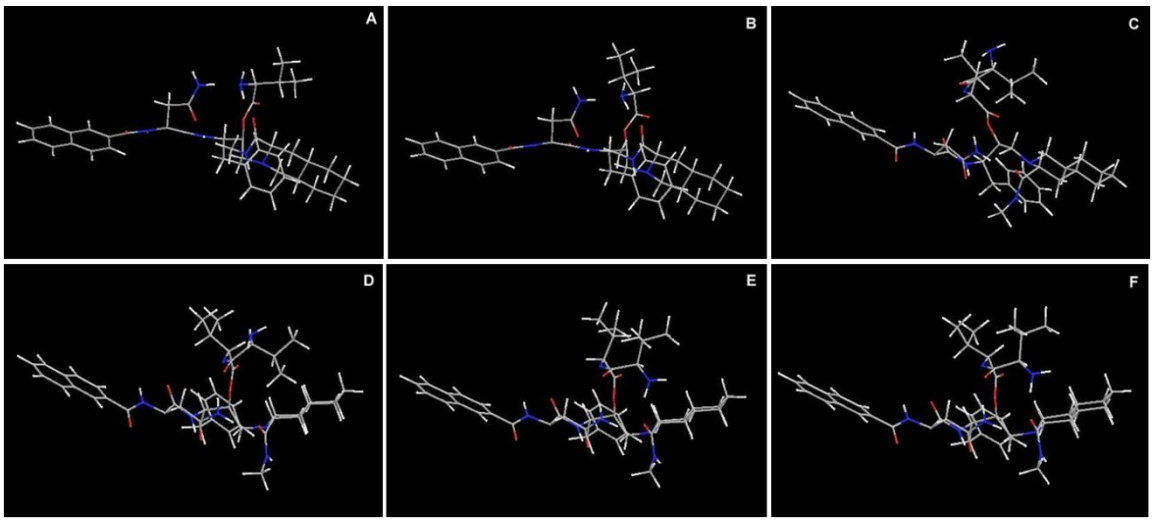


Figure 24. Structures of saquinavir stereoisomeric prodrugs

A. *L*-valine-saquinavir (LS)
B. *D*-valine-saquinavir (DS)
C. *L*-valine-*L*-valine-saquinavir (LLS)
D. *L*-valine-*D*-valine-saquinavir (LDS)
E. *D*-valine-*L*-valine-saquinavir (DLS)
F. *D*-valine-*D*-valine-saquinavir (DDS)

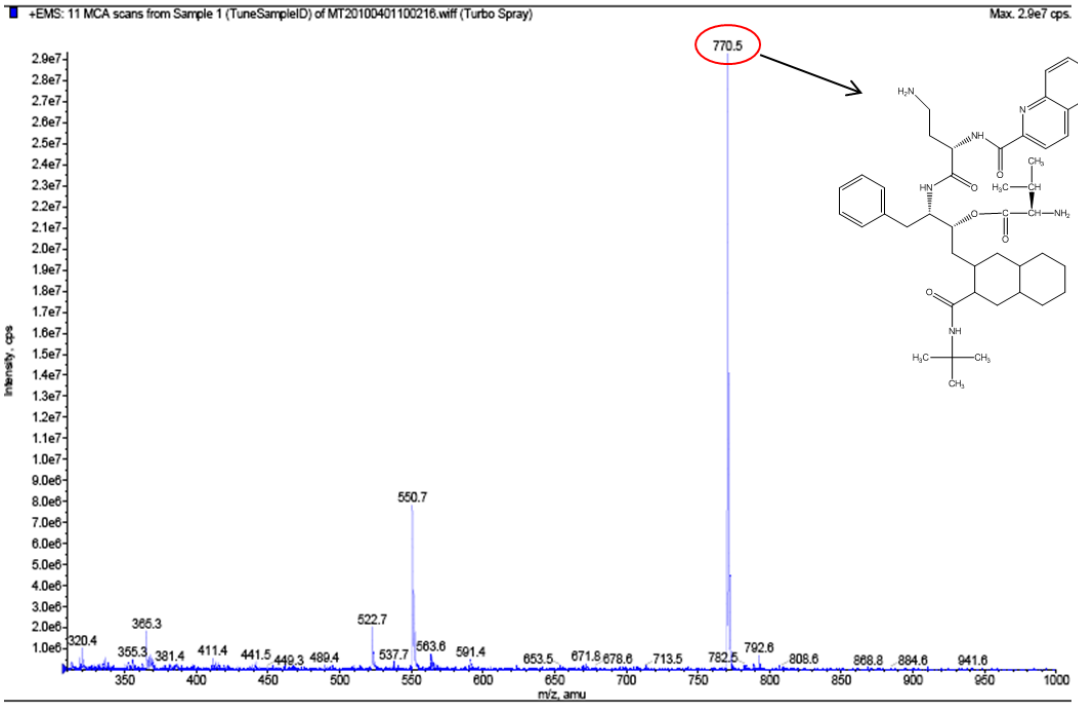


Figure 25. Mass spectrometry of *D*-valine-SQV (DS)

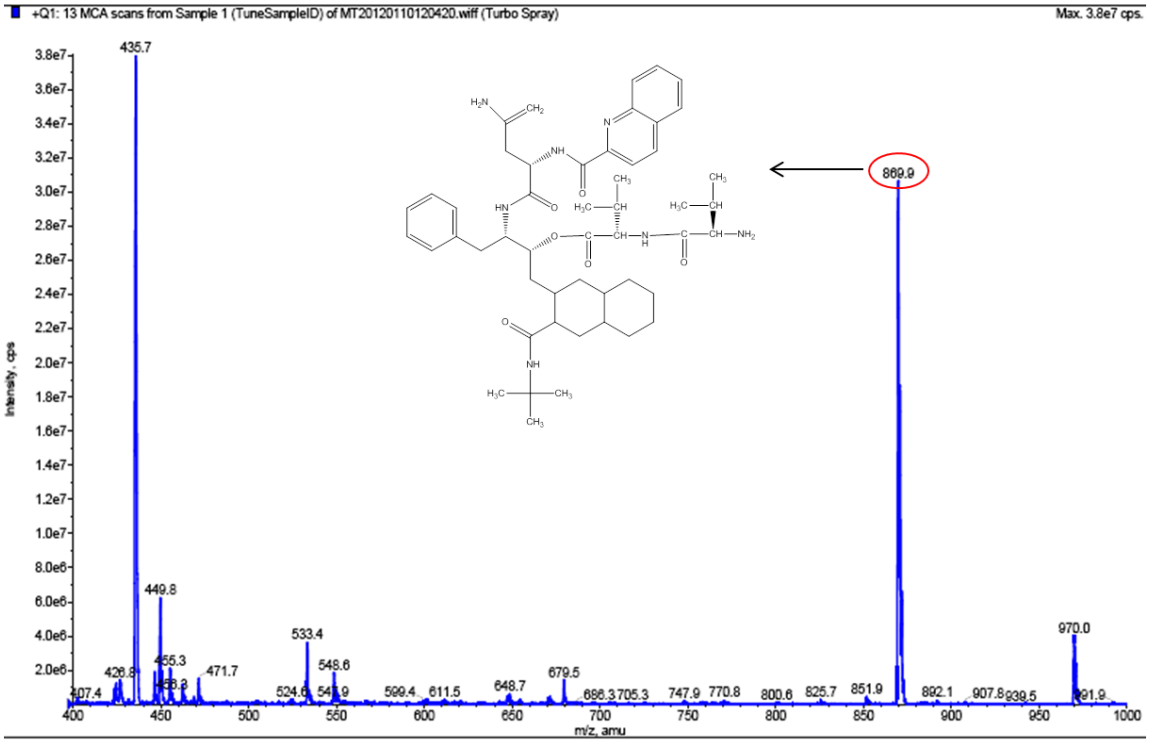


Figure 26. Mass spectrometry of *D*-valine- *L*-valine-SQV (DLS)

***D*-val-SQV**: LC/MS(M/z): 770.1; $^{1}$HNMR (DMSO-d6): δ 0.99 – 1.04 (m, 6H), 1.30 (s, 9H), 1.35- 1.36 (m, 1H), 1.52 – 1.57 (m, 2H), 1.64 – 1.67 (m, 4H), 1.71-1.97 (m, 4H), 2.24 – 2.29 (m, 2H), 2.56 – 2.73 (m, 3H), 2.84 – 2.89 (m, 2H),3.13 – 3.15 (m, 3H), 3.24 – 3.51 (m, 1H), 3.97(brs, 1H), 4.47 – 4.49 (m, 1H), 4.74 – 4.80 (m, 1H), 5.35 – 5.59 (brs, 1H), 6.96 – 7.01 (m, 1H), 7.08 – 7.10 (m, 3H), 7.24 – 7.25 (m, 2H), 7.58 (brs, 1H), 7.73 – 7.77 (m, 1H), 7.87 – 7.91 (m, 1H), 8.11 – 8.23 (m, 4H), 8.43 (brs, 3H), 8.60 – 8.62 (d, J = 8Hz 1H), 8.83 – 8.85 (d, J = 8Hz, 1H).

***L*-val-SQV**: LC/MS(M/z): 770.4; $^{1}$HNMR (DMSO-d6): δ 8.89 (d, 1H), 8.52 (m, 1H), 8.42 (bd, 4H), 8.21 (d, 2H), 8.08 (m, 1H), 7.86 (m, 1H), 7.74 (m, 1H), 7.63 (bd, 2H), 7.01–7.20 (m, 5H), 5.52 (m, 1H), 4.83 (m, 1H), 4.58 (m, 1H), 3.85 (m, 1H), 3.26 (m, 1H), 2.3–2.74 (m, 7H), 1.59–1.99 (m, 13H), 1.36 (s, 9H), 1.06 (dd, 6H).

***L*-val-*D*-val-SQV**: LC/MS(M/z): 870.5; $^{1}$HNMR (DMSO-d6): δ 0.92 – 1.09 (m, 12H), 1.13 - 1.35 (m, 14H), 1.52 - 1.96 (m, 9H), 2.08 – 2.23 (m, 2H), 2.50 – 2.67 (m, 2H), 2.93 – 3.53 (m, 5H), 3.77 – 3.86 (m, 1H), 4.33 – 4.53 (m, 1H), 4.76 – 4.81 (m, 1H), 5.25 – 5.29 (brs, 1H), 5.59 – 5.61(brs, 1H), 6.96 – 7.08 (m, 4H), 7.16 (brs, 2H), 7.51 (brs, 1H), 7.73 – 7.77 (m, 1H), 7.87 – 7.92 (m, 1H), 8.11 – 8.19 (m, 7H), 8.61 - 8.64 (m, 2H), 8.88 (brs, 1H).

***D*-val-*L*-val-SQV**: LC/MS(M/z): 870.2; $^{1}$HNMR (DMSO-d6): δ 0.87 – 0.99 (m, 12H), 1.15 - 1.33 (m, 14H), 1.38 - 1.99 (m, 8H), 2.15 – 2.23 (m, 2H), 2.64 – 2.71 (m, 3H), 3.23 – 3.41 (m, 3H), 3.84 – 4.05 (m, 2H), 4.36 – 4.38 (m, 1H), 4.49 – 4.53 (m, 2H), 4.74 – 4.78 (m, 1H), 5.46 – 5.49 (brs, 1H), 7.02 – 7.22 (m, 6H), 7.54 (brs, 1H), 7.73 – 7.77 (m, 1H), 7.88 – 7.91 (m, 1H), 8.02 – 8.18 (m, 7H), 8.60 – 8.69 (m, 2H), 8.80 – 8.82 (brs, 1H).

***D*-val-*D*-val-SQV**: LC/MS(M/z): 870.3; $^{1}$HNMR (DMSO-d6): δ 0.89 – 0.99 (m, 12H), 1.19 - 1.30 (m, 14H), 1.50 - 1.73 (m, 9H), 2.08 – 2.24 (m, 2H), 2.62 – 2.65 (m, 2H), 3.30 – 3.45 (m, 5H), 3.79 – 3.87 (m, 1H), 4.33 – 4.41 (m, 1H), 4.75 – 4.80 (m, 1H), 5.28 – 5.34 (brs, 1H), 5.51 – 5.61(brs, 1H), 6.96 – 7.08 (m, 4H), 7.21 (brs, 2H), 7.45 (brs, 1H), 7.73 – 7.77 (m, 1H), 7.87 – 7.91 (m, 1H), 8.10 – 8.19 (m, 7H), 8.58 - 8.62 (m, 2H), 8.82 (brs, 1H).

***L*-val-*L*-val-SQV**: LC/MS (M/z)870.4; $^{1}$HNMR (DMSO-d6): δ 8.78 (d, 1H), 8.62 (m, 1H), 8.19 (d, 2H), 8.10 (bd, 6H), 7.87 (m, 1H), 7.74 (m, 1H), 7.39 (bd, 2H), 6.95–7.05 (m, 5H), 5.24 (m, 1H), 4.83 (m, 1H), 3.77 (m, 5H), 1.81–3.01 (m, 21H), 1.28 (s, 9H), 0.94 (m, 12H).

**Quantitative Analysis**

HPLC

Retention time and quantitative limit for each prodrugs using HPLC analysis method are summarized in Table 5. Four stereoisomeric SQV dipeptide prodrugs showed varied retention times (8.09 min - 9.21 min) after injection into HPLC system. Similarly, two amino acid SQV prodrugs, LS and DS, also exhibited differential retention time, which is 7.62 min and 7.23 min, respectively. These results indicate that the observed prodrugs with same molecular formula and molecular weight have different spatial structure.

LC-MS/MS

The precursor and product ion generated for SQV, valine-SQV (VS), and valine-valine-SQV (VVS), and quantitative limit for each prodrugs using LC-MS/MS method

are summarized in Table 6. Results in the present study indicate that sensitivity of LC-MS/MS is much higher than HPLC.

Table 5. Parameters of HPLC analysis method for the dermination of SQV stereoisomeric prodrugs.

| | Retention time (min) | Lower limit of quantification (μM) |
|---|---|---|
| SQV | 5.32 | 0.2 |
| Dipeptide prodrugs | | |
| LLS | 8.71 | 0.5 |
| LDS | 8.40 | |
| DLS | 9.21 | |
| DDS | 8.09 | |
| Amino acid prodrugs | | |
| LS | 7.62 | 0.5 |
| DS | 7.23 | |

Table 6. Parameters for LC-MS/MS analysis method.

| | SQV | VS | VVS |
|---|---|---|---|
| Q1/Q3 | 671.4/570.3 | 770.6/367.3 | 869.7/266.3 |
| Lower limit of quantification (nM) | 1 | 5 | 20 |

## Discussion

In the present chapter, various SQV prodrugs conjugated with stereoisomeric amino acid valine or dipeptide valine-valine were synthesized successfully. Moreover, HPLC and LC-MS/MS analysis methods were developed for quantitative determination of the observed prodrugs.

# CHAPTER 5

# PHYSICOCHEMICAL PROPERTIES AND *IN VITRO* EVALUATION

## Rationale

Recent advances in transporter-targeted drug delivery indicated that "peptidomimetic" prodrugs could be recognized easily by the peptide transporter-mediated influx system and ferried across the epithelial membrane (Ganapathy et al., 1995). Moreover, structure modification reduces the interaction of the parent drug with efflux transporters. Therefore enhanced cellular permeation could be achieved by the cumulative effects of reducing secretion by efflux transporters and increasing absorption by influx transporters.

It has been reported that different stereoisomers of chiral drug molecules possess different biological properties (Siccardi et al., 2003; Wang et al., 2010). Stereoisomers are molecules that are identical in atomic constitution and bonding, but differ in the three-dimensional arrangement of the atoms. Conjugates attached with different stereoisomeric promoieties could be featured with various physicochemical and biological properties. Most amino acids currently applied in prodrug strategy are *L*-isomers. Major advantages to *L*-configurations include their natural occurrence in the body, as well as their rapid and specific recognition by peptide transporters (Pochopin et al., 1994; Sawada et al., 1999). *In vitro* permeability studies on *L*-valyl, *L*-leucyl, and *L*-phenylalanyl ester conjugates of indinavir and saquinavir demonstrated an increased translocation across Caco-2 cell monolayers (Fountoulakis and Suter, 2002). However, most *L*-isomeric derivatives have limited chemical or enzymatic stability (Pochopin et al., 1994; Talluri et al., 2008). In contrast, *D*-amino acid prodrugs of dapsone exhibited much better resistance to enzymatic hydrolysis and showed a longer residence time *in vivo* (Pochopin et al., 1994).

These findings give us strong support for studying stereoisomeric peptide prodrugs of SQV.

In this chapter, we provided a comparison of physicochemical and biological properties of SQV prodrugs synthesiszed in last chapter, including aqueous solubility, *in vitro* cytotoxicity, as well as chemical and enzymatic stability with respect to hydrolysis under physiological conditions. Affinities for specific proteins like efflux pumps (P-gp and MRP2) and influx peptide transporters, and permeability studies across *in vitro* cell monolayers have also been investigated here. Moreover, stereoselectivity in protein binding was evaluated in rat plasma in this study. The purpose of this screening is to select the most promising stereoisomeric dipeptide prodrug that could improve cellular permeation of parent drug SQV across intestinal barriers.

## Materials and Methods

### Materials

SQV mesylate was kindly donated by Hoffmann-La Roche. [$^{14}$C]Erythromycin (80 Ci/mmol) was obtained from American Radiolabeled Chemicals Inc. (St. Louis, MO). [$^{3}$H]glycylsarcosine ([$^{3}$H]Gly-Sar, 4Ci/mmol) was purchased from Moravek Biochemicals (Brea, CA). Madin-Darby canine kidney cells transfectant overexpressing hP-gp/MDR1 (MDCK-MDR1), hMRP2 (MDCK-MRP2), and wild type MDCK cells (MDCK-wt) were generously provided by Dr. P. Borst and Dr. A. Schinkel (The Netherlands Cancer Institute, Amsterdam, Netherland), respectively. Caco-2 and U937 cells were obtained from ATCC (Manassas, VA). TrypLE$^{TM}$ Express Stable Trypsin Replacement and Dulbecco's modified Eagle's Medium (DMEM) and RPMI-1640 were

obtained from Invitrogen (Carlsbed, CA). Fetal bovine serum (FBS) was purchased from Atlanta Biologicals (Lawenceville, GA). Sprague–Dawley rat plasma was purchased from Valley Biomedical Inc. (Winchester, VA). GF120918 was generously provided by GlaxoSmithKline Ltd. MK-571 was purchased from Biomol (Plymouth Meeting, PA). Triton X-100, HEPES, d-glucose and all other chemicals were purchased from Sigma Chemical Co (St. Louis, MO). Scintillation cocktail reagent was obtained from Fisher Scientific (Fair Lawn, NJ). BioRad protein estimation kit was obtained from BioRad (Hercules, CA). Transwell® inserts and 12-well tissue culture plates were purchased from Corning Costar Corp (Cambridge, MA). All chemicals were products of special reagent grade and used as such.

**Aqueous Solubility Study**

Generally 5 mg of compound was added to 2 ml of distilled deionized water in a 10 ml screw-capped glass tube. These tubes were shaken mechanically at 25 ℃ for 24 hrs. At the end of 24 hrs, the mixture was centrifuged at 12,500 rpm, 25 ℃ for 10 min. The supernatant was collected and filtered through 0.45 µm membrane (Nalgene syringe filter). The filtrate was appropriately diluted with water and drug concentration was measured with LC-MS/MS.

**Chemical Hydrolysis**

Chemical hydrolysis study of SQV prodrugs was determined in buffer over a pH range of 1.4 to 10.4. Buffers containing 50 mM of hydrochloric acid/ potassium chloride (pH 1.4), phthalate (pH 3.4 and 5.4) and phosphate (pH 7.4 and 10.4) were prepared for

this study and ionic strength was adjusted to 0.1 M. The pH was adjusted to within ±0.02 units of the target using hydrochloric acid or sodium hydroxide. Two hundred microliter of prodrug solution (230 μM) was incubated with 1.8 ml of buffers at 37 ℃ under various pH conditions for 48 hrs. Aliquot (100 μl) of samples was collected at predetermined time intervals and stored in −80 ℃ until future analysis by HPLC.

**Enzymatic Hydrolysis in Cell Homogenates**

Caco-2 cells were maintained in 75 $cm^2$ cell culture flasks for 21 days under same conditions as MDCK-MDR1 cells. Cells were isolated using a mechanical scraper after 3 times washing with DPBS (pH 7.4), and then were suspended in proper volumes of chilled water and homogenized using Multipro Variable Speed Homogenizer (DREMEL, Racine, WI) for 5 min on ice bath. Cell homogenates were centrifuged at 12,500 rpm, 4 ℃ for 10 min to remove debris, and supernatant was diluted properly to achieve a final protein concentration of 0.3 mg/ml. Protein content was determined according to the method of Bradford using BioRad protein estimation kit. Cell homogenates were warmed up at 37 ℃ for 15 min before stability studies. 1.8 ml of cell homogenate with 200 μl of prodrug solution (final concentration 23 μM) was incubated at 37˚C in a shaking water bath (60 rpm) for 3 hrs. Samples (100 μl) were collected at predetermined time intervals and an equal volume of ice-cold acetonitrile: methanol (5:4) mixture was added to stop the enzymatic hydrolysis. Samples were stored at −80˚C until further analysis by HPLC.

**Cell Culture**

MDCK-wt cells, MDCK-MDR1 cells (passages 5-12) and MDCK-MRP2 cells (passages 5-25) were maintained following the method in Chapter 3. Human leukemic monocyte lymphoma cell line U937 were maintained in suspension culture in RPMI-1640 supplemented with 10% (v/v) heat-inactivated FBS, 2 mM l-glutamine and 10 mM HEPES, at 37 ℃ in a humidified atmosphere of 5% $CO_2$.

**Cytotoxicity Assay**

Cellular toxicity study was performed using LDH Cytotoxicity Detection Kit (Takara Bio Co. St Louis, MO) on MDCK-wt cells. Cell suspension (200 µl/well) was added in the 96-well tissue culture plate at the density of 10,000 cells/well, and then incubated at 37 ℃, 5% $CO_2$ and 90% humidity. The medium was aspirated after 12 hours-postseeding, and 200 µl of assay medium (serum-free DMEM) with different concentrations (0−150 µM) of SQV or prodrugs was added to each well. Positive control (1% Triton X-100 in assay medium), negative control (only assay medium) and background control (assay medium in the wells without cells) were also evaluated at the same time. After 24 hours-incubation, 100 µl/well of supernatant was carefully transferred into corresponding wells of an optically clear 96-well flat bottom microtiter plate (MTP). Then 100 µl of dye mixture solution from LDH Cytotoxicity Detection Kit was added into each well and incubated for 20 min. Absorbance of the solutions was measured at 450 nm using DTX 880 Multimode Detector (Beckman Coulter, Brea, CA) and the LDH release was calculated in each of the drug treated wells and was compared with the control.

**Uptake Studies**

Cellular accumulation of SQV and prodrugs in MDCK-MDR1 and MDCK-MRP2 cells were conducted following the procedures in Chapter 3. U937 cells grown in RPMI 1640 with 10% (v/v) FBS were added into 1.5 ml centrifuge tube at the cell density of $4\times10^6$ cells/ml. Cells were then washed twice with DPBS (pH7.4) at 37°C. Uptake was initiated by addition of 10 μM of SQV and its prodrugs in above DPBS. After 30 min incubation at 37°C, drug uptake was terminated by rinsing the cells three times with ice-cold stop solution (200 mM KCl and 2 mM HEPES) followed by cell disruption with water at -80°C for 30 min. Cellular drug uptake was determined by LC-MS/MS and then was normalized by amount of protein measured using BioRad protein estimation kit in each tube.

**Transport Studies**

Drug transport across MDCK-MDR1 and MDCK-MRP2 cell monolayers were conducted following the procedures in Chapter 3.

**Determination of Protein Binding in Rat Plasma**

The protein binding of SQV and its stereoisomeric prodrugs in rat plasma were determined using ultra-filtration technique reported previously (Boffito et al., 2002). Briefly, stock solutions (100 μl) of SQV or prodrugs in isotonic phosphate-buffered saline (IPBS), pH 7.4, containing 8 g/L NaCl, 0.2 g/L KCl, 1.44 g/L $Na_2HPO_4$, and 0.24 g/L $KH_2PO_4$, were added into 900 μl blank rat plasma to yield final concentrations of 0.5 μM. Equal volume of fresh IPBS (pH7.4) replaced drug solutions to be used as control to evaluate non-specific adsorption and plasma binding. During the 30 min-equilibration at

37°C, spiked plasma samples were agitated gentlely every 10 min. Then 500 µl samples were transferred to Amicon ultra-0.5ml centrifugal filters (10 k NMWL, Millipore Corporation, Bedford, MA) and centrifuged at 10,000 ×g, 37°C, for 1 h. Around 250 µl of ultra-filtrate containing the unbound drug was obtained in basolateral chamber. After centrifugation, aliquots of filtered (200 µl) and unfiltered (20 µl, diluted with IPBS to 200 µl) samples were taken and analyzed using LC-MS/MS immediately to calculate protein binding of drugs in rat plasma. Unbound fraction ($f_u$) was calculated by the ratio of drug in the filtered samples to the sum of filtered and unfiltered samples.

**Sample Preparation and Analysis**

SQV and its prodrugs were analyzed by HPLC and LC-MS/MS which are described in Chapter 4. Samples for LC-MS/MS were prepared using liquid-liquid extraction technique. Briefly, 200 µl samples were added to 10 µl of internal standard (4 µM verapamil) and 400 µl of ice-cold *tert*-butyl methyl ether. All samples were vortexed for 2 min to extract the drug from the aqueous to organic phase. Then 300 µl of *tert*-butyl methyl ether was decanted and dried in vacuo (DD-4X GeneVac, Gardiner, NY). The residue was reconstituted in 70 µl of deionized distilled water containing 0.05% (v/v) cremophor EL. Subsequently 40 µl of reconstituted extract was injected onto a LC-MS/MS system for analysis. Relative extraction efficiency for SQV and its prodrugs was around 70%.

**Data and Statistical Analysis**

Apparent permeability coefficients $P_{app}$ (cm/s) were calculated by linear regression analysis on the time course plot of amount of drugs transported across cell monolayers.

$$P_{app} = \frac{TR_{cum}/dt}{C_0 \times A}$$

Where $TR_{cum}/dt$ is the flux rate of (pro)drug obtained from the slope of transport profile. *A* is the surface area of cell monolayers. $C_0$ is initial concentration of (pro)drug in the donor chambers.

All experiments were conducted at least in triplicate and repeated independently three or four times. The results were expressed as mean ± SD. Statistical significance was detected using Student's *t*-test. Difference between mean values was considered statistically significant at $p < 0.05$ and very statistically significant at $p < 0.01$.

## Results

### Apparent Aqueous Solubility

Results of the solubility study presented in Table 7 demonstrate that all stereoisomeric dipeptide prodrugs improved aqueous solubility over parent drug SQV (mesylate salt) to a certain extent. Solubilities of LLS, LDS, DLS and DDS were dramatically greater than that of SQV mesylate by around 2.8, 2.7, 2.6 and 2.5-fold, respectively. Amino acid prodrugs also displayed significant increase in aqueous solubility relative to SQV.

Table 7. Apparent aqueous solubility of SQV and its stereoisomeric prodrugs

| | Apparent aqueous solubility (mg/ml) |
|---|---|
| SQV (mesylate salt) | $1.34 \pm 0.22$ |
| Dipeptide prodrugs | |
| LLS | $3.73 \pm 0.20^{**}$ |
| LDS | $3.65 \pm 0.47^{**}$ |
| DLS | $3.52 \pm 0.27^{**}$ |
| DDS | $3.34 \pm 0.45^{**}$ |
| Amino acid prodrugs | |
| LS | $2.81 \pm 0.12^{**}$ |
| DS | $2.70 \pm 0.10^{**}$ |

Data represented are mean $\pm$ SD (n=4). ** $P < 0.01$ compared with SQV (mesylate salt).

**Chemical Hydrolysis in Buffer**

Effect of pH on hydrolysis of the SQV prodrugs was evaluated within the pH range of 1.4 to 10.4. The half lives ($t_{1/2}$) of each prodrug were estimated by plotting the natural logarithm of prodrug concentrations *versus* time (Table 8). All prodrugs showed a gradient increase in susceptibility to hydrolysis as pH was raised from acidic (pH 1-5) towards basic conditions (pH 7-10). The hydrolysis data indicate that SQV dipeptide conjugates were chemically more stable in comparison to amino acid prodrugs at all the pH levels. Besides, DDS appears to be most stable compared to other dipeptide conjugates.

Table 8. Degradation half lives (h) for various SQV prodrugs at different pH conditions.

| | pH1.4 | pH3.4 | pH5.4 | pH7.4 | pH10.4 |
|---|---|---|---|---|---|
| LLS | 336.4 ± 23.7 | 203.2 ± 11.3 | 49.3 ± 0.9 | 10.4 ± 0.6 | 7.2 ± 0.2 |
| LDS | 357.2 ± 18.9 | 228.7 ± 23.5 | 55.0 ± 2.1 | 12.9 ± 1.4 | 8.0 ± 0.4 |
| DLS | 364.7 ± 21.2 | 242.3 ± 14.6 | 55.1 ± 4.3 | 16.0 ± 1.8 | 9.3 ± 0.2 |
| DDS | 412.5 ± 14.4 | 249.3 ± 16.3 | 63.1 ± 1.8 | 19.9 ± 1.1 | 11.8 ± 0.4 |
| LS | 30.2 ± 1.7 | 15.1 ± 1.1 | 5.0 ± 0.6 | 2.5 ± 0.3 | 1.9 ± 0.2 |
| DS | 43.3 ± 3.3 | 38.3 ± 3.6 | 6.9 ± 0.8 | 3.2 ± 0.2 | 2.3 ± 0.1 |

Data represented are mean ± SD (n=4).

**Enzymatic Hydrolysis in Cell Homogenates**

The concentration profile for SQV prodrugs in Caco-2 cell homogenates at pH 7.4 for a period of 3 h is depicted in Figure 27. Regeneration of valine-SQV and SQV demonstrates the role of esterase and peptidase enzymes in the metabolism process. Dipeptide prodrugs are more stable than amino acid prodrugs in Caco-2 cell homogenates. LLS appears the least enzymatically stable compared to the other three dipeptide prodrugs. The percentage of LLS remaining in 0.25 mg/ml cell homogenates after 3-hour incubation was around 35%, while more than 70% of DLS, DDS, and LDS were detected in the samples. Table 9 displays the estimated degradation rate constants and half-lives obtained from linear regression of pseudo-first-order plots of prodrug concentration *versus* time in cell homogenate. DDS exhibited the highest enzymatic stability with a half life of 12.6 h. LLS showed 7-fold less stability compared to DDS. LDS and DLS showed similar moderate stability in response to enzymatic hydrolysis in Caco-2 cell homogenates.

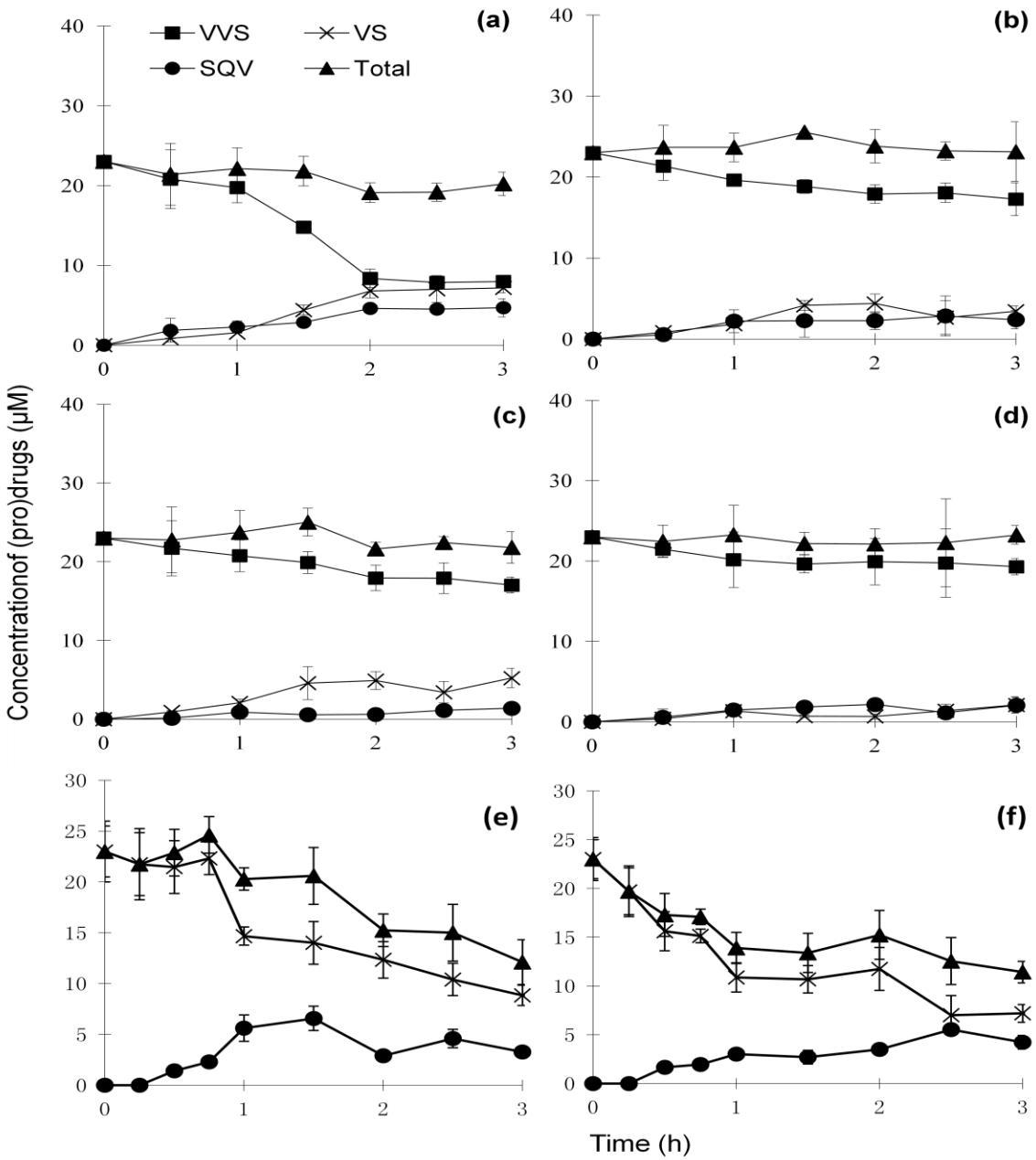


Figure 27. Degradation rate of SQV stereoisomeric dipeptide prodrugs (VVS, 23 μM) in 0.25 mg protein/ml Caco-2 cell homogenates and regeneration of relative amino acid prodrug (VS) and parent drug (SQV).

(a), LLS; (b), LDS; (c), DLS; and (d), DDS; (e), LS; and (f), DS. Each point represents mean ± SD (n=3).

Table 9. Degradation rate constants ($K_d$) and half lives ($t_{1/2}$) for various SQV prodrugs in 0.25 mg protein/ml Caco-2 cell homogenates.

| | $K_d$ ($h^{-1}$) | $t_{1/2}$ (h) |
|---|---|---|
| LLS | 0.4145 ± 0.0488 | 1.7 ± 0.2 |
| LDS | 0.0948 ± 0.0052 | 7.3 ± 0.4 |
| DLS | 0.0930 ± 0.0062 | 7.5 ± 0.5 |
| DDS | 0.0548 ± 0.0039 | 12.6 ± 0.9 |
| LS | 0.3060 ± 0.0322 | 2.3 ± 0.4 |
| DS | 0.2418 ± 0.0274 | 2.9 ± 0.3 |

Data represented are mean ± SD (n=3).

**Cytotoxicity Studies**

Lactate dehydrogenase (LDH) is a stable cytoplasmic enzyme present in most cells. It is released into cell culture medium upon damage of the cell membrane and could be detected to represent damage in cells. Results obtained after 24 hours-exposure of different amounts of SQV (pro)drugs (5 μM to 150 μM) to MDCK-wt cells are depicted in Figure 28. SQV and its prodrugs increased cellular toxicity in a concentration-dependant manner. In comparison to SQV, significantly less cellular toxicity was induced from prodrugs especially at higher concentrations. Two *D*-valine conjugate DDS displayed the least toxic on MDCK-wt cells at all concentration levels in this study.

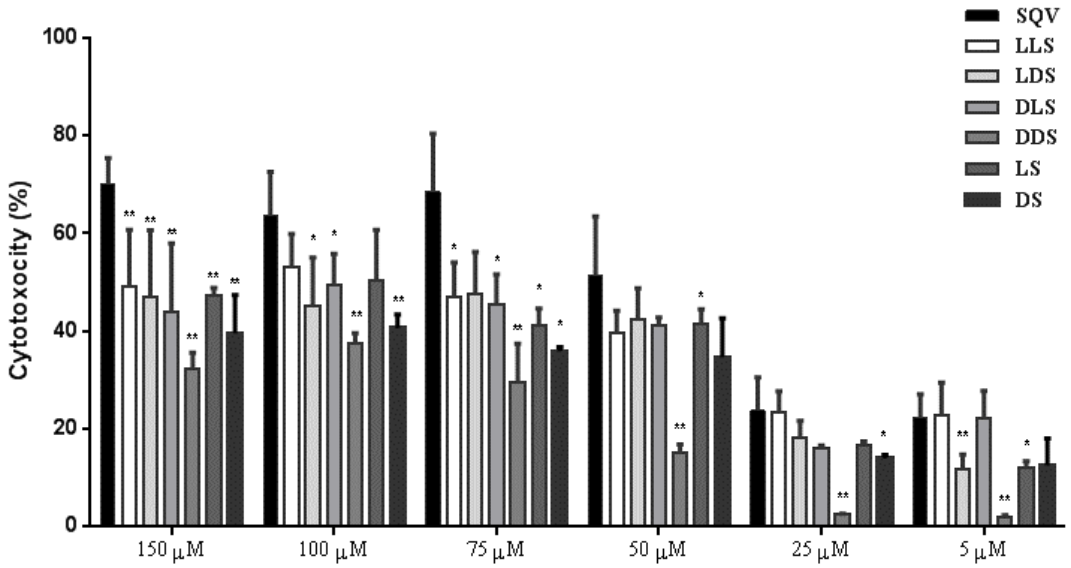


Figure 28. Cytotoxicity of SQV and stereoisomeric prodrugs after 24-hrs incubation on MDCK-wt cells.

Each point represents mean ± SD (n=4). *$P < 0.05$, and **$P < 0.01$ compared with SQV at same concentration.

**Affinity for Efflux Pumps**

Accumulation of [$^{14}$C]erythromycin (0.25 μCi/ml), a model substrate for both P-gp and MRP2, was determined in the presence of SQV or its peptide derivatives in MDCK cells to evaluate the affinity of prodrugs for P-gp or MRP2 efflux proteins. Results depicted in Figure 29 show that uptake of [$^{14}$C]erythromycin in MDCK-MDR1 cells in the presence of 75 μM of drugs were 286.7 ± 15.7% (SQV), 209.7 ± 10.0% (LLS), 214.9 ± 5.8% (LDS), 182.0 ± 17.5% (DLS), and 219.4 ± 8.7% (DDS), respectively. Similar results were also found in MDCK-MRP2 cells. Accumulation of [$^{14}$C]erythromycin was reduced significantly from 3-fold with SQV to less than 2-fold with various SQV stereoisomeric dipeptide prodrugs in both MDR1 and MRP2 cells.

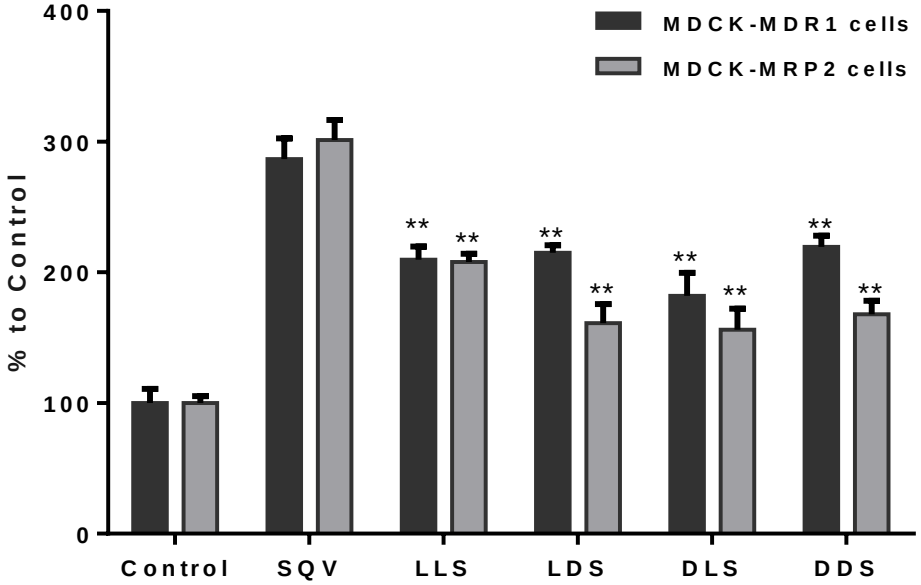


Figure 29. Uptake of [$^{14}$C]erythromycin (0.25 μCi/ml) in the absence (Control) or presence of 75 μM of SQV and its prodrugs in MDCK-MDR1 and MDCK-MRP2 cells. Each point represents mean ± SD (n=4). ***P*<0.01 compared with uptake of [$^{14}$C]erythromycin in the presence of SQV.

**Recognition by Peptide Transporters**

Gly-Sar is a good substrate for peptide transporters. Figure 30 shows that accumulation of [$^{3}$H]Gly-Sar was inhibited in the presence of 1 mM unlabeled Gly-Sar or 75 μM dipeptide (*L*-val-*L*-val) in both transfected MDCK cells. Dipeptide conjugates LLS, LDS, and DLS (75 μM) displayed significant inhibition to [$^{3}$H]Gly-Sar uptakes to the range of 65%-75% relative to control in MDCK-MDR1 cells, whereas SQV and DDS did not show any significant inhibition on [$^{3}$H]Gly-Sar uptake. Results in MDCK-MRP2 cells also exhibit similar inhibition effects on accumulation of [$^{3}$H]Gly-Sar. Percentage of

[$^3$H]Gly-Sar uptake observed for LLS, LDS, DLS, and DDS compared to the control was 73.4%, 72.3%, 73.9% and 94.5%, respectively.

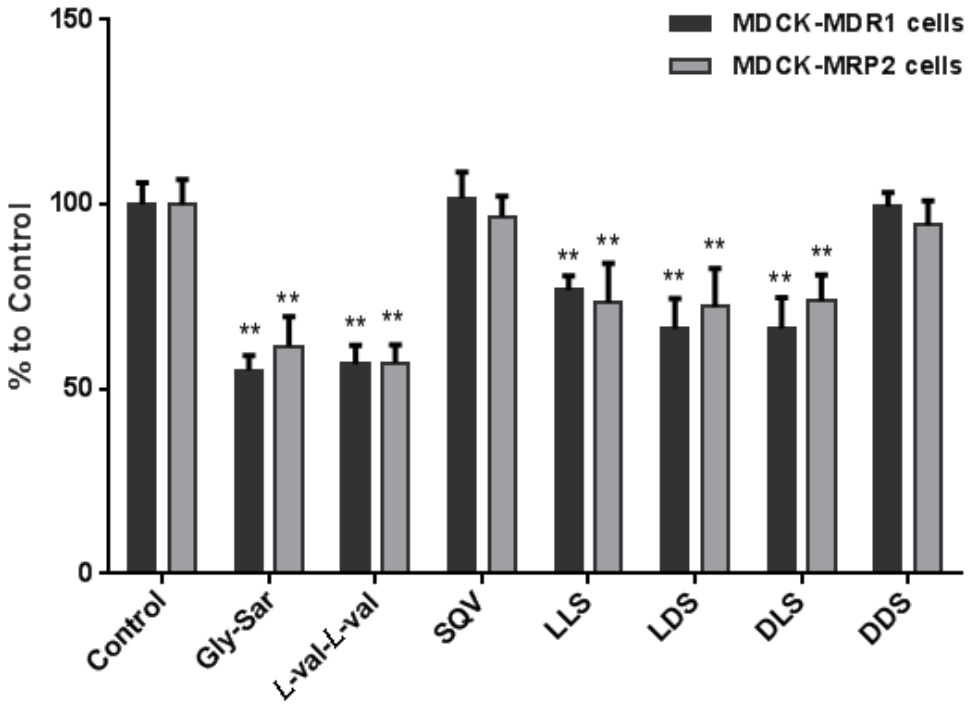


Figure 30. Uptake of [$^3$H] Gly-Sar (0.5 μCi/ml) in the absence (Control) or presence of unlabeled Gly-Sar (1 mM), *L*-val-*L*-val (75 μM), SQV (75 μM) or SQV prodrugs (75 μM) in MDCK-MDR1 and MDCK-MRP2 cells.

Each point represents mean ± SD (n=4). ** $P$<0.01 compared with control.

**Recognition by Human Leukemic Monocytes**

Human leukemic monocyte lymphoma cell line U937 was used in this study to compare cellular cumulation of SQV with its prodrug derivatives (10 μM) by lymphatic cells. Results in Figure 31 indicate that cellular uptake of amino acids prodrugs in U937 cells was about 90% of SQV. Dipeptide prodrugs showed slightly less monocytes uptake

than SQV. After 30 min incubation in U937 cells, cellular uptake of LLS, LDS, DLS, and DDS was observed to be 90.5±17.8%, 87.5±9.0%, 86.6±12.3%, and 78.6±11.2% of SQV, respectively.

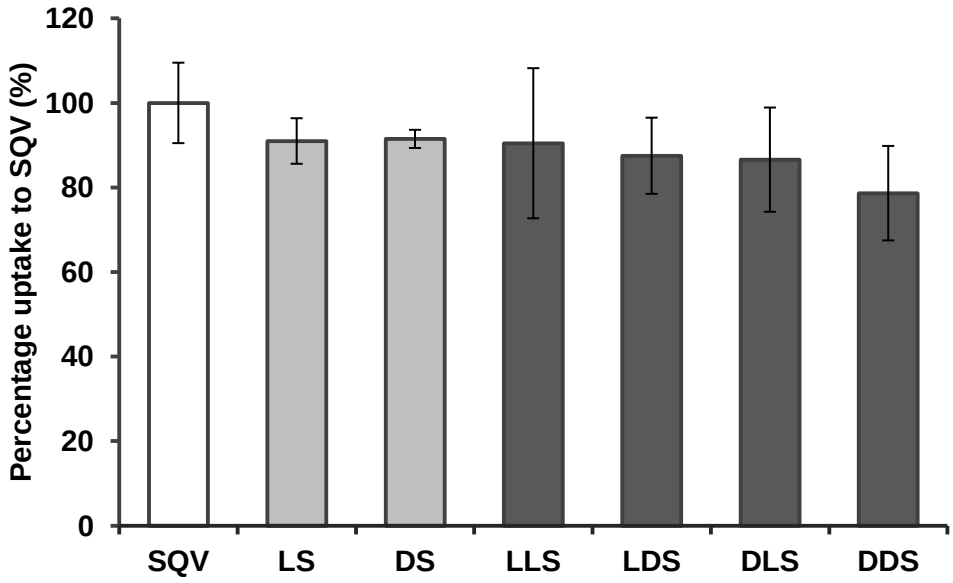


Figure 31. Uptake of SQV and prodrugs (10 μM) in human leukemic monocytes U937 cells. Each point represents mean ± SD (n=4).

**Transepithelial Permeability Determination**

To determine whether stereoisomeric prodrug modifications could actually improve absorption across intestinal epithelium, both apical-to-basolateral (A-B) and basolateral-to-apical (B-A) permeabilities for SQV and its prodrugs were measured across MDCK-MDR1 and MDCK-MRP2 cell monolayers. The transport studies were performed at pH 5.4 to reduce chemical hydrolysis since all dipeptide prodrugs of SQV showed higher stability in comparison to those at pH 7.4 (Table 8). Also, peptide transporters are more

active at acidic pH than at basic pH (Agarwal et al., 2007a). Figure 32 compares the bidirectional transport profiles of SQV in the presence or absence of P-gp inhibitor GF120918 (5 μM) and MRP inhibitor MK571 (50 μM). The A-B flux of SQV was less than B-A flux across both MDR1 and MRP2 cells. The presence of GF120918 and MK571 reduced the efflux ratio between B-A and A-B directions significantly to around 1.0 (Table 10). Furthermore, comparison of transepithelial transport between SQV and stereoisomeric prodrugs was evaluated by determining the apparent permeability coefficients ($P_{app}$) in both transport directions. Results in Table 10 indicate that A-B permeability of SQV was significantly enhanced by stereoisomeric prodrug modification, and B-A permeability was decreased on both MDR1 and MRP2 cell monolayers. Efflux ratios for prodrugs are in the range of 1.3 to 1.9 on MDCK-MDR1 cells and 1.1 to 1.4 on MDCK-MRP2 cells, respectively, which are much lower than that of SQV (4.50 on MDCK-MDR1 and 3.04 on MDCK-MRP2), but comparable to the values in the presence of P-gp inhibitor (1.14) and MRP inhibitor (1.00).

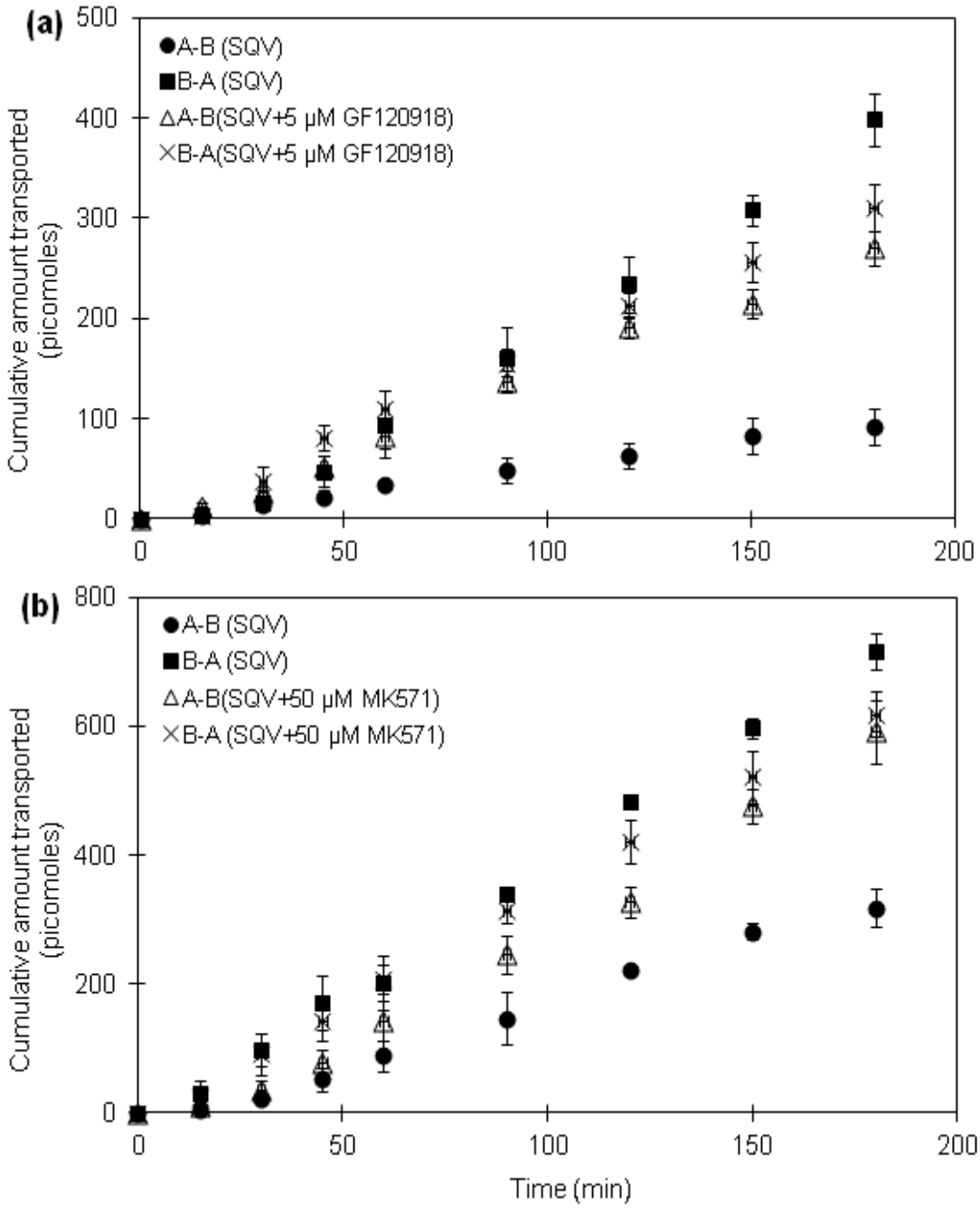


Figure 32. Bidirectional transepithelial transport of SQV (10 μM) across MDCK-MDR1 cell monolayers (a), or MDCK-MRP2 cell monolayers (b).

Each point represents mean ± SD (n=3).

Table 10. Apparent permeabilities ($P_{app}$) of SQV and stereoisomeric prodrugs on apical-to-basolateral direction (A-B) and basolateral-to-apical direction (B-A) across MDCK-MDR1 and MDCK-MRP2 cell monolayers.

| | MDCK-MDR1 cells | | | MDCK-MRP2 cells | | |
|---|---|---|---|---|---|---|
| | $P_{app}$(A-B) (cm/s, $\times 10^{-6}$) | $P_{app}$(B-A) (cm/s, $\times 10^{-6}$) | Efflux ratio | $P_{app}$(A-B) (cm/s, $\times 10^{-6}$) | $P_{app}$(B-A) (cm/s, $\times 10^{-6}$) | Efflux ratio |
| SQV | 0.90 ± 0.16 | 4.06 ± 0.48 | 4.50 | 2.47 ± 0.30 | 7.51 ± 0.24 | 3.04 |
| SQV+MK571 (50 μM) | ND | ND | ND | 5.95 ± 1.60 | 5.97 ± 0.81 | 1.00 |
| SQV+GF120 918(5 μM) | 2.66 ± 0.21 | 3.03 ± 0.33 | 1.14 | ND | ND | ND |
| LLS | 1.66 ± 0.09 | 2.27 ± 0.24 | 1.37 | 4.98 ± 0.45 | 5.72 ± 1.18 | 1.15 |
| LDS | 1.52 ± 0.31 | 2.13 ± 0.57 | 1.40 | 4.60 ± 1.35 | 6.08 ± 1.10 | 1.32 |
| DLS | 2.08 ± 0.43 | 2.69 ± 0.43 | 1.29 | 5.10 ± 0.98 | 5.90 ± 1.15 | 1.16 |
| DDS | 1.35 ± 0.14 | 2.52 ± 0.12 | 1.87 | 4.66 ± 0.57 | 6.61 ± 0.23 | 1.42 |

Data represented are mean ± SD (n=3). ND: not determined.

**Plasma Protein Binding**

Unbound fraction of SQV and various prodrugs in rat plasma were shown in Table 11. The $f_u$ value of SQV is 0.036 ± 0.005 at a concentration of 0.5 μM. *L*-valine conjugates LS and LLS showed significantly enhanced mean $f_u$ values to 0.086 and 0.060, respectively. Unbound drug proportion of DS and DDS, i.e. the prodrugs conjugated with *D*-valines, were observed to be reduced to 0.016 and 0.024 in plasma, respectively.

Table 11. Unbound fraction ($f_u$) of SQV and stereoisomeric prodrugs (0.5 μM) in rat plasma.

| | SQV | LS | DS | LLS | LDS | DLS | DDS |
|---|---|---|---|---|---|---|---|
| $f_u$ | 0.036±0.005 | 0.086±0.015** | 0.016±0.003** | 0.060±0.012* | 0.050±0.001* | 0.031±0.011 | 0.024±0.010 |

Data represented are mean ±SD ($n$ = 3). *$P$ < 0.05 and ** $P$ < 0.01 for statistical difference between SQV and prodrug values.

## Discussion

Apparent aqueous solubilities of all stereoisomeric val-val-SQV increased to more than 2-fold over SQV mesylate salt, and 1000-fold over SQV which is predicted as 2.47 μg/ml at 25°C (DrugBank database: DB01232). This increased solubility can be explained by three dimensional structure modification of SQV by amino acids. Generally the formation of hydrogen bonds between compounds and water molecules is considered to have strong influence on physical properties like aqueous solubility. The high hydrogen-bonding potential and the presence of charged amino groups in the promoiety val-val may dramatically contribute to the hydrophilicity of the conjugates. Similar results are obtained by MSX-4, a valine ester prodrug of the adenosine A2A receptor antagonist MSX-2, with an enhanced solubility to more than 73 times over its parent drug (Vollmann et al., 2008).

A good prodrug candidate after oral administration should be stable enough in gastrointestinal (GI) tract, and then be absorbed across intestinal mucosa and converted to intact parent drug following its transport. Degradation of peptide prodrug in GI tract can proceed either by enzyme-catalyzed hydrolysis or *via* a base-catalyzed hydrolysis yielding amino acid prodrug or parent drug directly. Therefore chemical and enzymatic stability studies will help in screening the ideal prodrug candidate for the further research. Results in Table 8 indicate that all stereoisomeric valine-SQV conjugates underwent acid/base hydrolysis in the pH range of 1.4 to 10.4. Chemical stability enhanced with the increased number of isomers in promoieties, suggesting that dipeptide conjugates are chemically more stable than amino acid conjugates. These results are consistent with previous observations (Anand et al., 2003; Patel et al., 2005). In comparison to *L*-valine

conjugates, the attachment of *D*-valine with SQV exhibited higher chemical stability under various pH conditions. The $t_{1/2}$ values of DS at different pH are either higher or comparable to that of LS, and two *D*-valine prodrug DDS displayed the longest degradation half lives at all pH conditions and is considered to be the most stable compound among all isomeric dipeptide prodrugs. Desiderio *et al.* also reported this stereoselective chemical stability. Approximately 42% of *D,L*-adenosylmethionine and 26% of *L,L*-adenosylmethionine were left after 14 days- incubation in sodium phosphate buffer (pH 2.5), respectively, indicating *L,L*-diastereoisomer showed a stronger chemical hydrolysis than the *D,L*-form (Desiderio et al., 2005). Since the physical pH of major portion of drug absorption in GI tract is ranged from 5 to 8, dipeptide conjugates of SQV with longer residence time in intestine could be better candidates for oral drug delivery in comparison to amino acid prodrugs.

Human colon adenocarcinoma cell line Caco-2 cells was used in metabolic hydrolysis study because it has been reported to be particularly abundant in many esterases like carboxylesterases and peptidases including aminopeptidases, dipeptidyl peptidases, endopeptidase, and membrane dipeptidase (Howell et al., 1992; Jumarie and Malo, 1994; Imai et al., 2005). These hydrolytic enzymes play an important role in the degradation of dipeptide prodrug to parent drug when it is absorbed across the intestinal mucosa. Time-course of various species formation in Caco-2 cell homogenates in Figure 27 illustrates that the hydrolysis pattern of SQV dipeptide prodrugs is compliant to the mechanism of metabolic degradation as demonstrated by the previous study (Anand et al., 2003). Dipeptide prodrug VVS was degraded to amino acid prodrug VS by peptidases and further to parent drug SQV by esterases. Formation of SQV directly from dipeptides

is also possible but the amount is very limited. Results in Table 9 indicate that LLS showed the least enzymatic stability in cell homogenates among all four stereoisomer prodrugs. Incorporation of *D*-isomer enhances the enzymatic stability of conjugation significantly. The half-lives of DLS and LDS are 4.4-fold and 4.3-fold longer than that of LLS, respectively. Two *D*-isomers conjugation DDS exhibits the most stability in cell homogenate, with a 7.4-fold longer half-life over LLS. This observation agrees well with the previously reported results (Pochopin et al., 1994; Fang et al., 2000; Talluri et al., 2008; Tsume et al., 2008). Different metabolic stability of dipeptides may due to their different affinities to hydrolytic enzymes. These stereoisomers could interact with hydrolases with different kinetic parameters since they have different three-dimensional structures. Results in this study indicate that LLS is an excellent substrate for hydrolases. The incorporation of *D*-valine might reduce the recognition by hydrolases, thus it decreases the interaction between conjugates and active site of the enzymes. Correspondingly, DDS displayed significantly enhanced stability in cell homogenates.

Cytotoxicity of SQV prodrugs was evaluated on MDCK-wt cells using LDH assay method. All prodrugs displayed similar or much lower toxicity in comparison to parent drug SQV. Additionally, the toxicity induced by prodrugs was stereoselective on MDCK-wt cells. *D*-isomer conjugations, especially DDS, showed relatively lower cytotoxicity than other stereoisomeric prodrugs. Our previous work measuring metabolic hydrolysis in cell homogenates might explain this sereoselecitive toxicity. DDS showed the least affinity to hydrolases compared to other dipeptide prodrugs. It would lead to less cellular accumulation of SQV from DDS degradation and consequently contribute to less cytotoxicity because SQV is more toxic than prodrugs. In contrast, LLS could be

degraded into SQV to a greater extent since it is a better substrate for hydrolytic enzymes, and thereby LLS displayed a higher toxicity on MDCK-wt cells.

Drug efflux proteins P-gp and MRP2, which are highly expressed in the intestinal mucosa, could be responsible for the low oral bioavailability of SQV (Washington et al., 1998; Huisman et al., 2002). Peptide prodrug modifications, including valine-valine drug derivatives, have been reported by our laboratory for their partial avoidance of efflux pump mediated transport (David et al., 2005; Agarwal et al., 2008; Jain et al., 2008). However, modification of the three-dimensional structure may affect the interaction of the substrate with the enzyme significantly. In this regard, comparison of the affinity of SQV and stereoisomeric valine-valine prodrugs towards efflux transporters was examined employing human MDR1 and MRP2 gene-transfected MDCK cell lines. These two cell lines are widely employed as in vitro models of intestinal epithelium for screening drug permeability (Irvine et al., 1999; Tang et al., 2002b; Tang et al., 2002a). Cellular uptake of [$^{14}$C]erythromycin was enhanced to 2.9-fold over the control with the administration of 75 μM SQV on MDCK-MDR1 cells, suggesting that the binding sites on P-gp were competitively occupied by SQV, thereby the cellular accumulation of another P-gp substrate erythromycin increased. However, equimolar amount of prodrugs exhibited significant reduction of [$^{14}$C]erythromycin uptake compared to SQV. Similar extent of inhibition was also observed on MDCK-MRP2 cells. These differential inhibitory activities indicate that all four stereoisomeric peptide modifications possess lower affinity for both P-gp and MRP2 relative to SQV, and consequently result in reduced cellular accumulation of [$^{14}$C]erythromycin.

Conversely, recognition of prodrugs by peptide transporters was the primary objective of our study. The presence of peptide transporters has been reported on MDCK cells (Brandsch et al., 1995; Agarwal et al., 2007a; Wang et al., 2013). Therefore accumulation of dipeptide Gly-Sar was determined on both MDCK-MDR1 and MDCK-MRP2 cells to evaluate the affinity of SQV prodrugs for peptide transporters in this study. Uptake of [$^3$H]Gly-Sar was inhibited by unlabeled Gly-Sar and val-val, suggesting the expression of peptide transporters on both MDCK-MDR1 and MDCK-MRP2 cell lines. Interaction between SQV prodrugs and peptide transporters is observed to be stereoselective. It is evident by the diminished cellular uptake of [$^3$H]Gly-Sar in the presence of LLS, LDS, and DLS, except two D-isomer conjugate DDS. These results are consistent with the previous studies that peptides containing *L*-amino acids showed higher interactions with peptide transporters than those containing *D*-amino acids (Tamai et al., 1988; Lister et al., 1995; Mitsuoka et al., 2007). Our findings in uptake studies clearly demonstrate that stereoisomeric prodrugs LLS, LDS, and DLS could be translocated into cells by peptide transporter mediated influx as well as bypass efflux transporters (P-gp and MRP2), whereas DDS may only evade efflux pumps and did not show reasonable affinity for the peptide transporters.

It has been reported that both tissue macrophages and blood monocytes can be infected with HIV-1 (Kedzierska and Crowe, 2002). Therefore cellular uptake of SQV and prodrug derivatives in lymphoma cells was also evaluated using U937 cells in this study. Results in Figure 31 demonstrate that all stereoisomeric prodrugs exhibit similar cellular uptake as parent drug SQV, suggesting that SQV uptake by lymphoma cells may not be influenced by valine-based prodrug modification proposed in this study.

Comparison of transepithelial flux of SQV on absorptive (apical-to-basolateral, A-B) and secretive (basolateral-to-apical, B-A) directions demonstrates the influence of efflux transporters which are located on the apical cell membrane. Results in Figure 32 and Table 10 exhibited a much lower absorptive transport of SQV compared to excretive transport. This asymmetric permeation is due to the involvement of efflux transporters present on apical cell membrane. Similar bidirectional transepithelial flux of SQV was obtained in the presence of GF120918 or MK571, inhibitors for P-gp and MRP2 respectively. It confirms that efflux activities of P-gp and MRP2 proteins are one of the major obstacles which limit intestinal absorption of SQV (Siccardi et al., 2003; Taub et al., 2005). Both MDCK-MDR1 and MDCK-MRP2 cell lines are originated from same wild type MDCK cells. However, the apparent permeabilities of peptide prodrugs across MDCK-MDR1 are different from MDCK-MRP2 monolayers (Table 10). It suggests a different capacity of peptide translocation in these two cell lines. Previous studies in our laboratory have reported that transfection of human efflux genes like MDR1 influences the functional activities and biological expression of endogenous transporters such as peptide transporters (Agarwal et al., 2007a; Wang et al., 2013). According to $P_{app}$ values summarized in Table 10, the bidirectional translocation of all prodrugs displayed insignificant asymmetry across both transfected MDCK cell lines. This increment may be due to combined effects of higher solubility and stability, less affinity for the efflux transporters and better recognition by peptide transporters. Among all stereoisomeric peptide prodrugs, the efflux ratio of DDS exhibited the least difference from SQV, suggesting its translocation across both MDCK cells is not as efficient as other isomeric conjugates. Even though DDS showed excellent chemical and enzymatic stability which

keeps more intact peptide prodrugs remaining in the 3 hours-transport study, the failure to be recognized by peptide transporters might attribute to its relatively low transepithelial permeation.

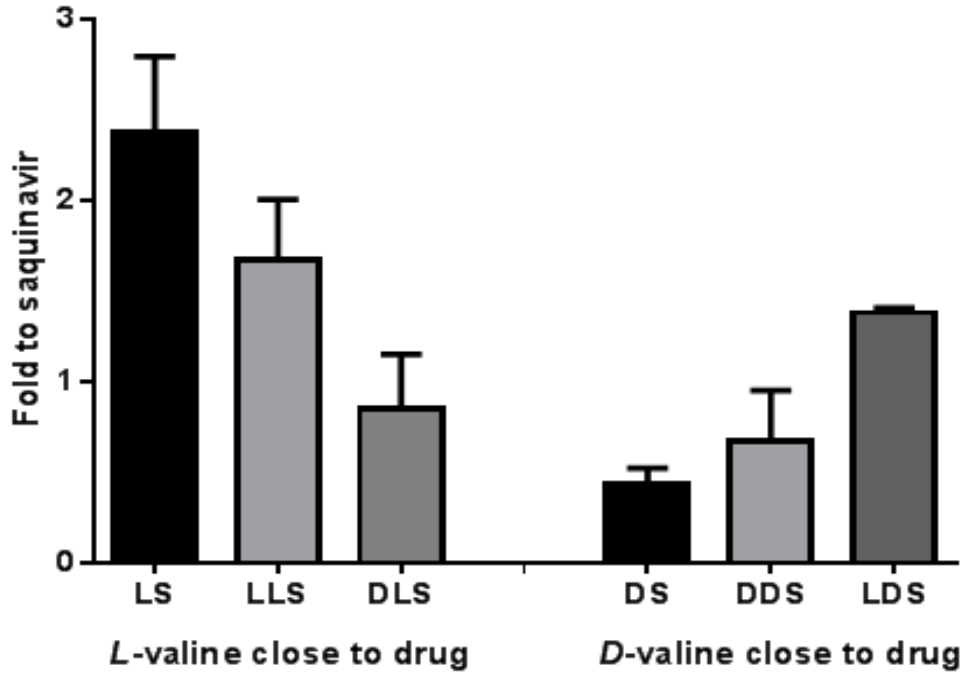


Figure 33. Comparison of unbound fraction ($f_u$) of SQV prodrugs with SQV in rat plasma.

Protein binding in plasma is one of the determinant characteristics for the evaluation of drug disposition in human because only unbound fraction is available for absorption and to elicit its pharmacological action to achieve therapeutic effects. HIV PIs exhibit moderate to high plasma proteins binding, especially to α1-acid glycoprotein (AAG), an acute phase plasma α-globulin glycoprotein (Acosta et al., 2000). In the present study, unbound fraction of SQV was determined *in vitro* using Sprague–Dawley rat plasma. The $f_u$ value of SQV was observed to be 0.036 ± 0.005, suggesting that only 3.6% of total amount of SQV in rat plasma remained free for antiretroviral activity. This result is

consistent with the previous findings that SQV is 98% bound to plasma proteins in human (Flexner, 1998). Significant stereoselectivity was observed in protein binding studies. Position of different isomers in promoieties plays a key role in protein binding of SQV dipeptide prodrugs. Comparison of unbound fractions of various prodrugs has been summarized in Figure 33. Generally, a reduced plasma protein binding is noted when *L*-valine is conjugated to SQV, conversely *D*-valine conjugated to parent drug SQV may contribute to increased protein binding. Moreover, type of terminal isomers in the promoieties can influence this stereoselective protein binding. Typically *D*-isomer on terminal position may reduce the unbound fraction, whereas *L*-isomer produces reverse effect. Because of the absence of any plasma proteins in *in vitro* studies, this differential plasma protein binding must be taken into consideration when interpreting *in vitro* data to estimate the *in vivo* pharmacokinetic or pharmacodynamic parameters.

The study in this chapter suggests that stereoisomeric peptide might be an attractive pro-moiety employed in transporter-targeted prodrug design. All valine-valine-SQV stereoisomeric modifications exhibit similar enhanced aqueous solubility as well as reduced affinity for efflux transporters, but significant stereoselectivity in cellular toxicity, plasma protein binding, chemical and enzyme-catalyzed hydrolysis, as well as recognizition by peptide transporters. Conjugation of *L*-valine to SQV illustrates higher affinity towards peptide transporters, lower protein binding but poor stability and higher toxicity, whereas incorporation of *D*-valine displays good stability and lower toxicity but weak binding with peptide transporters and less unbound fraction in plasma. Results in this chapter indicate that *D*-valine-*L*-valine-SQV and *L*-valine-*D*-valine-SQV might be

potential targeted prodrug candidates which improve intestinal absorption of SQV and enhance oral bioavailability.

# CHAPTER 6

# *IN VITRO* HYDROLYSIS AND ENZYMATIC METABOLISM STUDIES

## Rationale

Poor pharmacokinetics of orally administered SQV are often attributed to rapid and extensive first-pass metabolism in small intestine and liver (Eagling et al., 2002; Usansky et al., 2008). Cytochrome P450 3A (CYP3A) has been identified as the predominant subfamily of hepatic and intestinal CYP enzymes. It is responsible for oxidative biotransformation of more than 50% of drugs in humans and rats. SQV is metabolized primarily by CYP3A4 to mono- and di- hydroxylated metabolites with negligible antiviral activity in humans (Noble and Faulds, 1996; Decker et al., 1998; Parker and Houston, 2008). Mean $C_{max}$ and AUC values were significantly elevated when SQV hard gel formulation was co-administered with other CYP3A4 inhibitors i.e. ritonavir or indinavir (Kumar et al., 1996; Figgitt and Plosker, 2000). In addition, activity of efflux pump P-gp also plays a critical role in reducing SQV oral bioavailability (Kim et al., 1998a; Pal and Mitra, 2006). In comparison with other major secretary transporters like MRP2 located in rat jejunum, P-gp displays a dominating role on intestinal SQV absorption (Usansky et al., 2008). Transepithelial permeation of SQV across gut wall into systemic circulation is mainly restricted by P-gp, and consequently a larger fraction is available for pre-systemic biotransformation in GI tract. Optimizing oral administration of drugs with narrow therapeutic index is critically important, especially for chronically ill patients requiring long-term treatment. Many such agents are substrates for both CYP enzymes and efflux transport proteins. Absorption, distribution, and disposition of SQV have been reported to be significantly influenced by the dual effect of P-gp-mediated

efflux and CYP enzymes-mediated metabolism. Also, continuous use of SQV results in induction of P-gp at the target cells (Konig et al., 2010).

The study in this chapter was to describe the application of stereoisomeric peptide prodrug modification as a strategy to overcome these problems and provide an extensive understanding of the stereoselective resistance to hydrolytic and oxidative enzymes. In this chapter, the first purpose of this study is to investigate affinity of SQV and stereoisomeric peptide conjugates towards P-gp expressed on Caco-2 cell membrane. The second aim is to determine enzyme kinetic parameters for the oxidative metabolism mediated by CYP3A in rat liver microsomes. Bioconversion from prodrugs to the parent drug was also studied in rat plasma and intestinal homogenates since hydrolytic enzymes located in these tissues play an important role in cleaving ester and peptide bonds.

## Materials and Methods

### Materials

SQV mesylate was kindly donated by Hoffmann-La Roche. SQV stereoisomaric dipeptide prodrugs (LLS, LDS, DLS, and DDS) and amino acid prodrugs (LS and DS) were synthesized in our laboratory. Caco-2 cells were obtained from ATCC (Manassas, VA). [$^{3}$H]saquinavir (1.0 Ci/mmol) was purchased from Moravek Biochemicals (Brea, CA). Sprague–Dawley rat plasma was purchased from Valley Biomedical Inc. (Winchester, VA). IGS Sprague–Dawley rat liver microsomes were obtained from XenoTech LLC (Lenexa, Kansas). Bestatin was purchased from USB Corporation (Cleveland, Ohio). Eserine and 4-(hydroxymercuri)benzoic acid sodium salt (PHMB) were obtained from Sigma Chemical Co. (St. Louis, MO). Pefabloc® SC was purchased

from Fluka Chemical Corp. (Milwaukee, WI). TrypLE™ Express Stable Trypsin Replacement and Dulbecco's modified Eagle's Medium (DMEM) were obtained from Invitrogen (Carlsbed, CA). Fetal bovine serum (FBS) was purchased from Atlanta Biologicals (Lawenceville, GA). LY335979 (zosuquidar) was generously provided by Kanisa Pharmaceuticals, Inc. (San Diego, CA). Ketoconazole was obtained from Sigma Chemical Co. (St. Louis, MO). BioRad protein estimation kit was purchased from BioRad (Hercules, CA). Scintillation cocktail reagent was obtained from Fisher Scientific (Fair Lawn, NJ). Triton X-100, HEPES, D-glucose and all other chemicals and solvents were purchased from Sigma Chemical Co. (St. Louis, MO) or Fisher Scientific Co. (Pittsburgh, PA).

**Animals**

Male Sprague–Dawley rats weighing 200–250 grams were obtained from Charles River Laboratories (Wilmington, MA). Animals were used in accordance with the protocol approved by University of Missouri-Kansas City Institutional Animal Care and Use Committee (IACUC) and housed in Laboratory Animal Research Core (LARC) facilities at University of Missouri-Kansas City. Before experiments, all rates were fasted overnight with free access to water.

**Cell Culture**

Caco-2 cells were seeded at a density of 40,000 cells/$cm^2$ in 75 $cm^2$ cell culture flasks and incubated at 37°C, in a humidified atmosphere of 5% $CO_2$, 90% relative humidity. Cells were maintained in DMEM containing 10% heat-inactivated FBS, 20

mM HEPES, 29 mM sodium bicarbonate, 100 units/ml penicillin, and 100 μg/ml streptomycin. Medium was changed every alternate day. After 7-days postseeding, cells were harvested and passaged using TrypLE$^{TM}$ Express Stable Trypsin Replacement, and plated at the density of $2 \times 10^4$ cells /cm$^2$ on 12-well tissue culture plates for uptake studies, or and $7.5 \times 10^4$ cells /cm$^2$ on 12-well Transwell® inserts (diameter 12 mm, pore size 0.4μm) for transport studies. Studies using Caco-2 cells were performed after 18-23 days of growth.

**Uptake and Transport Studies**

Drug cellular accumulation and transport studies on Caco-2 cells were conducted following the methods described in Chapter 3.

**Metabolism Studies in Rat Liver Microsomes**

IGS Sprague–Dawley rat liver microsomes were employed to study affinity of the stereoisomeric prodrugs toward CYP3A relative to SQV. Incubations were conducted in Eppendorf tubes in a LabQuake® Tube Shaker (Barnstead Thermolyne Corp., Dubuque, Iowa) at 37°C. For inhibition study, depletion of SQV and prodrugs in the presence of specific CYP3A4 inhibitor ketoconazole (KTZ) was determined after 15 min-incubation in 1.0 mg protein/ml rat liver microsomes. Generally 135 μl of liver microsomes diluted in DPBS (pH7.4) with 10 mM magnesium chloride and 10 μM KTZ were pre-incubated at 37°C for 10 min. After adding 150 μl drug solutions (2 μM) with 10 μM KTZ, the reaction was initiated by adding 15 μl of pre-warmed NADPH generating system containing 5mM glucose 6-phosphate, 1 U/ml glucose 6-phosphate dehydrogenase, and

1mM β-nicotinamide adenine dinucleotide phosphate (NADP). Final concentrations for drugs and KTZ were 1 μM and 10 μM, respectively. Aliquots (100 μl) of samples were taken at 0 min and 15 min, and then 100 μl of ice-cold acetonitrile was added immediately to terminate metabolic reaction. Subsequently samples were centrifuged at 12,500 rpm, 4 °C for 5 min and the supernatant was stored at −80°C until further analysis by LC-MS/MS. Amounts of remained SQV and prodrugs in the absence of KTZ were also determined under same conditions.

For time dependent metabolism study, depletion of SQV and prodrugs was measured at the initial concentration of 1 μM for up to 2 hour-incubation in rat liver microsomes (0.2 mg protein/ml). Metabolic kinetic parameters including $K_m$ and $V_{max}$ were calculated by incubating SQV and its prodrugs with various concentrations over a range of 0.1-2.5 μM in 0.2 mg protein/ml rat liver microsomes for 5 min. The incubation followed the method mentioned in the inhibition study earlier. Samples (100 μl) were collected at predetermined time points. The metabolic reaction was terminated by adding equal volumes of ice-cold acetonitrile to the sample. Samples were stored at −80°C until further analysis. All incubations were performed in quadruplicate.

**Preparation of Intestinal Homogenates**

Male Sprague-Dawley rats (200-250 g) were euthanized by a lethal injection of sodium pentobarbital through the tail vein (100 mg/kg). Small intestine was exposed and jejunum segment was externalized. Intestinal tissues were homogenized in 10 ml chilled isotonic phosphate buffered saline (IPBS, pH 7.4) using Multipro Variable Speed Homogenizer (DREMEL, Racine, WI) for 5 min on ice bath. Subsequently, homogenates

were centrifuged at 14,000 ×g, 4°C for 25 min to remove cellular debris. The supernatant was diluted with IPBS properly to achieve a final protein concentration of 0.5 mg/ml. Protein content was determined according to the method of Bradford using BioRad protein estimation kit.

### *In vitro* Prodrug Hydrolysis in Rat Plasma and Intestinal Homogenates

Hydrolysis of SQV peptide prodrugs was determined in triplicate in rat plasma and intestinal homogenate in the presence or absence of various hydrolytic enzyme inhibitors. Frozen Sprague–Dawley rat plasma was thawed quickly before experiment and diluted to 90% (v/v) with IPBS (pH 7.4) to maintain the pH of solution. Prior to the initiation of hydrolysis study, plasma and intestinal homogenate were equilibrated at 37°C for 15 min after adding enzyme inhibitors. The concentrations for enzyme inhibitors PHMB, eserine, bestatin, and Pefabloc® AC were 1 mM, 1 mM, 0.5 mM, and 1 mM, respectively. Hydrolysis was initiated in a test tube by the addition of SQV prodrug solution to 1 ml plasma or intestinal homogenate in the presence or absence of enzyme inhibitor. Final prodrug concentration in the reaction mixture was 10 µM. Test tubes were incubated at 37°C in a shaking water bath (45 rpm) and aliquots (50 µl) were withdrawn at appropriate time intervals for up to 24 h. Samples were immediately diluted with 50 µl chilled acetonitrile to quench the reaction and centrifuged at 12,500 rpm for 15 min to precipitate protein. The supernatants were stored at−80°C until further analysis by LC-MS/MS.

### Sample Preparation and Analysis

All SQV and prodrug samples were prepared using liquid-liquid extraction technique following the procedure in Chapter 5. Analysis procedures using LC-MS/MS system have been described in Chapter 4.

**Data and Statistical Analysis**

For oxidative metabolism studies, elimination rate constant ($K_e$) and half life ($t_{1/2}$) of each drug in rat liver microsomes were calculated by plotting the natural logarithm of drug concentrations *versus* time. The data of metabolic rates (substrate turnover per minute per milligram microsomal protein) were fit to Michaelis-Menten equation by nonlinear regression to determine the kinetic parameters $K_m$ and $V_{max}$. Data modeling was conducted using KaleidaGraph (Synergy Software). *In vitro* intrinsic clearance ($CL_{int}$) was subsequently represented by dividing $V_{max}$ by $K_m$ as shown in the following equation.

$$V = \frac{V_{max} \times [S]}{K_m + [S]}$$

Where $V$ represents the total rate of uptake, $V_{max}$ is the maximum uptake rate for the carrier-mediated process, $K_m$ (Michaelis-Menten constant) is the concentration at half-saturation, and [$S$] is the substrate concentration.

For hydrolytic metabolism study in rat plasma and tissue homogenate, degradation rate constants ($K_d$) were calculated by plotting the natural logarithm of drug concentrations against time, and half lives ($t_{1/2}$) were estimated by degradation rate constants.

All experiments were conducted at least in triplicate and the results were expressed as mean ± S.E. Statistical significance was detected using Student's *t*-test. Difference

between mean values was considered statistically significant at $p < 0.05$ and very statistically significant at $p < 0.01$.

## Results

### Uptake and Transport in Caco-2 Cells

Cellular accumulation of [$^3$H]saquinavir (0.5 μCi/ml) was carried out in Caco-2 cells to determine whether stereoisomeric prodrug modifications could evade P-gp mediated efflux of SQV. Figure 34 shows that the accumulation of [$^3$H]saquinavir markedly increased about 2.5-fold in the presence of LY335979, a potent P-gp inhibitor, suggesting P-gp mediated SQV efflux was competitively inhibited. Similarly, around 2.2-fold increase in [$^3$H]saquinavir uptake with 50 μM of unlabelled SQV indicates that SQV is a good substrate for P-gp. However, the presence of equimolar SQV prodrugs showed only 1.2- to 1.4-fold increase in cellular uptake of [$^3$H]saquinavir, suggesting that the affinity to P-gp was significantly reduced by stereoisomeric prodrug modification ($P < 0.01$). No statistical difference was observed in the [$^3$H]saquinavir uptake when various SQV prodrugs presented in this study.

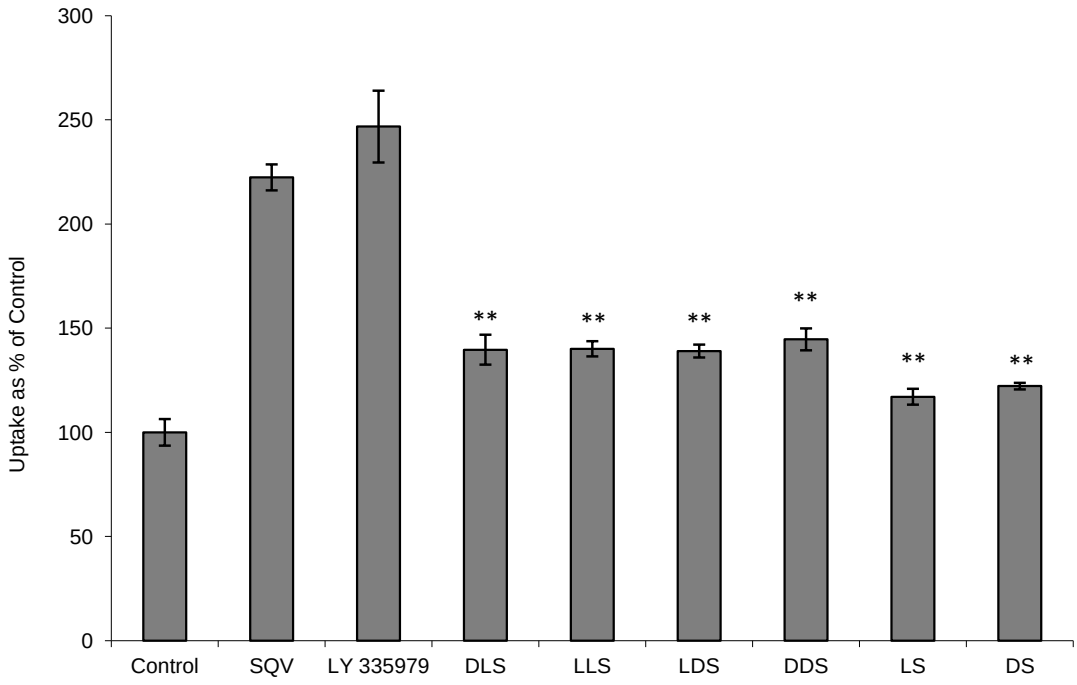


Figure 34. Cellular uptake of [$^{3}$H]saquinavir (0.5 μCi/ml) by Caco-2 cells in the absence (Control) and presence of P-gp inhibitor LY335979 (1 μM), SQV (50 μM) and various stereoisomeric prodrugs (50 μM).

Statistically significant difference (**$P < 0.01$) was observed in uptake between prodrugs and equimolar concentrations of SQV. Values are mean ± S.E. (n = 4).

Transepithelial transport of SQV and its stereoisomeric prodrugs were studied across Caco-2 cell monolayers. Cumulative amount of drug transported was plotted as a function of time. Since partial dipeptide prodrugs can be hydrolyzed to amino acid prodrugs and SQV by the enzymes present in cell cytoplasm during the transport process, amount of drugs transported into receiver chambers for prodrug transport studies was calculated as the sum of prodrugs and regenerated SQV. Bidirectional transport of SQV

across Caco-2 cells in Figure 35A demonstrates that absorptive flux (AB) of SQV was much lower than secretory direction (BA). The presence of specific P-gp inhibitor LY335979 (1 μM) can markedly increase absorptive permeability of SQV, and reduce its secretory permeability. Bidirectional transport of SQV prodrugs, amino acid prodrug DS and dipeptide prodrug DLS, across Caco-2 cell monolayers was illustrates in Figure 35B. All transport-time profiles of SQV prodrugs showed similar linear relationship over the time course of 3 hours (profiles of other prodrugs are not shown here). In comparison with SQV, a less asymmetric permeation was observed by all prodrugs. Values of apparent permeabilities ($P_{app}$) of SQV and stereoisomeric prodrugs across Caco-2 cell monolayers are summarized in Table 12. Efflux ratios, the ratio of $P_{app}$ on BA direction to AB direction, were obtained to be 4.98 and 1.32 for SQV in the absence and presence of LY335979, respectively. The efflux ratios for prodrugs are in the range of 1.2 to 2.8, which are much lower than unmodified SQV, but comparable to the value observed in the presence LY335979. Prodrugs with *L*-valine as promoiety showed higher permeability relative to *D*- isomer conjugates. Efflux ratio for LS across Caco-2 monolayer is 1.22, about half of DS. The order of efflux ratio for dipeptide SQV prodrugs is LLS < DLS < LDS < DDS.

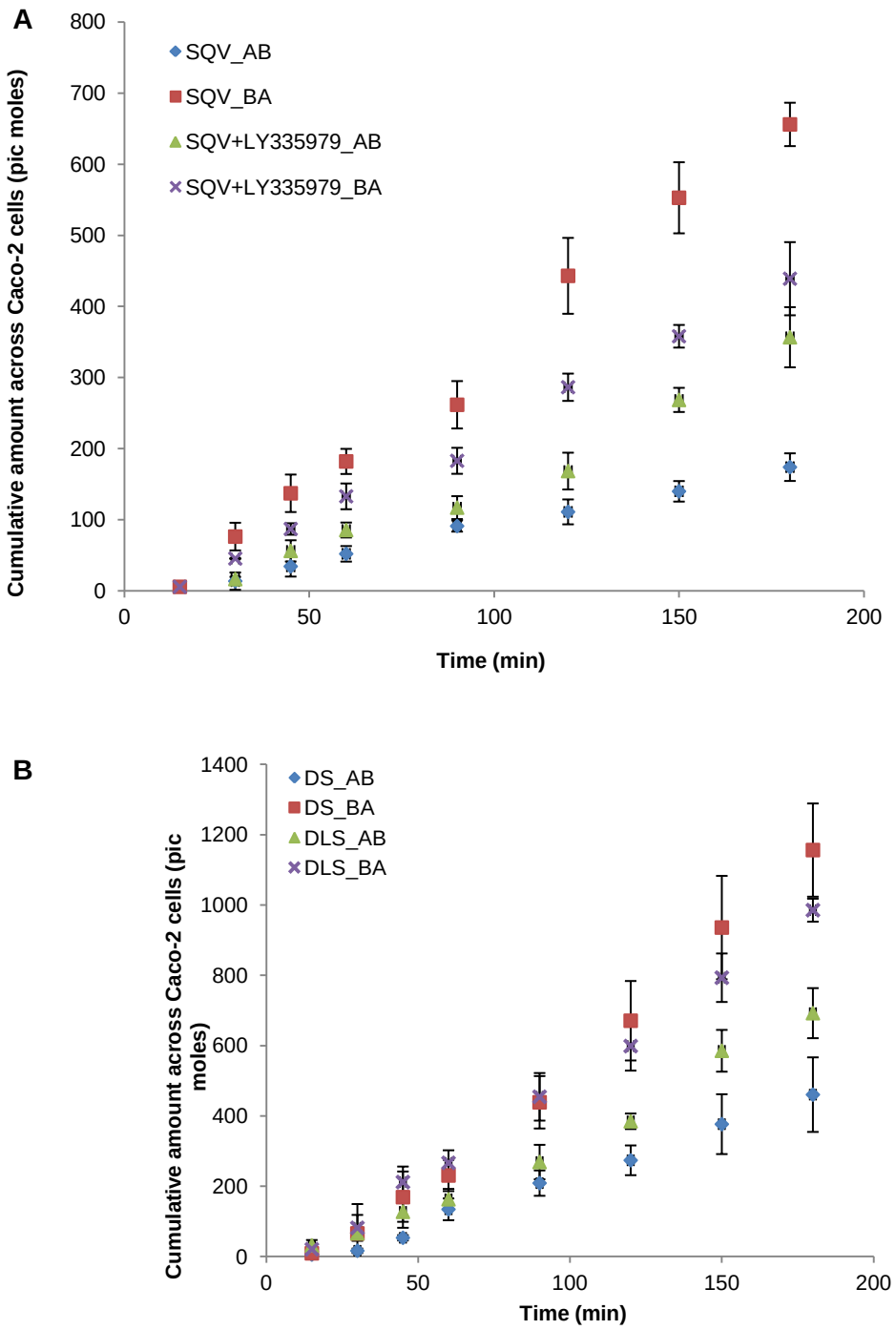


Figure 35. Bidirectional transepithelial transport of SQV (10 μM) in the presence and absence of P-gp inhibitor LY335979 (1 μM) (A), and SQV prodrugs DS and DLS (25 μM) (B) across Caco-2 cell monolayers (mean ± S.E, *n* = 4).

Table 12. Bidirectional apparent permeabilities ($P_{app}$) of SQV and stereoisomeric prodrugs across Caco-2 cell monolayers (mean ± S.E, $n$ = 4).

| | $P_{app}$(AB) ($\times 10^{-6}$ cm/s) | $P_{app}$(BA) ($\times 10^{-6}$ cm/s) | Efflux ratio |
|---|---|---|---|
| SQV | 1.62 ± 0.28 | 8.06 ± 0.85 | 4.98 |
| SQV + LY335979 (1 μM) | 3.57 ± 0.28 | 4.73 ± 0.25 | 1.32 |
| Amino acid prodrugs | | | |
| LS | 2.76 ± 0.21 | 3.38 ± 0.02 | 1.22 |
| DS | 1.88 ± 0.18 | 4.83 ± 0.22 | 2.57 |
| Dipeptide prodrugs | | | |
| LLS | 2.84 ± 0.14 | 3.32 ± 0.15 | 1.17 |
| LDS | 2.47 ± 0.23 | 3.99 ± 0.10 | 1.62 |
| DLS | 2.71 ± 0.02 | 3.85 ± 0.22 | 1.42 |
| DDS | 2.09 ± 0.13 | 5.91 ± 0.14 | 2.83 |

AB: on apical-to-basolateral direction; BA: basolateral-to-apical direction; Efflux ratio = $P_{app}$ (BA)/$P_{app}$ (AB).

**Inhibitory Hepatic Metabolism**

Depletion of SQV and prodrugs (1 μM) was determined in the presence or absence of specific CYP3A inhibitor KTZ (10 μM) after 15-min incubation in 1 mg protein/ml rat liver microsomes (Figure 36). The percentage SQV remaining was only 10.8% ± 0.8% at the end of experiment. However, it significantly increased by more than 8-fold to 86.4% ± 8.7% when co-administered with KTZ. In comparison with SQV, all dipeptide and amino acid prodrugs exhibited improved stability against hepatic metabolism. Around 57% - 72% of valine-SQV prodrugs and 80% - 96% of stereoisomeric valine-valine conjugates

remained unchanged after 15-min of incubation in rat liver microsomes. In addition, all prodrugs appeared to be more stable in the presence of 10 μM KTZ. Less than 10% of biotransformation was noted.

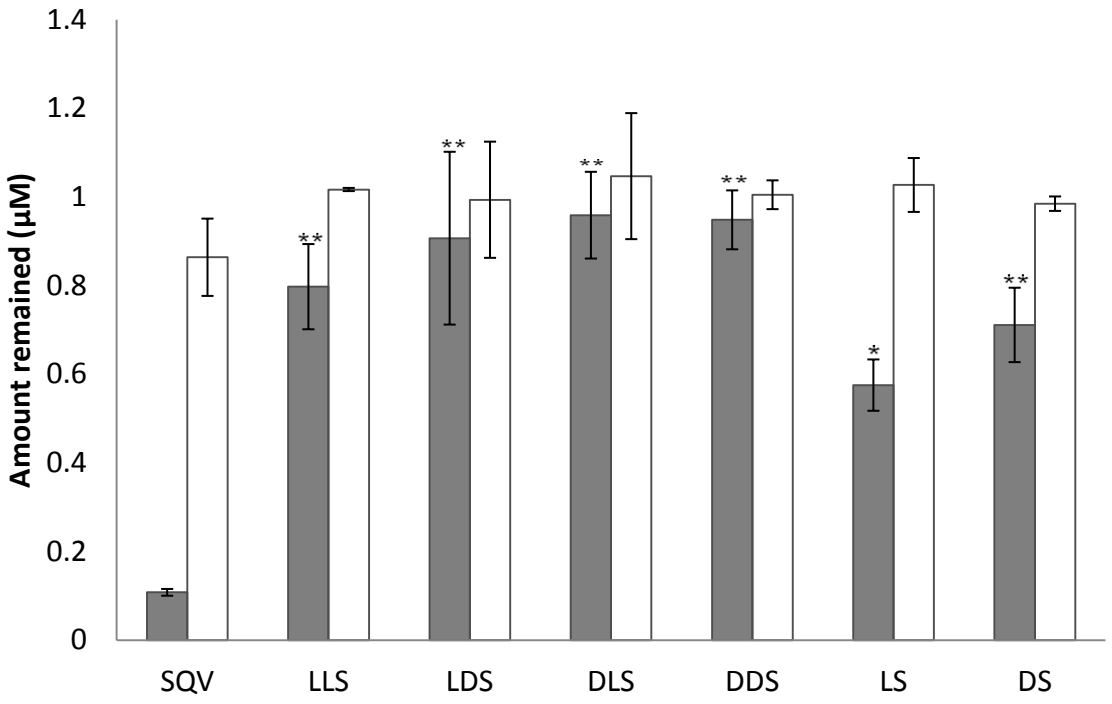


Figure 36. Amount of remained SQV and prodrugs in the absence or presence of CYP 3A inhibitor ketoconazole (10 μM) after 15 min incubation in 1.0 mg/ml rat liver microsomes (mean ± S.E, $n = 4$).

Close bar: 1 μM of substrate; Open bar: 1 μM of substrate and 10 μM of ketoconazole. *$P < 0.05$, and **$P < 0.01$ compared with SQV.

**Time Dependent Hepatic Metabolism**

Time dependent metabolism study was performed in 0.2 mg protein/ml rat liver microsomes for 2 h (Figure 37). Compared with prodrugs, SQV showed maximum

instability towards hepatic metabolic enzymes. Almost 100% SQV underwent biotransformation to inactive metabolites after 1-h incubation. Dipeptide prodrugs exhibited longer residence time than amino acid prodrugs. DDS showed the longest resistance to hepatic enzymes with about 75% of the drug remaining unchanged after 2-h incubation. All depletion profiles displayed logarithm-linear relationship over the time course studied. Elimination rate constants ($K_e$) and half lives ($t_{1/2}$) are summarized in Table 13. The shortest half life (7.3 ± 1.3 min) and the fastest biotransformation rate (0.0949 ± 0.0169 $min^{-1}$) were observed for SQV in microsomal solutions. Dipeptide and amino acid prodrugs were less susceptible to hepatic enzymes, with significantly longer half lives by 12- to 40- fold and 6- to 7- fold relative to SQV, respectively. Additionally, *D*-isomer conjugates appear to be more enzymatically stable over *L*-isomer conjugates. The half life of DS (55.9±7.9 min) was longer than LS (46.5±7.8 min), and DDS exhibited the longest residence with the half life of 296.2±25.8 min, which is 3 times more than LLS.

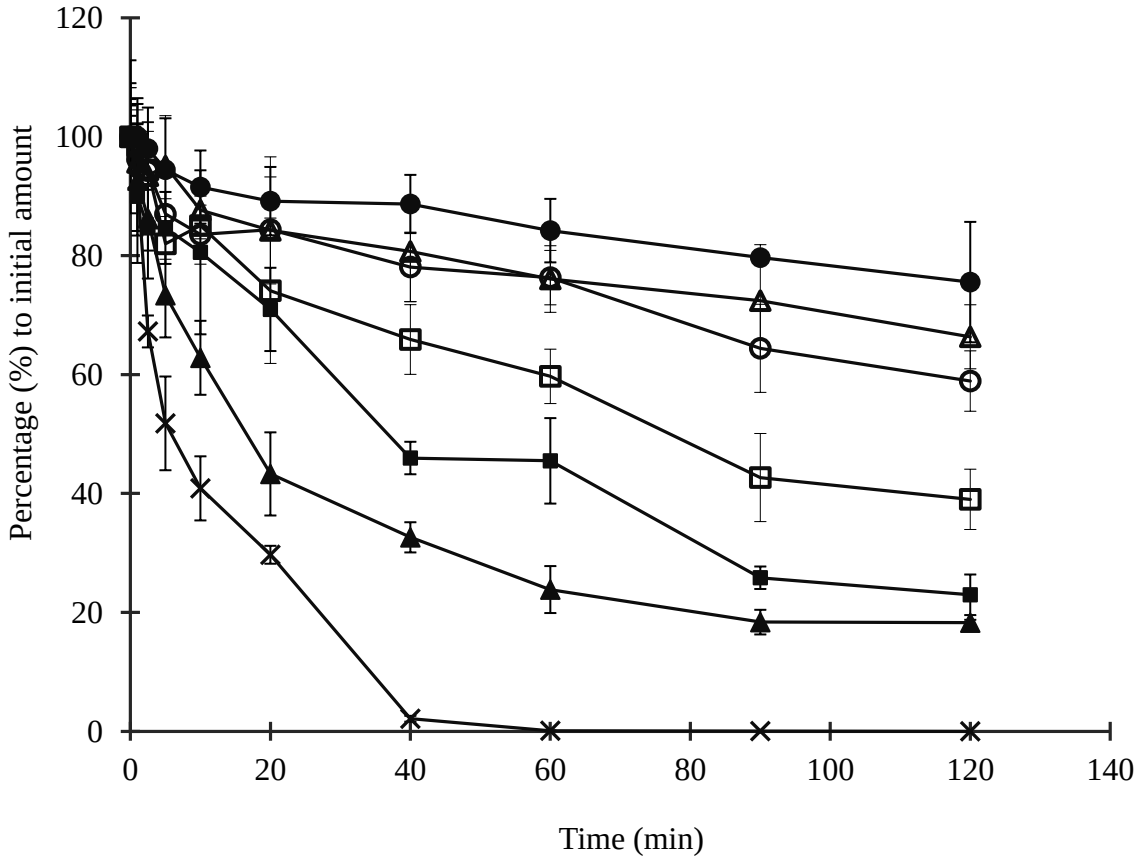


Figure 37. Time dependent metabolism for SQV and various prodrugs in 0.2 mg protein/ml rat liver microsomes (mean ± S.E, *n* = 4).

×, SQV; ▲, LS; ■, DS; □, LLS; ○, LDS; Δ, DLS; ●, DDS.

Table 13. Elimination rate constants ($K_e$) and half lives ($t_{1/2}$) for SQV and various stereoisomeric prodrugs in 0.2 mg protein/ml rat liver microsomes (mean ± S.E, $n$ = 4).

| | $K_e$ ($min^{-1}$) | $t_{1/2}$ (min) |
|---|---|---|
| SQV | 0.0949 ± 0.0169 | 7.3 ± 1.3 |
| Amino acid prodrugs | | |
| LS | 0.0149 ± 0.0025 | 46.5 ± 7.8 |
| DS | 0.0124 ± 0.0018 | 55.9 ± 7.9 |
| Dipeptide prodrugs | | |
| LLS | 0.0078 ± 0.0012 | 88.9 ± 13.2 |
| LDS | 0.0039 ± 0.0003 | 177.7 ± 15.6 |
| DLS | 0.0031 ± 0.0003 | 223.6 ± 20.8 |
| DDS | 0.0023 ± 0.0002 | 296.2 ± 25.8 |

**Concentration Dependent Hepatic Metabolism**

Figure 38 depicts the relationship between metabolic rate and substrate concentration for SQV, LS and LLS. Oxidative biotransformation of SQV and stereoisomeric prodrugs follows Michaelis-Menten kinetics in rat liver microsomes. Kinetic parameters $K_m$ and $V_{max}$ were calculated and are listed in Table 14. Apparent $K_m$ for SQV (0.41 ± 0.06 μM) was increased by 2 to 5 times after prodrug modification, suggesting that this approach significantly reduced the affinity of SQV towards CYP-mediated phase I metabolism. Among the prodrugs studied, DDS was most stable towards metabolic enzymes, with a $K_m$ value of 1.98 ± 0.27 μM. Application of *L*- or *D*- isomers in conjugation also played an important role in enzyme recognition. The $K_m$ values for LS and DS were 0.64 μM and 0.98 μM, respectively, suggesting that the *D*- isomer conjugations display less affinity towards hepatic enzymes. This result is consistent with results from dipeptide

prodrugs. Apparent $K_m$ values for LLS and DDS determined in this study were 1.06 µM and 1.57 µM, respectively. Estimates of *in vitro* intrinsic clearance ($CL_{int}$) summarized in Table 14 primarily represent the disparity in turnover of rat liver microsomes. The *in vitro* intrinsic clearance of SQV in microsomes was calculated as 1.85 ± 0.20 ml/min/mg microsomal protein. Significantly lower $CL_{int}$ estimates were observed for all prodrugs in comparison with SQV. DLS showed the most reduced turnover rate at 0.78 ± 0.13 ml/min/mg protein, with 60% less metabolites generated relative to parent drug SQV.

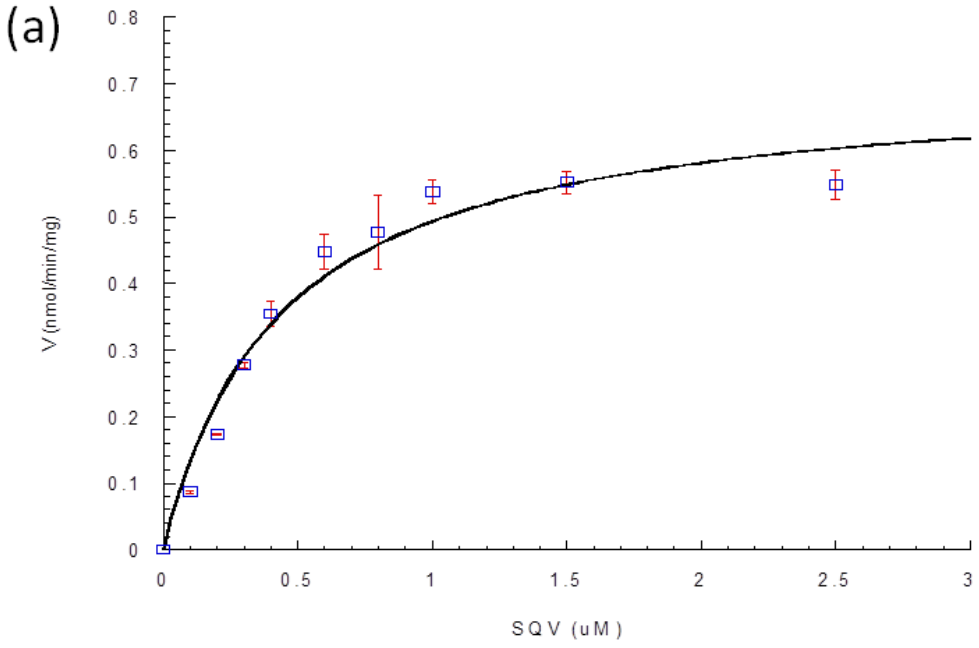

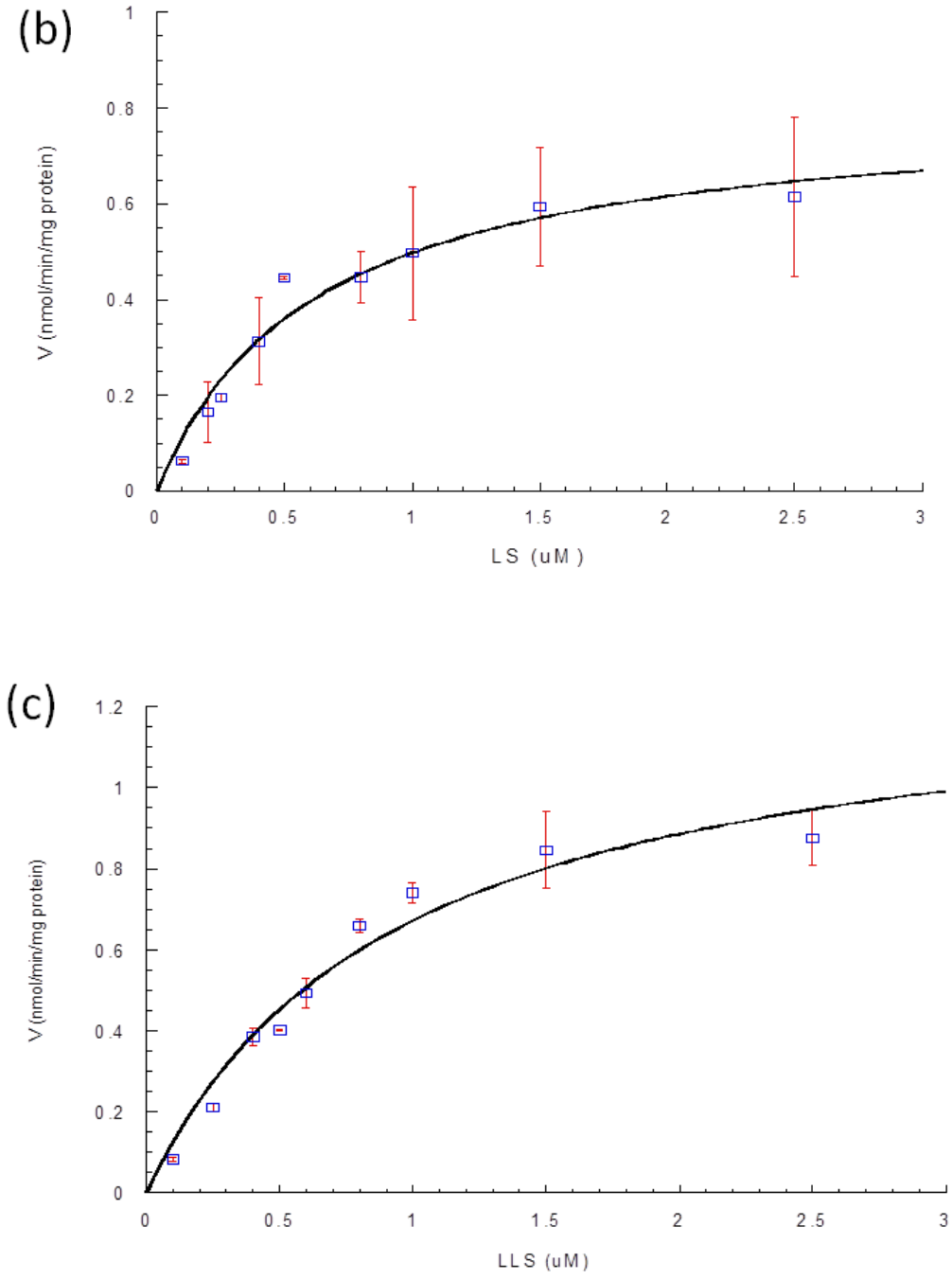


Figure 38. Relationship between metabolic rate and substrate concentration for SQV (a), LS (b) and LLS (c) in 0.2 mg protein/ml rat liver microsomes (mean ± S.E, *n* = 4).

Table 14. Kinetic parameters $K_m$, $V_{max}$ and *in vitro* intrinsic clearance ($CL_{int}$) of saquinavir and stereoisomeric prodrugs in 0.2 mg protein/ml rat liver microsomes (mean ± S.E., $n = 4$).

| | $K_m$ (μM) | $V_{max}$ (nmol/min/mg protein) | $CL_{int}$ (ml/min/mg protein) |
|---|---|---|---|
| SQV | 0.41 ±0.06 | 0.749 ±0.030 | 1.85 ±0.20 |
| Amino acid prodrugs | | | |
| LS | 0.64 ±0.23 | 0.856 ±0.073* | 1.43 ±0.31* |
| DS | 0.98 ±0.13** | 1.318 ±0.122** | 1.35 ±0.04** |
| Dipeptide prodrugs | | | |
| LLS | 1.06 ±0.30** | 1.369 ±0.292** | 1.30 ±0.15** |
| LDS | 1.15 ±0.38** | 1.304 ±0.406** | 1.14 ±0.04** |
| DLS | 1.33 ±0.12** | 1.031 ±0.125** | 0.78 ±0.13** |
| DDS | 1.57 ±0.09** | 1.467 ±0.127** | 0.93 ±0.03** |

*$P < 0.05$, and **$P < 0.01$ compared with SQV.

**Hydrolytic Degradation in Rat Tissues**

Stability of various SQV stereoisomeric valine-valine prodrugs was evaluated in rat plasma and intestinal homogenates to identify the contribution of structural modification to enzymatic hydrolysis. Results in Figure 39 indicate that LLS may be the least enzymatically stable among all four dipeptide prodrugs. The estimated half lives (Table 15) of LLS in rat intestinal homogenates (0.5 mg protein/ml) and plasma were 2.4 ± 0.1 h and 7.8 ± 0.1 h, respectively. DDS exhibited relatively higher enzymatic stability with half lives of 24.1 ± 0.5 h and 40.0 ± 5.0 h in rat intestinal homogenates and plasma,

which are around 10- fold and 5- fold higher over LLS, respectively. Our studies also indicate that all SQV dipeptide prodrugs displayed more susceptibility to hydrolytic enzymes in rat intestine as compared to plasma.

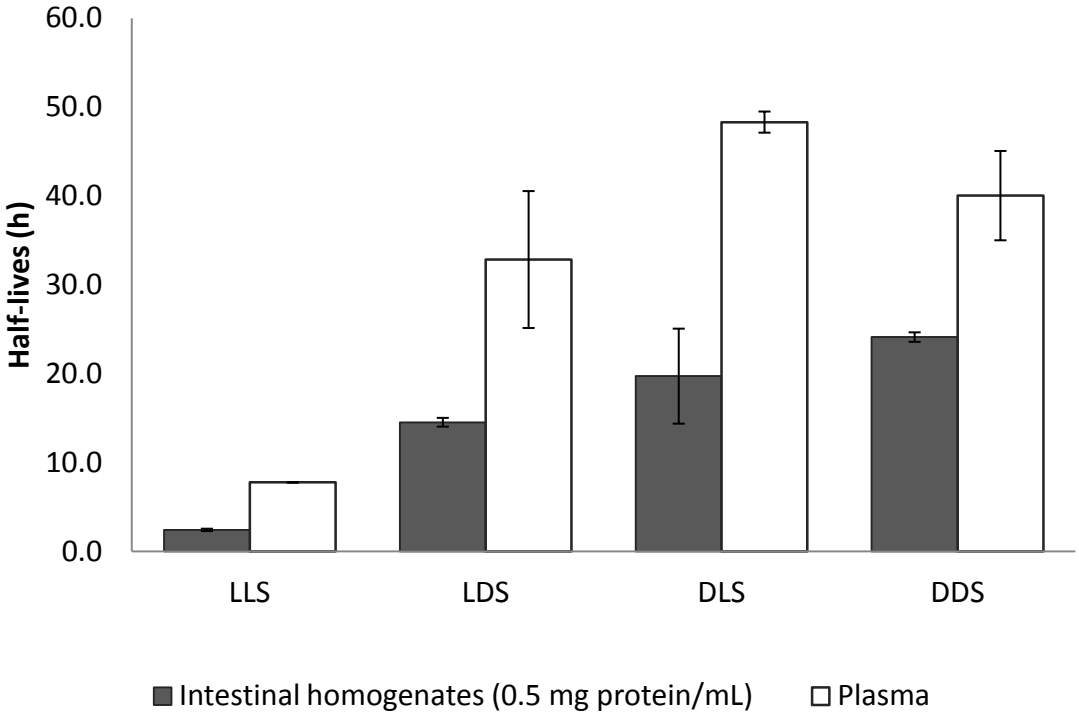


Figure 39. Half-lives of SQV stereoisomeric peptide prodrugs in rat plasma and intestinal homogenates (mean ±S.E, n = 4).

**Hydrolytic Degradation in the Presence of Enzyme Inhibitors**

Hydrolysis study of SQV stereoisomeric valine-valine prodrugs was performed in the presence of various classes of enzyme inhibitors to illustrate the enzyme class responsible for drug degradation in rat tissues. In rat intestinal homogenates (Table 15), addition of specific aminopeptidase inhibitor bestatin (0.5 mM) resulted in a complete inhibition for

the hydrolysis of LLS, LDS and DLS, but no effect was noted with DDS. Degradation of LLS was partially inhibited by irreversible serine hydrolase inhibitor pefabloc SC (1 mM), which did not prevent hydrolysis of the other three SQV dipeptide prodrugs. Half lives of LLS, LDS and DDS in rat intestinal homogenates were improved by different extents by both carboxylesterase inhibitor PHMB (1 mM) and cholinesterase reversible inhibitor eserine (1 mM), while stability of DLS remained unaffected with 1 mM PHMB.

Inhibition of SQV dipeptide prodrug hydrolysis in rat plasma has also been illustrated in Table 15. LLS hydrolysis was completely inhibited by both esterase inhibitors PHMB (1 mM) and eserine (1 mM), and peptidase inhibitors bestatin (0.5 mM) and pefabloc® SC (1 mM). However, half lives of LDS, DLS and DDS were significantly improved only when coadministered with 1 mM PHMB. Bestatin, pefabloc®SC and eserine showed no measurable inhibition to the hydrolysis of these three dipeptide prodrugs in rat plasma.

Table 15. Half-lives (h) of SQV stereoisomeric dipeptide prodrugs in the presence of different enzyme inhibitors (mean ±S.E, n = 4).

| | Rat intestinal homogenates | | | | Rat plasma | | | |
|---|---|---|---|---|---|---|---|---|
| | LLS | LDS | DLS | DDS | LLS | LDS | DLS | DDS |
| Drug alone | 2.4 ±0.1 | 14.5 ±0.5 | 19.7 ±5.3 | 24.1 ±0.5 | 7.8 ±0.1 | 32.8 ±7.7 | 48.3 ±1.2 | 40.0 ±5.0 |
| Drug and various hydrolyse inhibitors | | | | | | | | |
| PHMB (1mM) | 9.3 ±3.9** | 21.0 ±2.5* | 16.9 ±3.0 | 45.5 ±8.7** | 17.7 ±1.2** | 40.9 ±0.9* | 61.7 ±11.8* | 62.7 ±13.4** |
| Eserine (1mM) | 8.3 ±1.9** | 19.3 ±0.3* | 41.0 ±11.5** | 31.5 ±7.6* | 19.5 ±3.4** | 21.8 ±3.0 | 39.4 ±11.7 | 31.1 ±6.9 |
| Bestatin (0.5mM) | 33.2 ±8.8** | 28.0 ±3.7** | 44.9 ±13.0** | 24.3 ±0.7 | 44.3 ±8.4** | 27.4 ±5.3 | 42.6 ±6.4 | 31.8 ±4.2 |
| Pefabloc® SC (1mM) | 5.3 ±0.4* | 12.9 ±0.3 | 14.3 ±1.6 | 14.8 ±3.5 | 43.9 ±8.9** | 37.9 ±0.9 | 42.5 ±4.4 | 38.1 ±0.3 |

*$P$ < 0.05, and **$P$ < 0.01 compared with drug alone.

## Discussion

Previous work from our laboratory has reported that affinity of PI drugs towards P-gp can be reduced by conjugating with different *L*-amino acids (Jain et al., 2005; Agarwal et al., 2008). Cellular uptake performed in this study provides the evidence that *D*-isomeric SQV conjugates also partially circumvent P-gp. Colon carcinoma cell line Caco-2 is an extensively used *in vitro* oral drug absorption model due to its similar epithelial cell characteristics and efflux proteins expression to human jejunum (Taipalensuu et al., 2001). In our study, cellular [$^3$H]saquinavir uptake in Caco-2 cells showed a 2.5-fold enhancement in the presence of LY335979, a potent P-gp inhibitor, confirming that SQV is a high-affinity substrate for P-gp. SQV prodrugs linked to various stereoisomeric amino acid promoieties demonstrated only 50-60% of [$^3$H]saquinavir uptake relative to equimolar concentration of unlabeled SQV. This altered inhibition profile observed for SQV prodrugs indicates that the modification of three-dimensional structure can affect the interaction between the substrate and P-gp, regardless of *L*- or *D*- isomers in conjugates.

Subsequent studies were carried out to determine the transepithelial flux of SQV and its prodrugs on both absorptive and secretory directions across Caco-2 cell monolayers. A similar bidirectional transepithelial SQV flux was obtained when P-gp, which is located on the apical surface of Caco-2 cells, was inhibited by LY335979. It provides additional evidence that efflux transport mediated by P-gp is one of the major obstacles to limit intestinal SQV absorption. Apparent $P_{app}$ values summarized in Table 12 indicate that bidirectional translocation of all prodrugs displayed less asymmetry than SQV. This increment in absorptive permeation is probably due to lower affinity for the efflux pump

P-gp. Interestingly, efflux ratios between secretory and absorptive transport exhibited somewhat stereoselectivity. The rank order of efflux ratio is LLS < LS < DS < DDS. LLS showed the maximally reduced efflux ratio relative to SQV. Whereas the efflux ratio observed for DDS exhibited the closest value to SQV, suggesting that its transepithelial accumulation is not as efficient as other isomeric prodrugs. Such stereoselective permeation of SQV prodrugs may indicate variable structural affinity for peptide transporters. It has been reported that drugs linked to small peptides (so called as peptide prodrugs) can be recognized easily as substrates by the peptide transporter-mediated influx system and ferried across the epithelial membrane (Ganapathy and Leibach, 1996; Katragadda et al., 2006). However, peptides containing *L*-amino acids displayed higher affinity towards peptide transporters than those containing *D*-amino acids (Lister et al., 1995; Mitsuoka et al., 2007). Previous uptake studies of stereoisomeric valine-valine-SQV on MDCK cells also indicated that prodrugs conjugated with *L*-isomer can be recognized by peptide transporters, whereas double *D*-isomeric derivative, DDS did not show any comparable affinity for these influx transporters. Therefore incorporation of *D*-valine in the peptide conjugate might lead to only partial recognition by peptide transporters, resulting in low transepithelial permeation across intestinal epithelium. Nevertheless, all prodrugs including DDS showed relatively higher transepithelial accumulation than the parent drug SQV. This result demonstrates a combined effect of the evasion of P-gp-mediated efflux and recognition by peptide transporters. Since the majority of SQV delivered by oral route is absorbed in the small intestine, overcoming the rate limiting barrier expressed by high-level of P-gp improves drug permeability

across intestinal epithelium and shut down repetitive exposure to metabolizing enzymes in intestinal lumen.

SQV is known to be metabolized primarily by hepatic and intestinal CYP3A4 to mono- and di- hydroxylated metabolites in humans (Fitzsimmons and Collins, 1997; Eagling et al., 2002; Parker and Houston, 2008). Tremendous SQV biotransformation has also been reported in rat liver microsomes (Treijtel et al., 2009). Two major P450 isoforms CYP3A2 and CYP3A1, oligomerically related to human CYP3A4, have been identified in rat liver (Nelson et al., 1996). Thus oxidative metabolism of SQV and its derivatives was also investigated in rat liver microsomes. KTZ is a potent CYP3A inhibitor at low concentrations in human (Michaud et al., 2010). Incubation of KTZ (10 μM) with 1.0 mg/ml microsomes showed significant inhibitory effects on SQV biotransformation, confirming the previous findings that SQV is a substrate of rat hepatic CYP3A enzymes. In comparison to SQV, a remarkablely less biotransformation was observed by prodrug modification, ranging from 2-fold lower for LS to 20-fold lower for DLS and DDS. Time-course of biotransformation also illustrates that stability in 0.2 mg protein/ml microsomes follows the rank order of parent drug < amino acid derivatives < dipeptide derivatives. This result is possibly due to the modification of three-dimensional structure of SQV. Bonding interactions between the functionalities of substrates and complementary sites on enzyme surface have considerable steric constraints. Thus the "fit" between SQV and active site of CYP3A enzymes is reduced by conjugating chiral promoieties. Less affinity for enzyme was observed for molecules with larger spatial structure modification. Additionally, such weakened interaction exhibited significant stereospecificity due to different prolonged elimination $t_{1/2}$ values in rat hepatic

microsomes. DDS is found to be the most stable in liver microsomes with the half life of 3-fold longer than LLS and 42-fold longer than SQV. Correspondingly, SQV attached with one *D*-valine in dipeptide promoity, like DLS and LDS, showed moderate prolonged residence time as compared with LLS and DDS. This result suggests that introducing a *D*-isomer into SQV can reduce its susceptibility to oxidative biotransformation driven by rat hepatic CYP3A.

To date, much less information is available on *in vitro* metabolic kinetics of SQV in rat liver microsomes. It has been reported that the $K_m$ and $V_{max}$ values for SQV in male Sprague-Dawley rat liver microsomes are 0.042 μM and 0.446 nmol/min/mg protein, respectively (Parker and Houston, 2008). These parameters differed from those estimated in our study (Table 14), probably due to the differences in methodology. Significantly higher $K_m$ for peptide prodrugs excluding LS was obtained as compared to SQV (0.41 μM), indicating that its affinity towards metabolizing enzyme CYP3A can be reduced by prodrug modification. Previous conclusion about stereoselective interaction between SQV prodrugs and enzymes is further interpreted by $K_m$ determination. The $K_m$ values for DDS, DS and LS were 1.57 μM, 0.98 μM, and 0.64 μM, respectively, indicating the order of affinity for CYP3A enzymes is DDS < DS < LS. Therefore increasing the number of *D*-valine in SQV prodrugs might lead to an enhanced stability in rat liver microsomal samples.

A true intrinsic clearance of free drug, defined as the volume of liver water cleared of drug in unit time *in vivo*, is influenced by many system dependent parameters such as protein binding, hepatocyte-medium partition and molecular diffusion (Treijtel et al., 2009). The ratio of $V_{max}$ /$K_m$, a measure of *in vitro* intrinsic clearance ($CL_{int}$), generally

considered to be a simple and useful approach to extrapolate the activity of metabolizing enzymes *in vivo* (Miners et al., 2006; Treijtel et al., 2009). Thus $CL_{int}$ estimates based on rat liver microsomal kinetic data in this study were generated to predict the "true" hepatic clearance rates of SQV and prodrugs. Comparison of $CL_{int}$ in Table 14 indicates that SQV showed the most rapid turnover rate in rat liver microsomes. Biotransformation rate of SQV amino acid derivatives was found to be higher than dipeptide prodrugs in this study. SQV attached with chiral promoieties displayed a distinct stereochemical preference in that an "*L*" configuration in promoiety result in a relatively rapid clearance by CYP3A. Such disparity in *in vitro* elimination may contribute to the differential clearance catalyzed by hepatic or intestinal CYP3A in first-pass effect following oral administration.

Aforementioned data provide evidence that, in comparison with amino acid prodrugs, SQV dipeptide conjugates exhibited higher potential to evade oxidative metabolism. Thus dipeptide prodrug modification might be a more promising strategy to overcome this dual CYP3A/P-gp-mediated oral bioavailability barrier. However, besides oxidative enzymes, the phase II conjugation enzymes are present ubiquitously in all biological fluids and tissues. Dipeptide prodrugs can be degraded to amino acid prodrugs or parent drug SQV by various hydrolases during the process of absorption and distribution. Hence it is critical to optimize bioconversion rates of orally administered prodrugs in gut, liver and plasma.

Rat intestine and plasma were chosen as the most relevant media for hydrolysis studies because they are possible sites where bioconversion takes place. Similarly, stereoselective interaction was observed between prodrugs and hydrolytic enzymes. LLS

has been observed to be the least enzymatically stable in both rat intestinal homogenates and plasma among four dipeptide prodrugs. Stereoisomers interact with hydrolases resulting in different kinetic parameters due to their differential three-dimensional structures. It seems that spatial structure of *D*-configuration does not fit well to the active site of enzymes. Such reduced recognition by hydrolase may possibly contribute to the significantly enhanced stability of prodrugs attached with *D*-valine in tissues. This observation coincidences well with the previously reported results (Fang et al., 2000; Talluri et al., 2008; Tsume et al., 2008). Additionally, all prodrugs showed slower degradation rates and longer half lives in rat plasma than in rat intestinal homogenates. This result may attribute to the less enzyme capacity or concentration expressed in plasma.

Valine-valine-SQV can be hydrolyzed at two positions, either at the ester bond or peptide bond. Therefore esterases and peptidases can play a key role in modulating the degradation rate of these dipeptide prodrugs. Among the peptidases located in intestinal brush border, aminopeptidase and serine hydrolase are proficient in cleaving peptide bonds in conjugated promoieties to generate amino acid prodrugs. Inhibitory data indicate that aminopeptidase appeared to be the principal peptidase in the bioconversion process of valine-valine-SQV. After co-administration with potent aminopeptidase inhibitor bestatin, half lives for LLS, LDS, and DLS in rat intestinal homogenates significantly increased by 13.8-, 1.9-, and 2.3-fold, respectively. However, serine hydrolase inhibitor Pefabloc® SC only produced limited inhibition to hydrolysis of LLS in both rat plasma and intestinal homogenates. It is also important to note that chirality of the valine residue in SQV prodrugs dictates bioconversion rate mediated by peptidase. Enzyme specificity

towards the drug is mainly based on preferred residues adjacent to the scissile bond. Results from inhibitory studies indicate that peptidase favors *L*-configuration, since incorporation of *L*-valine leads to more susceptibility to peptidases.

Generally, hydrolysis of all four SQV dipeptide prodrugs was inhibited by both cholinesterase inhibitor eserine and carboxylesterase inhibitor PHMB. Such inhibitory effect by PHMB was observed in both rat plasma and intestine, whereas eserine showed remarkable inhibitory effect only in rat intestinal samples. Usually esterases are expressed throughout the body, but the activity of these hydrolytic enzymes varies in different tissues. Serum carboxylesterase activity in Sprague-Dawley rat has been reported as 6158 nmol/ml serum/min, significantly higher than that of serum cholinesterase (Clement and Erhardt, 1990). Such differential activity clearly explains the results that hydrolysis of prodrugs was decelerated by both carboxylesterase and cholinesterase inhibitors in rat intestinal homogenates, but was only reduced by carboxylesterase inhibitor in rat plasma. Two *L*-valine derivative LLS still presented a remarkable enhancement in $t_{1/2}$ when coadministered with esterase inhibitors. But no expectant stereoselective interaction with esterases was observed in this study because hydrolysis of DDS was also inhibited by esterase inhibitors.

Enzymatic hydrolysis is considered a complicated process. Hydrolysis of drugs is often mediated by more than one enzyme at different sites. The bioconversion rate of SQV dipeptide prodrugs should be determined by the combined effects of esterases and peptidases. According to the results shown in Table 15, *L*-valine-*L*-valine-SQV showed extremely rapid bioconversion and poor stability in biological media. This result indicates

that LLS might be hydrolyzed rapidly into SQV in gut or plasma, thereby leading to low oral bioavailability caused by intestinal or hepatic first-pass metabolism.

# CHAPTER 7

# EVALUATION OF *IN VITRO/IN VIVO* BIOAVAILABILITY

## Rationale

In the previous chapters, we have reported that stereoisomeric dipeptide prodrugs exhibited enhanced cellular accumulation and transepithelial transport as compared with the parent drug SQV in *in vitro* cell models. This improvement may be achieved by the cumulative effects of evasion of efflux activities and CYP-mediated metabolisms as well as facilitated transport by peptide transport system. But no direct evidence shows that these prodrugs can overcome the absorption and metabolic barriers *in vivo*, and exhibit enhanced oral bioavailability over SQV.

Drug pharmacokinetics including absorption, distribution, metabolism and elimination (ADME) are complicated processes in the body. Numerous transporters and enzymes are involved in these processes and contribute to drug disposition in systemic circulation. *In vitro* cell culture models provide a simple but extremely useful way to evaluate the molecular mechanisms of drug transport and metabolism, but the absence of tissue crosstalks occurring *in vivo* limits application of these single cell lines in drug screening. Recently physiologically based *in vitro* co-culture cell systems of enterocytes and hepatocytes have been developed to provide cell culture environment close to *in vivo* ADME processes (Ouattara et al., 2011; Rossi et al., 2012). These *in vitro* cell co-cultures offer a new testing platform to simulate more reliable *in vivo* drug disposition processes. Bioavailability of a drug is defined as the fraction of the dose that appears intact in the systemic circulation. Major factors influencing drug oral bioavailability include drug permeation across intestinal mucosa, enzymatic degradation and biotransformation

occurring in gut wall and liver. Therefore a static cell system MDCK cells overexpressed human MDR1 gene and CYP3A4 enzyme (MMC) co-cultivated with human hepatoma cell line HepG2 was developed in this study to estimate kinetic parameters related to *in vivo* ADME such as bioavailability. MMC has been characterized as a reliable *in vitro* model for assessing drug intestinal absorption and enteric CYP3A4–mediated metabolism (Kwatra et al., 2012), and HepG2 has been widely applied as a useful cell model in drug metabolism and toxicity studies (Roe et al., 1993; Donato et al., 2008). In this study MMC is employed to study transepithelial transport and metabolism of SQV and its prodrugs in the intestinal lumen. After crossing intestinal barrier such as MMC growing in Transwell filter, their hepatic metabolism in blood circulation can be evaluated by HepG2 cells growing in receiving chamber.

In this chapter the *in vitro* bioavailability of SQV and its dipeptide prodrugs was estimated using this MMC/HepG2 co-culture system. Subsequently oral absorption studies were performed via oral gavage to male Sprague-Dawley rats to investigate the pharmacokinetics of dipeptide prodrugs *in vivo*. Plasma concentration of parent drug SQV regenerated from these prodrugs was also compared to the SQV administered orally to rats.

## Materials and Methods

### Chemicals

Madin-Darby canine kidney cells transfectant overexpressing human P-gp/MDR1 (MDCK-MDR1) was generously provided by Dr. Peter Borst, Netherlands Cancer Institute (Amsterdam, Netherland). Stable transfection of MDCK-MDR1 cell with human

CYP3A4 enzyme (MMC) was conducted in our laboratory (Kwatra et al., 2012). HepG2 cells were obtained from American Type Culture Collection (Manassas, VA). TrypLE$^{TM}$ Express Stable Trypsin Replacement, modified Eagle's Medium (MEM) with Earle's B salt solution and Dulbecco's modified Eagle's Medium (DMEM) were obtained from Invitrogen (Carlsbed, CA). Fetal bovine serum (FBS) was purchased from Atlanta Biologicals (Lawenceville, GA). Ketoconazole, quinidine, hydroxyl ethyl piperazine ethane sulfonic acid (HEPES), D-glucose, propylene glycol, triton X-100, cremophor EL and all other chemicals and solvents were purchased from Sigma-Aldrich Co. (St. Louis, MO) or Fisher Scientific Ltd.,Co. (Pittsburgh, PA).

**Animals**

Male Sprague–Dawley rats with jugular vein cannulated catheters, weighing 200–250 grams, were obtained from Charles River Laboratories International, Inc. (Wilmington, MA). Animals were used in accordance with the protocol approved by University of Missouri-Kansas City Institutional Animal Care and Use Committee (IACUC) and housed in Laboratory Animal Research Core (LARC) facilities at University of Missouri-Kansas City. Before experiments, all rates were fasted overnight with free access to water.

**Cell Culture**

MMC and HepG2 cells were seeded in 75 $cm^2$ cell culture flasks and incubated at 37°C, in a humidified atmosphere of 5% $CO_2$, 90% relative humidity. MMC cells were maintained in DMEM containing 10% heat-inactivated FBS, 20 mM HEPES, 29 mM

sodium bicarbonate, 100 units/ml penicillin, and 100 μg/ml streptomycin. HepG2 cells were maintained in MEM with Earle's B salt solution supplemented with 10% FBS, 2 mM *L*-glutamine, 0.1 mM MEM non-essential amino acids, 1 mM sodium pyruvate, 1.5 g/L sodium bicarbonate, 100 units/ml penicillin, and 100 μg/ml streptomycin. Medium was changed every alternate day. After 7-days postseeding, cells were harvested and passaged using TrypLE™ Express Stable Trypsin Replacement, and seeded on 12-well Transwell® inserts (diameter 12 mm, pore size 0.4μm, Corning, Lowell, MA) at the density of $7.5 \times 10^4$ cells /$cm^2$ for MMC cells, and 12-well tissue culture plates at the density of $2 \times 10^4$ cells /$cm^2$ for HepG2 cells, respectively.

**Construction of *in vitro* MMC/HepG2 Co-culture Model**

MMC cells and HepG2 cells were grown separately for 5-7 days before the experiment. The monolayer integrity of MMC was monitored by measuring transepithelial electrical resistance (TEER) values using volt–ohm meter (EVOM-G, World Precision Instruments, Sarasota, FL). Only the monolayers with TEER values of around 600 Ω•$cm^2$ were used as permeability barriers. Before the experiments, both cell lines were washed twice with IPBS (pH7.4). Then 12-well Transwell inserts on which MMC cells have been cultured were installed to 12-well tissue culture plates growing HepG2 heptocytes to form co-culture system (Figure 40).

**Assessment of *in vitro* Bioavailability**

The *in vitro* bioavailability of SQV and its prodrugs was evaluated and compared using MMC/HepG2 co-culture system constructed in this study. Working volumes of the

apical (AP) and basolateral (BL) compartments were 0.5 and 1.5 ml, respectively. IPBS (pH 7.4) in the absence (as control) or presence of P-gp inhibitor (75 µM quinidine) and/or CYP3A4 inhibitor (10 µM ketoconazole) were added in both AP and BL chambers. After 15 min-preincubation, various SQV (10 µM) and prodrug (25 µM) solutions with or without the above inhibitors were used to replace IPBS in AP chambers to initiate transport process. Selection of donor concentrations is dependent on the detection of SQV and prodrugs in receiver chambers. Aliquots (200 µl) were withdrawn from BL chambers at predetermined time intervals over a period of 3 h and replaced with same volume of fresh transport medium (fresh IPBS, pH 7.4, or different inhibitor solutions in IPBS, pH7.4) to maintain sink conditions. Samples were stored at −80ºC until further analysis using LC-MS/MS.

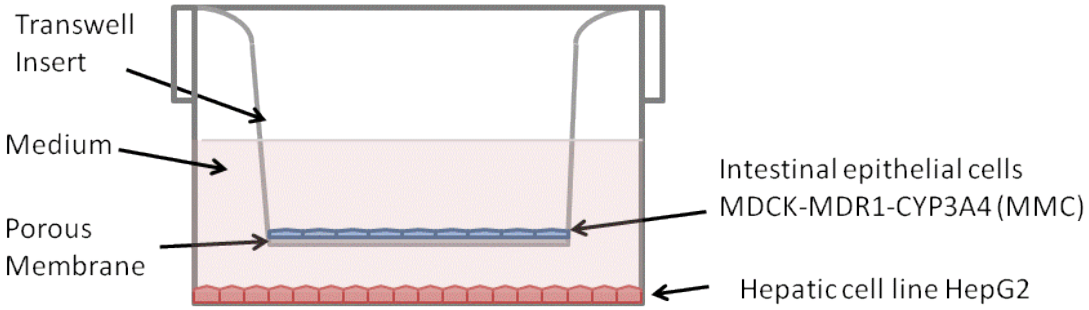


Figure 40. Construction of *in vitro* co-culture cell model MMC/HepG2.

**Oral Absorption Studies**

Oral absorption studies of SQV and prodrugs LDS and DLS were carried out at an equivalent dose of 30 mg/kg for didpeptide prodrugs corresponding to 25mg/kg SQV.

Solvent system employed to prepare drug solutions was 50:50 (v/v) propylene glycol and water. Rats were divided into 3 groups. According to statistical results of Power Analysis for two-group independent sample t-test (G*Power 3.1.7 version, University of Kiel, Germany), sample size was designed to be 3 animals for each group in this study. Maximum dose volume 0.8 ml was administered by oral gavage. Blood samples (200 μl) were collected from the jugular vein cannula at pre-determined time intervals over a period of 8 h post dosing. Heparinized saline (100 μl, 10 IU/ml) was injected through the vein to prevent clots in the catheter and maintain a fairly constant fluid volume. At the end of experiment animals were euthanized by administering an excess dose of sodium pentobarbital (100 mg/kg). Blood samples were collected in heparin-coated micro-centrifuge tubes and centrifuged at 5000 ×g, 4°C for 10 min to separate plasma. The plasma samples were immediately diluted with 50 μl ice-cold acetonitrile and centrifuged at 5000 ×g, 4°C for 15 min to precipitate protein. The supernatants were decanted and dried in vacuo (DD-4X GeneVac, Gardiner, NY) and the residue was stored at −80°C until further analysis by LC-MS/MS.

**Sample Preparation and Analysis**

All SQV and prodrug samples were prepared using liquid-liquid extraction technique following the procedure in Chapter 5. Analysis procedures using LC-MS/MS system have been described in Chapter 4.

**Data Analysis**

Apparent permeability coefficients $P_{app}$ (cm/s) were calculated by linear regression analysis on the time course plot of amount of drugs transported across MMC cell monolayers.

$$P_{app} = \frac{TR_{cum}/dt}{C_0 \times A}$$

where $TR_{cum}/dt$ is the flux rate of SQV or prodrugs obtained from the slope of transport profile. $A$ is the surface area of cell monolayers. $C_0$ is initial concentration of (pro)drugs in apical chambers of MMC/HepG2 co-culture system.

Pharmacokinetic parameters were calculated with noncompartmental analysis (NCA) of plasma drug concentration-time profiles upon oral administrations of SQV and prodrugs DLS and LDS using Phoenix WinNonlin professional v6.1 (Pharsight Corp., Mountain View, CA).

All experiments were conducted at least in triplicate. Results from *in vivo/in vivo* experiments are expressed as mean ± standard error (SE). Statistical significance was detected using Student's *t* test. Difference between mean values was considered significant at $p < 0.05$ and very significant at $p < 0.01$.

## Results

### *In vitro* Bioavailability Prediction using MMC/HepG2 system

Co-culture cell system MMC/HepG2 was developed in this study to simulate the most relevant environment of drug's disposition *in vivo*. *In vitro* bioavailability of SQV and its prodrugs was predicted by determination of absorptive apparent permeability ($P_{app}$) on apical to basolateral direction across this co-culture cell model. Results in Figure 41

indicate that, in comparison with SQV with a $P_{app}$ value of (0.62 ± 0.02) × $10^{-6}$ cm/s, a significantly higher permeability was obtained by all prodrugs tested. LDS and DLS exhibited the most enhanced $P_{app}$ across MMC/HepG2 co-culture, which were observed to be 4- fold (2.50 × $10^{-6}$ cm/s) and 3.5- fold (2.17 × $10^{-6}$ cm/s) higher than SQV, respectively. Two amino acid prodrugs LS and DS also displayed higher $P_{app}$ values than SQV, but to a less extent as compared with dipeptide prodrugs, suggesting a relative lower *in vitro* bioavailability than dipeptide derivatives of SQV.

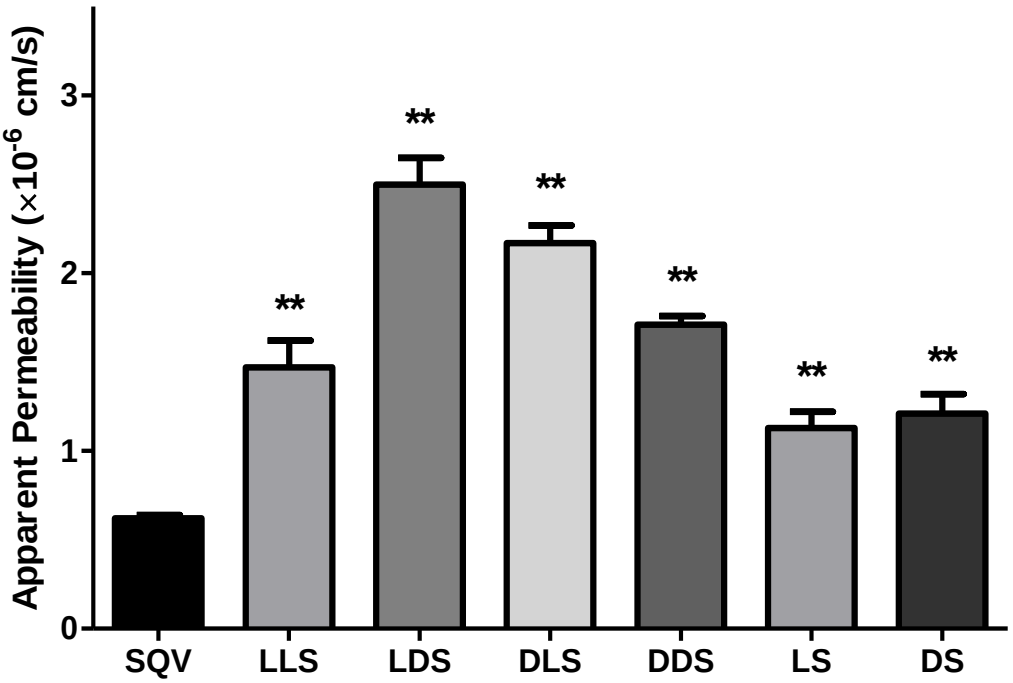


Figure 41. Apparent permeability of absorptive transport of SQV and its stereoisomeric prodrugs across *in vitro* cell co-culture cell model MCC/HepG2.

Each data point represents mean ± SE (n=4). ** $P$ < 0.01 for statistical difference between SQV and prodrug values.

Then permeability studies of SQV and prodrugs across co-culture MMC/HepG2 cell system were evaluated in the presence of efflux pump inhibitor quinidine (75 μM) and/or metabolizing enzyme inhibitor ketoconazole (10 μM). Results are summarized in Table 16. Co-administration of qunidine, ketoconazole and quinidine+ketoconazole contributed to a 3-, 3- and 3.5- times enhancement in absorptive permeability of SQV, respectively. All prodrugs also generated enhanced permeabilities, but to a lower extent relative to SQV. A 1.5-2.5 times higher permeability was observed in the presence of both qunidine and ketoconazole than drug alone. Among dipeptide prodrugs, LLS appears to be the most susceptive to metabolizing enzymes, with $P_{app}$ of $(3.49 \pm 0.28) \times 10^{-6}$ cm/s when co-administered with 10 μM ketoconazole, about 2.4- fold higher than it alone.

Table 16. Apparent permeabilities ($P_{app}$, $\times 10^{-6}$ cm/s) of SQV and stereoisomeric prodrugs across *in vitro* co-culture cell model MMC/HepG2.

| | SQV | LS | DS | LLS | LDS | DLS | DDS |
|---|---|---|---|---|---|---|---|
| Drug alone | 0.62±0.02 | 1.13±0.09** | 1.21±0.11** | 1.47±0.15** | 2.50±0.15** | 2.17±0.10** | 1.71±0.05** |
| +Quinidine (75 μM) | 1.82±0.08 | 1.26±0.10 | 1.41±0.03 | 2.21±0.14 | 3.32±0.20 | 3.23±0.32 | 2.03±0.09 |
| +Ketoconazole (10 μM) | 1.81±0.14 | 1.60±0.02 | 1.59±0.20 | 3.49±0.28 | 3.67±0.12 | 3.41±0.30 | 2.05±0.08 |
| +Quinidine (75 μM) & Ketoconazole (10 μM) | 2.15±0.05 | 1.88±0.05 | 1.84±0.10 | 3.69±0.04 | 4.28±0.18 | 4.30±0.12 | 2.36±0.38 |

Data represented are mean ±SE ($n$ = 4). ** $P < 0.01$ for statistical difference between SQV and prodrug values.

**Oral Administration in Rats**

Plasma concentration versus time profiles for SQV and equivalent dose of dipeptide prodrugs LDS and DLS after single oral administration have been illustrated in this study (Figure 42, 43). Pharmacokinetic parameters after oral dosing of SQV and prodrugs in rats are outlined in Table 17. Following oral aqueous gavage dosing with SQV, initial drug absorption was rapid with a $t_{max}$ value of 0.22 h and $C_{max}$ value of 46.1 ± 6.1 nM, and followed by rapid drug elimination. Subsequently a second SQV absorption peak appeared at about 3 h followed again by rapid elimination (Figure 42). Whereas only one absorption peak was obtained after oral administration of LDS and DLS, and the $t_{max}$ values were estimated to be about 2.0 h and 3.0 h, respectively (Figure 43). In comparison to parent drug, both prodrugs showed remarkably enhanced $C_{max}$, about 8-fold (366.3 ± 89.1 nM for LDS) and 1.5-fold (66.4 ± 7.3 nM for DLS) higher than SQV. As indicated in Table 17, $AUC_{0\text{-}8h}$ values of LDS (1846.14 ± 478.29 h·nmol/l) and DLS (377.95 ± 90.50 h·nmol/l) were 10-fold and 2-fold higher than that of SQV (178.58 ± 16.08 h·nmol/l), respectively. These results are consistent with what we found in *in vitro* studies. Therefore prodrug modifications showed higher absorptive permeability across intestinal barrier probably due to evasion of P-gp-mediated efflux as well as facilitated transport by peptide transporters. Prodrug LDS also exhibited lower clearance (10 times less) and longer mean residence time (MRT) (1.3-fold higher) than SQV (Table 17), probably due to lower rate of enzymatic metabolism.

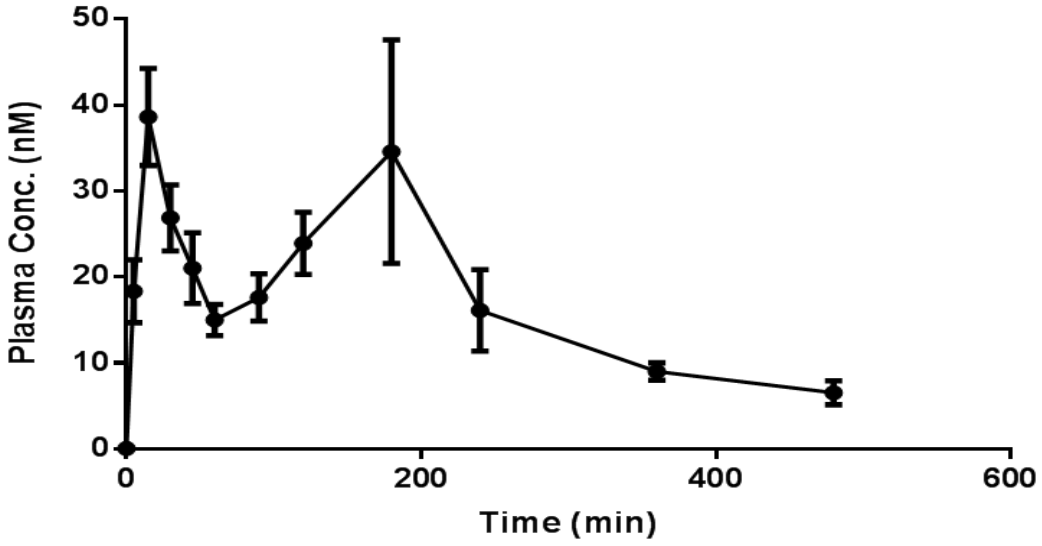


Figure 42. Plasma concentration-time profile of SQV after oral administration (25 mg/kg) in rats. Each data point represents mean ± SE (n=3).

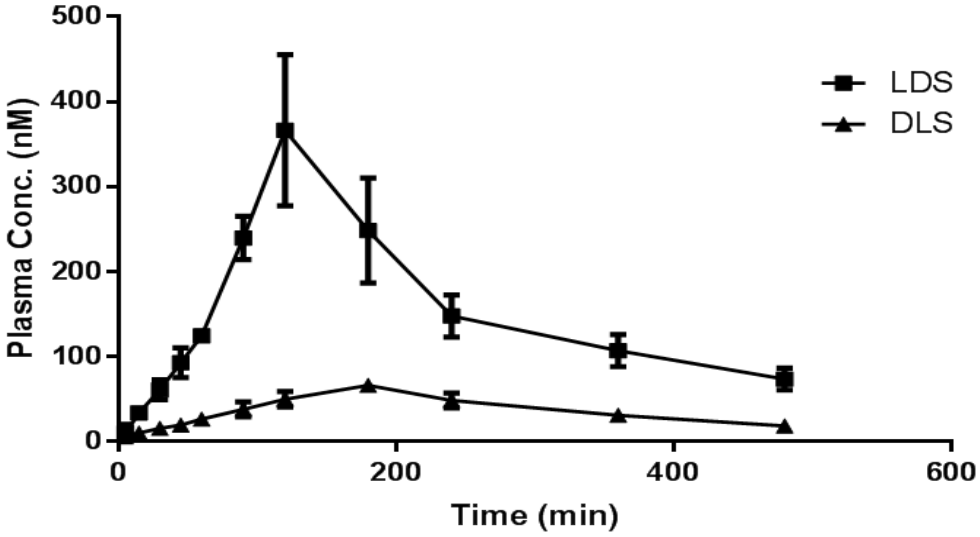


Figure 43. Plasma concentration-time profiles of SQV stereoisomeric dipeptide prodrugs LDS and DLS after single oral administration (30 mg/kg) in rats. Each data point represents mean ± SE (n=3).

Table 17. Estimated pharmacokinetic parameters of SQV and equivalent dose of prodrugs after oral administration in rats.

| Parameter | SQV | LDS | DLS |
|---|---|---|---|
| Lambda_z (1/h) | 0.2320 ± 0.0910 | 0.1700 ± 0.0490 | 0.2540 ± 0.0364 |
| Half-life (h) | 3.9 ± 1.1 | 5.2 ± 2.1 | 2.8 ± 0.4 |
| $t_{max}$ (h) | 3.0 | 2.0 | 3.0 |
| $C_{max}$ (nM) | 46.1 ± 6.1 | 366.3 ± 89.1 | 66.4 ± 7.3 |
| $AUC_{(0\text{-}8h)}$ (h ·nmol/l) | 178.58 ± 16.08 | 1846.14 ± 478.29 | 377.95 ± 90.50 |
| Clearance (l/h/kg) | 210.8 ± 19.8 | 20.9 ± 5.1 | 99.2 ± 19.3 |
| MRT (h) | 5.66 ± 0.86 | 7.52 ± 2.11 | 5.53 ± 0.49 |

Data are reported as means ± SE (n=3).

**Determination of SQV Regenerated from Prodrugs**

Plasma concentration versus time profile of SQV and regenerated SQV from equivalent dose of dipeptide prodrugs LDS and DLS after oral administration are illustrated in Figure 44. In comparison to DLS, much more SQV was released by LDS in blood during 8-hour time period. Unlike oral SQV, which showed rapid decrease in plasma concentration after 3 hours of dosing, regeneration of SQV from dipeptide prodrug LDS was observed to slowly rise during the 8-hour process. It suggests that prodrug LDS might provide a controlled release of the active parent drug SQV, and maintain relatively high and steady level.

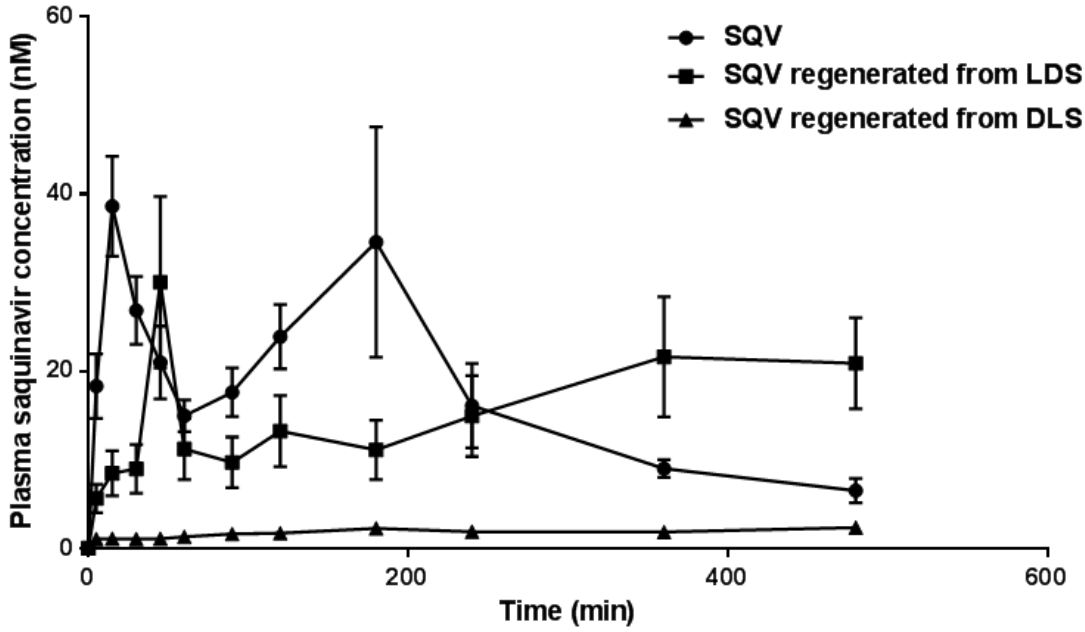


Figure 44. Plasma concentration-time profiles of (regenerated) SQV after oral administration of SQV (25 mg/kg) or its stereoisomeric dipeptide prodrugs LDS and DLS (30 mg/kg) in rats. Each data point represents mean ± SE (n=3).

## Discussion

According to the findings in the previous chapters, all stereoisomeric prodrugs of SQV displayed an enhanced transepithelial transport across Caco-2 cells and human *MDR* gene-transfected MDCK cells (Chapters 5 and 6). A significantly higher stability against CYP3A-mediated oxidative metabolism was also observed by these prodrug modifications in rat hepatic microsomes (Chapter 6). These improvements are believed to be achieved by the cumulative effects of enhanced absorption (targeting influx peptide transporters) and decreased elimination (circumventing efflux pumps and metabolic enzymes). But there was no direct evidence demonstrating that oral bioavailability can be

improved by this prodrug modification. Therefore in the present study, bioavailability of SQV and stereoisomeric prodrugs was first estimated by measuring apparent permeabilities employing a static *in vitro* ADME simulation co-culture cell model.

The bioavailability prediction using *in vitro* co-culture cell models has been proved to be a valuable drug screening method and attracted a lot of interest in recent years (Castrillon et al., 2009; Ouattara et al., 2011). Limitations of MMC/HepG2 co-cultures include relatively lower metabolic activity in HepG2 cells, such as CYP enzymes levels, as compared with primary cultured hepatocytes, and the absence of bloodborne factors that participate in tissue crosstalks occurring *in vivo* (Westerink and Schoonen, 2007; Lin et al., 2012). Yet it is a simple and accessible testing interface to predict kinetic mechanisms of orally administered drugs. Apparent $P_{app}$ values summarized in Table 16 indicate that a significant enhancement in oral bioavailability was observed by prodrugs as compared with SQV. This incremental permeability of SQV prodrugs provides the evidence that intestinal SQV permeation and its metabolic stability against enteric and hepatic enzymes can be improved by prodrug modifications. This result was further confirmed by inhibitory transport studies with specific P-gp and CYP3A4 inhibitors. An enhancement in absorptive permeabilities of prodrugs on MMC/HepG2 was less than that of SQV in the presence of quinidine or ketoconazole, suggesting that affinity of SQV towards efflux pumps and enzymes has been partially overcome by prodrug modification. Moreover, this *in vitro* bioavailability prediction appears to be stereoselective. Among dipeptide prodrugs, DDS exhibited the highest stability against metabolizing enzymes and the least affinity for P-gp efflux (Table 16), but its bioavailability was estimated to be much less than LDS and DLS, about 70% for LDS and 80% for DLS (Figure 41). It is

probably due to poor recognition of *D*-valines in promoiety of the prodrug by peptide transporter. LDS and DLS appear to be the best prodrug candidates since these two compounds might exhibit the most enhanced bioavailabilities over parent drug SQV. Taking into account of protein unbound fraction (Table 11), the concentration of unbound LDS is 5.5-fold higher than unbound SQV in rat plasma, and unbound DLS is about 3 times more than free SQV.

Subsequently *in vivo* bioavailability of SQV and the best prodrug candidates LDS and DLS was determined in male Sprague–Dawley rats. Figure 42 illustrates that the double absorption peaks and relatively rapid absorption and elimination were observed in the plasma concentration versus time profile after oral dosing with SQV mesylate salt in rats. This result is probably due to the low drug solubility in gut fluid, rapid metabolism and reabsorption. Rats do not have gall bladder, but enterohepatic circulation (EHC) exists in rats since bile can be excreted into the duodenum by the cannulated bile duct (Kuipers et al., 1985; van Wijk et al., 2001). Thus, once hydrophobic SQV was absorbed in systemic circulation, it was eliminated rapidly and transported into bile, and SQV in bile may be reabsorbed back into intestine and form the second absorption peak. This result is confirmed by the previous reports (Buchanan et al., 2008).

Higher $C_{max}$ and AUC values were observed by prodrugs relative to SQV, particularly LDS exhibited a dramatically higher AUC and $C_{max,}$ which are about 10- and 8- fold higher than SQV, respectively. Moreover prodrug LDS exhibited longer MRT, lower terminal elimination rate (lambda_z) and slower clearance values, suggesting that it is much more stable in blood circulation than parent drug SQV. All of these data taken together provide evidence that oral bioavailability of prodrugs is greater than SQV. These

*in vivo* observations are consistent with what we found with *in vitro* MMC/HepG2 co-culture system. Oral bioavailability followed the same rank order of LDS > DLS > SQV in both *in vitro* and *in vivo* studies. But LDS showed remarkably higher bioavailability in rats than *in vitro* cell-based model. Such differential results may be due to the variety of expression and activities of enzymes and transporters under physiological conditions and cell-based milieu. In comparison with fresh-isolated primary human hepatocytes, hepatic cell line HepG2 shows significantly lower levels of phase I drug-metabolizing enzymes and moderately lower levels of phase II enzymes (Lin et al., 2012). Besides, MDCK cell lines have been reported for the reduced activity of peptide transporters after transfecting with human *MDR* genes (Wang et al., 2013). Therefore such disparity in activities of enzymes and transporters may contribute to the differential absorption and biotransformation of SQV prodrugs, and subsequently display extremely different bioavailability.

Although we observed that prodrugs show higher oral bioavailability than SQV, it is critical to determine the amount of SQV regenerated from prodrugs into the systemic circulation because the antiviral activity (such as $IC_{50}$ for HIV-1) of SQV is always higher than its prodrugs (Farese-Di Giorgio et al., 2000; Gaucher et al., 2004). LDS and DLS have been considered to be the best prodrug candidates according to *in vitro* studies. However, plasma concentration of SQV regenerated from LDS was much higher than DLS in rats. It indicates that LDS is more susceptive towards hydrolytic enzymes present in rats compared to DLS, and ester bond between parent drug and pro-moiety *L*-valine-*D*-valine- of LDS is easier to be cleaved to release more free and active SQV in the systemic circulation as compared to DLS. Results in Figure 44 also demonstrate a

controlled, prolonged release of SQV regenerated from LDS, suggesting that prodrug *L*-valine-*D*-valine-SQV may be a good substitute for SQV in clinical application. LDS can provide a continuous and effective therapeutic plasma concentration, as well as prevent development of resistant viral strains. It is critically important for drugs with narrow therapeutic index like SQV, especially for patients with chronic disease such as HIV-1 infection requiring long-term treatment.

In conclusion, the study in this chapter is the first investigation to evaluate pharmacokinetics of stereoisomeric valine-based SQV prodrugs using both *in vitro* and *in vivo* models. Our studies indicate an overall good correlation between *in vitro* and *in vivo* results. Oral bioavailability of SQV can be enhanced significantly by dipeptide derivative *L*-valine-*D*-valine-SQV. This enhancement is attributed to the cumulative effects of higher intestinal permeation facilitated by peptide transporters and evasion of both P-gp-mediated efflux and CYP-mediated biotransformation. These findings demonstrate that peptide transporter-targeted prodrug strategy has enormous promise for improving the intestinal absorption and oral bioavailability of poorly absorbed antiviral agent saquinavir via the oral route of administration.

# CHAPTER 8

# SUMMARY AND RECOMMENDATIONS

## Summary

Clinical application of SQV is remarkably limited by its low oral bioavailability. Low aqueous solubility, high affinity for efflux proteins, fast CYP-mediated metabolism and high plasma protein binding are considered to be the major obstacles contributing to poor bioavailability of SQV. The purpose of this dissertation project is to design new transporter-targeted prodrugs to circumvent these biological and physicochemical barriers, and consequently to improve oral bioavailability and therapeutic outcomes of SQV.

SQV is a high-affinity substrate for both efflux pumps and metabolizing enzymes. Hence our first purpose of this project is to modify molecular structure by conjugating with specific dipeptide pro-moieties, thereby to reduce the interaction between SQV and these proteins/enzymes. Moreover, peptide transporters essential for the intake and transport of various "peptidomimetic" xenobiotics are expressed on the cellular membranes of various tissues including intestine. So SQV dipeptide prodrugs proposed in this project could be recognized easily by the peptide transporter-mediated influx system and ferried across the epithelial membrane. In addition, typically different stereoisomeric prodrugs exhibit varied stereoselectivity in biological and physicochemical properties such as aqueous solubility, plasma protein binding, and enzymatic hydrolysis. With this background, a series of stereoisomeric valine-SQV (*L*- and *D*-) and valine-valine-SQV (*L*-*L*-, *L*-*D*-, *D*-*L*-, and *D*-*D*-) were designed and identified in this project (Chapter 4), and their *in vitro* and *in vivo* evaluations are demonstrated in the following chapters. Overall assessment of these transporter-targeted prodrugs has been summarized in Table 18.

Table 18. Overall i*n vitro/in vivo* evaluations of transporter-targeted dipeptide prodrugs synthesized in this project to overcome major obstacles of SQV in oral administration

| | Stereoisomeric dipeptide prodrugs | | | |
|---|---|---|---|---|
| | LLS | LDS | DLS | DDS |
| Major problems of SQV | | | | |
| Low aqueous solubility | ↑ | ↑ | ↑ | ↑ |
| High affinity for efflux pumps | ↓ | ↓ | ↓ | ↓ |
| Fast CYP metabolism | ↓ | ↓ | ↓ | ↓ |
| High plasma protein binding | ↓ | ↓ | ↑ | ↑ |
| Properties of prodrugs | | | | |
| Recognition by PepT | Yes | Yes | Yes | No |
| Stability against hydrolytic enzymes | LLS << LDS ≤ DLS < DDS | | | |
| Bioavailability evaluation | | | | |
| *In vitro* co-culture cell model | SQV < LLS ≈ DDS < DLS < LDS | | | |
| Single dose of oral administration to rats | | ↑↑↑ | ↑ | |

With regards to the four major unfavorable properties of SQV, all four dipeptide prodrugs showed improved aqueous solubility and reduced affinity for both efflux pumps (P-gp and MRP2) and CYP3A enzymes as compared with parent drug SQV (Table 18). Plasma protein binding was found to be stereoselective, because LLS and LDS showed less protein binding than SQV whereas DDS and DLS exhibited higher protein binding levels in rat plasma. These findings indicate that dipeptide prodrug modification provides

a good strategy to overcome biological obstacles contributing to low oral bioavailability of SQV.

Interaction between proposed prodrugs and influx peptide transporters as well as their degradation catalyzed by hydrolytic enzymes were then investigated, and results are compared in Table 18. All prodrugs except DDS can be recognized by peptide transporters-mediated influx system expressed on cellular membrane surface of *in vitro* cell-based models. Hydrolysis studies performed in rat intestinal homogenates and plasma demonstrate that prodrugs with *D*-valine in pro-moieties exhibited significantly reduced biodegradation, and the rank order of stability against hydrolytic enzymes has been obtained to be LLS << LDS ≤ DLS < DDS.

Based on these *in vitro* observations, LDS and DLS could be the best prodrug candidates possessing both high affinity for influx transport system and proper resistance against hydrolytic enzymes. This result was confirmed by the prediction of *in vitro* bioavailability using a MMC/HepG2 co-culture cell system (Table 18). Enhanced apparent transepithelial permeabilities over SQV were achieved by all stereoisomeric prodrug modifications, and LDS exhibited the most enhanced bioavailability as compared with SQV. Finally *in vivo* absorption studies after single-dose oral administration in rats further proved that specific stereoisomeric dipeptide prodrugs like LDS could be applied to improve oral bioavailability of SQV.

Additionally, since MDCK cell lines transfected with various human *MDR* genes have been widely used as *in vitro* cell-based permeability screening models, influence of human efflux transporters (P-gp, MRP2 and BCRP) on the functional activities, and gene and protein expression of endogenous influx peptide transporters in these cell lines was

also evaluated in this dissertation project (Chapter 4). Results demonstrate that overexpression of *MDR* genes can reduce PepT function probably due to the phenomenon of transporter-compensation resulting in down-regulation of endogenous genes. It may provide some mechanistic insight into possible reasons for underestimation in drug screening using these cell models.

## Recommendations

Besides the poor oral bioavailability, low brain absorption is another major challenge in current SQV application for the treatment of HIV infection. Inability to attain sufficient SQV concentration in CNS results in persistent viral replication and a HIV sanctuary site in the brain parenchyma. Expression of peptide transporters (i.e. PepT2) in brain is relatively low, whereas amino acid transport systems such as large neutral amino acid transporter (LAT) exhibit high expression on the BBB. Consequently amino acid prodrugs, which are regenerated from dipeptide prodrugs, may be easily identified and ferried by these amino acid transporters and reach in brain. However, the proposed amino acid prodrug valine-SQV shows poor enzymatic stability regardless of *L*- or *D*- isomers, and very low levels of valine-SQV can be detected in rat plasma. Therefore stereoisomeric SQV prodrugs conjugating with other amino acid pro-moieties, such as leucine, histidine and glutamine, can be developed in future studies. Firstly, different amino acid pro-moieties may contribute to varied enzymatic hydrolysis of prodrugs, and more stable amino acid prodrugs could be obtained by these dipeptide prodrugs. Secondly, other dipeptide prodrugs like histidine-based dipeptide prodrug could be

recognized by other carrier-mediated influx systems expressed on the BBB, such as peptide/histidine transporter 1 (PHT1), and reach CNS at high levels.

Other structural modifications may be also applied in the proposed transporter-targeted stereoisomeric prodrug strategy, such as attaching a linker or spacer between parent drug and dipeptide ligand. This linker/spacer could be carbon chains with varying length. Properties of prodrugs such as solubility, enzymatic stability, anti-HIV activity, and transepithelial permeability may be significantly changed due to the conjugation of linker/spacer. Therefore, modification of molecular structure of pro-moieties will facilitate the development of SQV prodrugs with optimized pharmacokinetic and pharmacodynamic properties.

APPENDIX

My Orders | My Library | My Profile | Welcome zwdhf@mail.umkc.edu | Log out | Help

My Orders > Orders > All Orders

# License Details

This is a License Agreement between Zhiying Wang ("You") and Elsevier ("Elsevier"). The license consists of your order details, the terms and conditions provided by Elsevier, and the payment terms and conditions.

Get the printable license.

| | |
|---|---|
| License Number | 3181550895413 |
| License date | Jul 03, 2013 |
| Licensed content publisher | Elsevier |
| Licensed content publication | International Journal of Pharmaceutics |
| Licensed content title | Influence of overexpression of efflux proteins on the function and gene expression of endogenous peptide transporters in MDR-transfected MDCKII cell lines |
| Licensed content author | Zhiying Wang,Dhananjay Pal,Ashaben Patel,Deep Kwatra,Ashim K. Mitra |
| Licensed content date | 30 January 2013 |
| Licensed content volume number | 441 |
| Licensed content issue number | 1–2 |
| Number of pages | 10 |
| Type of Use | reuse in a thesis/dissertation |
| Portion | full article |
| Format | both print and electronic |
| Are you the author of this Elsevier article? | Yes |
| Will you be translating? | No |
| Order reference number | None |
| Title of your thesis/dissertation | Transporter-Targeted Prodrug Delivery to Improve Oral Bioavailability of Saquinavir |
| Expected completion date | Jul 2013 |
| Elsevier VAT number | GB 494 6272 12 |
| Permissions price | 0.00 USD |
| VAT/Local Sales Tax | 0.00 USD |
| Total | **0.00 USD** |

Back

# License Details

This is a License Agreement between Zhiying Wang ("You") and John Wiley and Sons ("John Wiley and Sons"). The license consists of your order details, the terms and conditions provided by John Wiley and Sons, and the payment terms and conditions.

Get the printable license.

| | |
|---|---|
| License Number | 3175550816019 |
| License cate | Jun 24, 2013 |
| Licensed content publisher | John Wiley and Sons |
| Licensed content publication | Journal of Pharmaceutical Sciences |
| Licensed content title | Stereoselective evasion of P-glycoprotein, cytochrome P450 3A, and hydrolases by peptide prodrug modification of saquinavir |
| Licensed copyright line | Copyright © 2012 Wiley Periodicals, Inc. |
| Licensed content author | Zhiying Wang,Dhananjay Pal,Ashim K. Mitra |
| Licensed content date | May 18, 2012 |
| Start page | 3199 |
| End page | 3213 |
| Type of use | Dissertation/Thesis |
| Requestor type | Author of this Wiley article |
| Format | Electronic |
| Portion | Full article |
| Will you be translating? | No |
| **Total** | **0.00 USD** |

| | |
|---|---|
| **Subject:** | Re: abhipublications.org :: New Inquery |
| **From:** | Managing Editor (ABHI Publications) (managingeditor@abhipublications.org) |
| **To:** | yingziby@yahoo.com; |
| **Date:** | Tuesday, June 25, 2013 5:07 AM |

Dear Sir,
you are cordially welcome to use your work in your dissertation.

---

*Regards,*
*Managing Editor*
*ABHI Publications*
www.abhipublications.org

On Tue, Jun 25, 2013 at 3:37 AM, <yingziby@yahoo.com> wrote:

**Enquery Details**

Dear Admin

| | | |
|---|---|---|
| Full Name | : | Zhiying Wang |
| Address | : | 2464 Charlotte St, HSB 5219 |
| Mobile | : | 1-816-235-5506 |
| Email | : | yingziby@yahoo.com |
| Query | : | Hello, I am graduate student of Division of Pharmaceutical Sciences, at University of Missouri-Kansas City. I am the author of the work "Wang Z, Luo S, Sheng Y, Samanta S, Pal D, Mitra AK. Stereoisomeric Peptide Prodrug Modification to Improve Intestinal Absorption of Saquinavir: Synthesis and in Vitro Evaluation. International Journal of Pharmacy and Engineering (IJPE) 2013, 1(2):93-112" published in your journal. I request your permission to use this work in my dissertation. |

With regards

**ABHI Publications, India (Since 2013)**
**Managing Editor**
Email: managingeditor@abhipublications.org

REFERENCES

(1998) Guidelines for the use of antiretroviral agents in HIV-infected adults and adolescents. Department of Health and Human Services and Henry J. Kaiser Family Foundation. *MMWR Recomm Rep* **47**:43-82.

Acosta EP, Kakuda TN, Brundage RC, Anderson PL and Fletcher CV (2000) Pharmacodynamics of human immunodeficiency virus type 1 protease inhibitors. *Clin Infect Dis* **30 Suppl 2**:S151-159.

Adamson CS, Salzwedel K and Freed EO (2009) Virus maturation as a new HIV-1 therapeutic target. *Expert Opin Ther Targets* **13**:895-908.

Adibi SA and Mercer DW (1973) Protein digestion in human intestine as reflected in luminal, mucosal, and plasma amino acid concentrations after meals. *J Clin Invest* **52**:1586-1594.

Agarwal S, Boddu SH, Jain R, Samanta S, Pal D and Mitra AK (2008) Peptide prodrugs: improved oral absorption of lopinavir, a HIV protease inhibitor. *Int J Pharm* **359**:7-14.

Agarwal S, Jain R, Pal D and Mitra AK (2007a) Functional characterization of peptide transporters in MDCKII-MDR1 cell line as a model for oral absorption studies. *Int J Pharm* **332**:147-152.

Agarwal S, Pal D and Mitra AK (2007b) Both P-gp and MRP2 mediate transport of Lopinavir, a protease inhibitor. *Int J Pharm* **339**:139-147.

Agoram B, Woltosz WS and Bolger MB (2001) Predicting the impact of physiological and biochemical processes on oral drug bioavailability. *Adv Drug Deliv Rev* **50 Suppl 1**:S41-67.

An G and Morris ME (2010) Effects of single and multiple flavonoids on BCRP-mediated accumulation, cytotoxicity and transport of mitoxantrone in vitro. *Pharm Res* **27**:1296-1308.

Anand B, Nashed Y and Mitra A (2003) Novel dipeptide prodrugs of acyclovir for ocular herpes infections: Bioreversion, antiviral activity and transport across rabbit cornea. *Curr Eye Res* **26**:151-163.

Ananworanich J, Gayet-Ageron A, Ruxrungtham K, Chetchotisakd P, Prasithsirikul W, Kiertiburanakul S, Munsakul W, Raksakulkarn P, Tansuphasawadikul S, LeBraz M, Jupimai T, Ubolyam S, Schutz M and Hirschel B (2008) Long-term efficacy and safety of first-line therapy with once-daily saquinavir/ritonavir. *Antivir Ther* **13**:375-380.

Arnaiz JA, Mallolas J, Podzamczer D, Gerstoft J, Lundgren JD, Cahn P, Fatkenheuer G, D'Arminio-Monforte A, Casiro A, Reiss P, Burger DM, Stek M and Gatell JM (2003) Continued indinavir versus switching to indinavir/ritonavir in HIV-infected patients with suppressed viral load. *AIDS* **17**:831-840.

Backman JT, Olkkola KT and Neuvonen PJ (1996) Rifampin drastically reduces plasma concentrations and effects of oral midazolam. *Clin Pharmacol Ther* **59**:7-13.

Balimane PV, Chong S, Patel K, Quan Y, Timoszyk J, Han YH, Wang B, Vig B and Faria TN (2007) Peptide transporter substrate identification during permeability screening in drug discovery: comparison of transfected MDCK-hPepT1 cells to Caco-2 cells. *Arch Pharm Res* **30**:507-518.

Bartlett JG (1990) Management of patients with asymptomatic HIV infection. *Md Med J* **39**:150-155.

Beery E, Rajnai Z, Abonyi T, Makai I, Bansaghi S, Erdo F, Sziraki I, Heredi-Szabo K, Kis E, Jani M, Marki-Zay J, Toth GK and Krajcsi P (2012) ABCG2 modulates chlorothiazide permeability--in vitro-characterization of its interactions. *Drug Metab Pharmacokinet* **27**:349-353.

Belman AL (2002) HIV-1 infection and AIDS. *Neurol Clin* **20**:983-1011.

Biegel A, Knutter I, Hartrodt B, Gebauer S, Theis S, Luckner P, Kottra G, Rastetter M, Zebisch K, Thondorf I, Daniel H, Neubert K and Brandsch M (2006) The renal type H+/peptide symporter PEPT2: structure-affinity relationships. *Amino Acids* **31**:137-156.

Boerner P, Evans-Laying M, U HS and Saier MH, Jr. (1986) Polarity of neutral amino acid transport and characterization of a broad specificity transport activity in a kidney epithelial cell line, MDCK. *J Biol Chem* **261**:13957-13962.

Boffito M, Hoggard PG, Reynolds HE, Bonora S, Meaden ER, Sinicco A, Di Perri G and Back DJ (2002) The unbound percentage of saquinavir and indinavir remains constant throughout the dosing interval in HIV positive subjects. *Br J Clin Pharmacol* **54**:262-268.

Boll M, Herget M, Wagener M, Weber WM, Markovich D, Biber J, Clauss W, Murer H and Daniel H (1996) Expression cloning and functional characterization of the kidney cortex high-affinity proton-coupled peptide transporter. *Proc Natl Acad Sci U S A* **93**:284-289.

Brandsch M, Ganapathy V and Leibach FH (1995) H(+)-peptide cotransport in Madin-Darby canine kidney cells: expression and calmodulin-dependent regulation. *Am J Physiol* **268**:F391-397.

Brandsch M, Knutter I and Bosse-Doenecke E (2008) Pharmaceutical and pharmacological importance of peptide transporters. *J Pharm Pharmacol* **60**:543-585.

Buchanan CM, Buchanan NL, Edgar KJ, Little JL, Ramsey MG, Ruble KM, Wacher VJ and Wempe MF (2008) Pharmacokinetics of saquinavir after intravenous and oral dosing of saquinavir: hydroxybutenyl-beta-cyclodextrin formulations. *Biomacromolecules* **9**:305-313.

Buchler M, Konig J, Brom M, Kartenbeck J, Spring H, Horie T and Keppler D (1996) cDNA cloning of the hepatocyte canalicular isoform of the multidrug resistance protein, cMrp, reveals a novel conjugate export pump deficient in hyperbilirubinemic mutant rats. *J Biol Chem* **271**:15091-15098.

Buss N, Snell P, Bock J, Hsu A and Jorga K (2001) Saquinavir and ritonavir pharmacokinetics following combined ritonavir and saquinavir (soft gelatin capsules) administration. *Br J Clin Pharmacol* **52**:255-264.

Castrillon L, Fernandez-Nava Y, Maranon E, Garcia L and Berrueta J (2009) Anoxic-aerobic treatment of the liquid fraction of cattle manure. *Waste Manag* **29**:761-766.

Chan DC and Kim PS (1998) HIV entry and its inhibition. *Cell* **93**:681-684.

Chandra S, Mondal D and Agrawal KC (2009) HIV-1 protease inhibitor induced oxidative stress suppresses glucose stimulated insulin release: protection with thymoquinone. *Exp Biol Med (Maywood)* **234**:442-453.

Chen G, Zhang D, Jing N, Yin S, Falany CN and Radominska-Pandya A (2003) Human gastrointestinal sulfotransferases: identification and distribution. *Toxicol Appl Pharmacol* **187**:186-197.

Chen LF, Hoy J and Lewin SR (2007) Ten years of highly active antiretroviral therapy for HIV infection. *Med J Aust* **186**:146-151.

Cheng T, Zhao Y, Li X, Lin F, Xu Y, Zhang X, Li Y, Wang R and Lai L (2007) Computation of octanol-water partition coefficients by guiding an additive model with knowledge. *J Chem Inf Model* **47**:2140-2148.

Clement JG and Erhardt N (1990) Serum carboxylesterase activity in various strains of rats: sensitivity to inhibition by CBDP (2-/o-cresyl/4H:1:3:2-benzodioxaphosphorin-2-oxide). *Arch Toxicol* **64**:414-416.

Clotet B (2004) Strategies for overcoming resistance in HIV-1 infected patients receiving HAART. *AIDS Rev* **6**:123-130.

Collet L, Veuillet E, Chanal JM, Desreux V, Mermet B, Disant F and Morgon A (1992) [Study of the ototoxicity of amikacin and netilmicin using provoked acoustic oto-emissions and high-frequency audiometry]. *Pathol Biol (Paris)* **40**:990-992.

Constantinides PP and Wasan KM (2007) Lipid formulation strategies for enhancing intestinal transport and absorption of P-glycoprotein (P-gp) substrate drugs: in vitro/in vivo case studies. *J Pharm Sci* **96**:235-248.

Cooray HC, Blackmore CG, Maskell L and Barrand MA (2002) Localisation of breast cancer resistance protein in microvessel endothelium of human brain. *Neuroreport* **13**:2059-2063.

Cornwell MM and Smith DE (1993) SP1 activates the MDR1 promoter through one of two distinct G-rich regions that modulate promoter activity. *J Biol Chem* **268**:19505-19511.

Czernik PJ, Little JM, Barone GW, Raufman JP and Radominska-Pandya A (2000) Glucuronidation of estrogens and retinoic acid and expression of UDP-glucuronosyltransferase 2B7 in human intestinal mucosa. *Drug Metab Dispos* **28**:1210-1216.

Daniel H and Kottra G (2004) The proton oligopeptide cotransporter family SLC15 in physiology and pharmacology. *Pflugers Arch* **447**:610-618.

David S, Barros V, Cruz C and Delgado R (2005) In vitro effect of free and complexed indium(III) against Mycobacterium tuberculosis. *FEMS Microbiol Lett* **251**:119-124.

Decker CJ, Laitinen LM, Bridson GW, Raybuck SA, Tung RD and Chaturvedi PR (1998) Metabolism of amprenavir in liver microsomes: role of CYP3A4 inhibition for drug interactions. *J Pharm Sci* **87**:803-807.

Desiderio C, Cavallaro RA, De Rossi A, D'Anselmi F, Fuso A and Scarpa S (2005) Evaluation of chemical and diastereoisomeric stability of S-adenosylmethionine in aqueous solution by capillary electrophoresis. *J Pharm Biomed Anal* **38**:449-456.

Dodiya SS, Chavhan SS, Sawant KK and Korde AG (2011) Solid lipid nanoparticles and nanosuspension formulation of Saquinavir: preparation, characterization, pharmacokinetics and biodistribution studies. *J Microencapsul* **28**:515-527.

Donato MT, Lahoz A, Castell JV and Gomez-Lechon MJ (2008) Cell lines: a tool for in vitro drug metabolism studies. *Curr Drug Metab* **9**:1-11.

Doyle L and Ross DD (2003) Multidrug resistance mediated by the breast cancer resistance protein BCRP (ABCG2). *Oncogene* **22**:7340-7358.

Doyle LA, Yang W, Abruzzo LV, Krogmann T, Gao Y, Rishi AK and Ross DD (1998) A multidrug resistance transporter from human MCF-7 breast cancer cells. *Proc Natl Acad Sci U S A* **95**:15665-15670.

Duong M, Petit JM, Martha B, Galland F, Piroth L, Walldner A, Grappin M, Buisson M, Duvillard L, Chavanet P and Portier H (2006) Concentration of circulating oxidized

LDL in HIV-infected patients treated with antiretroviral agents: relation to HIV-related lipodystrophy. *HIV Clin Trials* **7**:41-47.

Eagling VA, Back DJ and Barry MG (1997) Differential inhibition of cytochrome P450 isoforms by the protease inhibitors, ritonavir, saquinavir and indinavir. *Br J Clin Pharmacol* **44**:190-194.

Eagling VA, Wiltshire H, Whitcombe IW and Back DJ (2002) CYP3A4-mediated hepatic metabolism of the HIV-1 protease inhibitor saquinavir in vitro. *Xenobiotica* **32**:1-17.

Engeland K and Maret W (1993) Extrahepatic, differential expression of four classes of human alcohol dehydrogenase. *Biochem Biophys Res Commun* **193**:47-53.

Eriksson T, Bjorkman S and Hoglund P (2001) Clinical pharmacology of thalidomide. *Eur J Clin Pharmacol* **57**:365-376.

Ernest CS, 2nd, Hall SD and Jones DR (2005) Mechanism-based inactivation of CYP3A by HIV protease inhibitors. *J Pharmacol Exp Ther* **312**:583-591.

Faesch R (1991) [A case from practice (209). Gilbert syndrome]. *Schweiz Rundsch Med Prax* **80**:208-209.

Fang G, Konings WN and Poolman B (2000) Kinetics and substrate specificity of membrane-reconstituted peptide transporter DtpT of Lactococcus lactis. *J Bacteriol* **182**:2530-2535.

Farese-Di Giorgio A, Rouquayrol M, Greiner J, Aubertin AM, Vierling P and Guedj R (2000) Synthesis and anti-HIV activity of prodrugs derived from saquinavir and indinavir. *Antivir Chem Chemother* **11**:97-110.

Fei YJ, Kanai Y, Nussberger S, Ganapathy V, Leibach FH, Romero MF, Singh SK, Boron WF and Hediger MA (1994) Expression cloning of a mammalian proton-coupled oligopeptide transporter. *Nature* **368**:563-566.

Figgitt DP and Plosker GL (2000) Saquinavir soft-gel capsule: an updated review of its use in the management of HIV infection. *Drugs* **60**:481-516.

Fitzsimmons ME and Collins JM (1997) Selective biotransformation of the human immunodeficiency virus protease inhibitor saquinavir by human small-intestinal cytochrome P4503A4: potential contribution to high first-pass metabolism. *Drug Metab Dispos* **25**:256-266.

Flanagan SD, Cummins CL, Susanto M, Liu X, Takahashi LH and Benet LZ (2002) Comparison of furosemide and vinblastine secretion from cell lines overexpressing multidrug resistance protein (P-glycoprotein) and multidrug resistance-associated proteins (MRP1 and MRP2). *Pharmacology* **64**:126-134.

Flexner C (1998) HIV-protease inhibitors. *N Engl J Med* **338**:1281-1292.

Fountoulakis M and Suter L (2002) Proteomic analysis of the rat liver. *J Chromatogr B Analyt Technol Biomed Life Sci* **782**:197-218.

Gallant JE (2004) Protease-inhibitor boosting in the treatment-experienced patient. *AIDS Rev* **6**:226-233.

Ganapathy ME, Brandsch M, Prasad PD, Ganapathy V and Leibach FH (1995) Differential recognition of beta -lactam antibiotics by intestinal and renal peptide transporters, PEPT 1 and PEPT 2. *J Biol Chem* **270**:25672-25677.

Ganapathy V and Leibach FH (1996) Peptide transporters. *Curr Opin Nephrol Hypertens* **5**:395-400.

Gao F, Bailes E, Robertson DL, Chen Y, Rodenburg CM, Michael SF, Cummins LB, Arthur LO, Peeters M, Shaw GM, Sharp PM and Hahn BH (1999) Origin of HIV-1 in the chimpanzee Pan troglodytes troglodytes. *Nature* **397**:436-441.

Garcia-Lerma JG and Heneine W (2001) Resistance of human immunodeficiency virus type 1 to reverse transcriptase and protease inhibitors: genotypic and phenotypic testing. *J Clin Virol* **21**:197-212.

Gaucher B, Rouquayrol M, Roche D, Greiner J, Aubertin AM and Vierling P (2004) Prodrugs of HIV protease inhibitors-saquinavir, indinavir and nelfinavir-derived from diglycerides or amino acids: synthesis, stability and anti-HIV activity. *Org Biomol Chem* **2**:345-357.

Giacomini KM, Huang SM, Tweedie DJ, Benet LZ, Brouwer KL, Chu X, Dahlin A, Evers R, Fischer V, Hillgren KM, Hoffmaster KA, Ishikawa T, Keppler D, Kim RB, Lee CA, Niemi M, Polli JW, Sugiyama Y, Swaan PW, Ware JA, Wright SH, Yee SW, Zamek-Gliszczynski MJ and Zhang L Membrane transporters in drug development. *Nat Rev Drug Discov* **9**:215-236.

Giacomini KM, Huang SM, Tweedie DJ, Benet LZ, Brouwer KL, Chu X, Dahlin A, Evers R, Fischer V, Hillgren KM, Hoffmaster KA, Ishikawa T, Keppler D, Kim RB, Lee CA, Niemi M, Polli JW, Sugiyama Y, Swaan PW, Ware JA, Wright SH, Yee SW, Zamek-Gliszczynski MJ and Zhang L (2010) Membrane transporters in drug development. *Nat Rev Drug Discov* **9**:215-236.

Gibbs JP, Yang JS and Slattery JT (1998) Comparison of human liver and small intestinal glutathione S-transferase-catalyzed busulfan conjugation in vitro. *Drug Metab Dispos* **26**:52-55.

Gisolf EH, Enting RH, Jurriaans S, de Wolf F, van der Ende ME, Hoetelmans RM, Portegies P and Danner SA (2000) Cerebrospinal fluid HIV-1 RNA during treatment with ritonavir/saquinavir or ritonavir/saquinavir/stavudine. *AIDS* **14**:1583-1589.

Gomez DY, Wacher VJ, Tomlanovich SJ, Hebert MF and Benet LZ (1995) The effects of ketoconazole on the intestinal metabolism and bioavailability of cyclosporine. *Clin Pharmacol Ther* **58**:15-19.

Gradhand U and Kim RB (2008) Pharmacogenomics of MRP transporters (ABCC1-5) and BCRP (ABCG2). *Drug Metab Rev* **40**:317-354.

Gumbleton M and Audus KL (2001) Progress and limitations in the use of in vitro cell cultures to serve as a permeability screen for the blood-brain barrier. *J Pharm Sci* **90**:1681-1698.

Gyalrong-Steur M, Bogner JR and Seybold U (1999) Changes in lipid profiles after switching to a protease inhibitor-containing cART--unfavourable effect of fosamprenavir in obese patients. *Eur J Med Res* **16**:85-92.

Hall HI, Song R, Rhodes P, Prejean J, An Q, Lee LM, Karon J, Brookmeyer R, Kaplan EH, McKenna MT and Janssen RS (2008) Estimation of HIV incidence in the United States. *JAMA* **300**:520-529.

Hall HI SR, Rhodes P, Prejean J, An Q, Lee LM, Karon J, Brookmeyer R, Kaplan EH, McKenna MT, Janssen RS; HIV Incidence Surveillance Group. (2008) HIV prevalence estimates--United States, 2006. *MMWR Morb Mortal Wkly Rep* **57**:1073-1076.

Hallenberger S, Bosch V, Angliker H, Shaw E, Klenk HD and Garten W (1992) Inhibition of furin-mediated cleavage activation of HIV-1 glycoprotein gp160. *Nature* **360**:358-361.

Han HK and Amidon GL (2000) Targeted prodrug design to optimize drug delivery. *AAPS PharmSci* **2**:E6.

Hantz H, Adesuyi A and Adebayo O (2001) Differential effects of U46619 on renal regional hemodynamics in the rat: involvement of endothelin. *J Pharmacol Exp Ther* **299**:372-376.

Hashizume T, Imaoka S, Mise M, Terauchi Y, Fujii T, Miyazaki H, Kamataki T and Funae Y (2002) Involvement of CYP2J2 and CYP4F12 in the metabolism of ebastine in human intestinal microsomes. *J Pharmacol Exp Ther* **300**:298-304.

Hiscott J, Kwon H and Genin P (2001) Hostile takeovers: viral appropriation of the NF-kappaB pathway. *J Clin Invest* **107**:143-151.

Holmstock N, Annaert P and Augustijns P (2012) Boosting of HIV protease inhibitors by ritonavir in the intestine: the relative role of cytochrome P450 and P-glycoprotein inhibition based on Caco-2 monolayers versus in situ intestinal perfusion in mice. *Drug Metab Dispos* **40**:1473-1477.

Honda K, Komatsu T, Koyama F, Kubota A, Kawakami K, Asakura H, Uno Y, Kitazawa T, Hiraga T and Teraoka H (2011) Expression of two novel cytochrome P450 3A131 and 3A132 in liver and small intestine of domestic cats. *J Vet Med Sci* **73**:1489-1492.

Horio M, Chin KV, Currier SJ, Goldenberg S, Williams C, Pastan I, Gottesman MM and Handler J (1989) Transepithelial transport of drugs by the multidrug transporter in cultured Madin-Darby canine kidney cell epithelia. *J Biol Chem* **264**:14880-14884.

Howell S, Kenny AJ and Turner AJ (1992) A survey of membrane peptidases in two human colonic cell lines, Caco-2 and HT-29. *Biochem J* **284 ( Pt 2)**:595-601.

Hu M, Subramanian P, Mosberg HI and Amidon GL (1989) Use of the peptide carrier system to improve the intestinal absorption of L-alpha-methyldopa: carrier kinetics, intestinal permeabilities, and in vitro hydrolysis of dipeptidyl derivatives of L-alpha-methyldopa. *Pharm Res* **6**:66-70.

Huisman MT, Smit JW, Crommentuyn KM, Zelcer N, Wiltshire HR, Beijnen JH and Schinkel AH (2002) Multidrug resistance protein 2 (MRP2) transports HIV protease inhibitors, and transport can be enhanced by other drugs. *AIDS* **16**:2295-2301.

Hulot JS, Villard E, Maguy A, Morel V, Mir L, Tostivint I, William-Faltaos D, Fernandez C, Hatem S, Deray G, Komajda M, Leblond V and Lechat P (2005) A mutation in the drug transporter gene ABCC2 associated with impaired methotrexate elimination. *Pharmacogenet Genomics* **15**:277-285.

Hutt AJ and O'Grady J (1996) Drug chirality: a consideration of the significance of the stereochemistry of antimicrobial agents. *J Antimicrob Chemother* **37**:7-32.

Imai T, Imoto M, Sakamoto H and Hashimoto M (2005) Identification of esterases expressed in Caco-2 cells and effects of their hydrolyzing activity in predicting human intestinal absorption. *Drug Metab Dispos* **33**:1185-1190.

Irie M, Terada T, Okuda M and Inui K (2004) Efflux properties of basolateral peptide transporter in human intestinal cell line Caco-2. *Pflugers Arch* **449**:186-194.

Irvine JD, Takahashi L, Lockhart K, Cheong J, Tolan JW, Selick HE and Grove JR (1999) MDCK (Madin-Darby canine kidney) cells: A tool for membrane permeability screening. *J Pharm Sci* **88**:28-33.

Ito K, Suzuki H, Horie T and Sugiyama Y (2005) Apical/basolateral surface expression of drug transporters and its role in vectorial drug transport. *Pharm Res* **22**:1559-1577.

Jain R, Agarwal S, Majumdar S, Zhu X, Pal D and Mitra AK (2005) Evasion of P-gp mediated cellular efflux and permeability enhancement of HIV-protease inhibitor saquinavir by prodrug modification. *Int J Pharm* **303**:8-19.

Jain R, Agarwal S, Mandava NK, Sheng Y and Mitra AK (2008) Interaction of dipeptide prodrugs of saquinavir with multidrug resistance protein-2 (MRP-2): evasion of MRP-2 mediated efflux. *Int J Pharm* **362**:44-51.

Jain R, Duvvuri S, Kansara V, Mandava NK and Mitra AK (2007) Intestinal absorption of novel-dipeptide prodrugs of saquinavir in rats. *Int J Pharm* **336**:233-240.

Jani M, Szabo P, Kis E, Molnar E, Glavinas H and Krajcsi P (2009) Kinetic characterization of sulfasalazine transport by human ATP-binding cassette G2. *Biol Pharm Bull* **32**:497-499.

Jedlitschky G, Leier I, Buchholz U, Barnouin K, Kurz G and Keppler D (1996) Transport of glutathione, glucuronate, and sulfate conjugates by the MRP gene-encoded conjugate export pump. *Cancer Res* **56**:988-994.

Josephson F, Allqvist A, Janabi M, Sayi J, Aklillu E, Jande M, Mahindi M, Burhenne J, Bottiger Y, Gustafsson LL, Haefeli WE and Bertilsson L (2007) CYP3A5 genotype has an impact on the metabolism of the HIV protease inhibitor saquinavir. *Clin Pharmacol Ther* **81**:708-712.

Jumarie C and Malo C (1994) Alkaline phosphatase and peptidase activities in Caco-2 cells: differential response to triiodothyronine. *In Vitro Cell Dev Biol Anim* **30A**:753-760.

Kaminsky LS and Zhang QY (2003) The small intestine as a xenobiotic-metabolizing organ. *Drug Metab Dispos* **31**:1520-1525.

Karlsson Hedestam GB, Fouchier RA, Phogat S, Burton DR, Sodroski J and Wyatt RT (2008) The challenges of eliciting neutralizing antibodies to HIV-1 and to influenza virus. *Nat Rev Microbiol* **6**:143-155.

Katragadda S, Talluri RS and Mitra AK (2006) Modulation of P-glycoprotein-mediated efflux by prodrug derivatization: an approach involving peptide transporter-mediated influx across rabbit cornea. *J Ocul Pharmacol Ther* **22**:110-120.

Kauffmann HM, Vorderstemann B and Schrenk D (2001) Basal expression of the rat, but not of the human, multidrug resistance protein 2 (MRP2) gene is mediated by CBF/NF-Y and Sp1 promoter-binding sites. *Toxicology* **167**:25-35.

Kaul DR, Cinti SK, Carver PL and Kazanjian PH (1999) HIV protease inhibitors: advances in therapy and adverse reactions, including metabolic complications. *Pharmacotherapy* **19**:281-298.

Kedzierska K and Crowe SM (2002) The role of monocytes and macrophages in the pathogenesis of HIV-1 infection. *Curr Med Chem* **9**:1893-1903.

Kim AE, Dintaman JM, Waddell DS and Silverman JA (1998a) Saquinavir, an HIV protease inhibitor, is transported by P-glycoprotein. *J Pharmacol Exp Ther* **286**:1439-1445.

Kim RB, Fromm MF, Wandel C, Leake B, Wood AJ, Roden DM and Wilkinson GR (1998b) The drug transporter P-glycoprotein limits oral absorption and brain entry of HIV-1 protease inhibitors. *J Clin Invest* **101**:289-294.

Knutter I, Rubio-Aliaga I, Boll M, Hause G, Daniel H, Neubert K and Brandsch M (2002) H+-peptide cotransport in the human bile duct epithelium cell line SK-ChA-1. *Am J Physiol Gastrointest Liver Physiol* **283**:G222-229.

Knutter I, Wollesky C, Kottra G, Hahn MG, Fischer W, Zebisch K, Neubert RH, Daniel H and Brandsch M (2008) Transport of angiotensin-converting enzyme inhibitors by H+/peptide transporters revisited. *J Pharmacol Exp Ther* **327**:432-441.

Kodaira H, Kusuhara H, Ushiki J, Fuse E and Sugiyama Y (2010) Kinetic analysis of the cooperation of P-glycoprotein (P-gp/Abcb1) and breast cancer resistance protein (Bcrp/Abcg2) in limiting the brain and testis penetration of erlotinib, flavopiridol, and mitoxantrone. *J Pharmacol Exp Ther* **333**:788-796.

Kohl NE, Emini EA, Schleif WA, Davis LJ, Heimbach JC, Dixon RA, Scolnick EM and Sigal IS (1988) Active human immunodeficiency virus protease is required for viral infectivity. *Proc Natl Acad Sci U S A* **85**:4686-4690.

Konig J, Nies AT, Cui Y, Leier I and Keppler D (1999) Conjugate export pumps of the multidrug resistance protein (MRP) family: localization, substrate specificity, and MRP2-mediated drug resistance. *Biochim Biophys Acta* **1461**:377-394.

Konig SK, Herzog M, Theile D, Zembruski N, Haefeli WE and Weiss J (2010) Impact of drug transporters on cellular resistance towards saquinavir and darunavir. *J Antimicrob Chemother* **65**:2319-2328.

Krishnamachary N and Center MS (1993) The MRP gene associated with a non-P-glycoprotein multidrug resistance encodes a 190-kDa membrane bound glycoprotein. *Cancer Res* **53**:3658-3661.

Kuipers F, Havinga R, Bosschieter H, Toorop GP, Hindriks FR and Vonk RJ (1985) Enterohepatic circulation in the rat. *Gastroenterology* **88**:403-411.

Kumar GN, Rodrigues AD, Buko AM and Denissen JF (1996) Cytochrome P450-mediated metabolism of the HIV-1 protease inhibitor ritonavir (ABT-538) in human liver microsomes. *J Pharmacol Exp Ther* **277**:423-431.

Kuo YC and Yu HW (2011) Transport of saquinavir across human brain-microvascular endothelial cells by poly(lactide-co-glycolide) nanoparticles with surface poly-(gamma-glutamic acid). *Int J Pharm* **416**:365-375.

Kuteykin-Teplyakov K, Luna-Tortos C, Ambroziak K and Loscher W (2010) Differences in the expression of endogenous efflux transporters in MDR1-transfected versus wildtype cell lines affect P-glycoprotein mediated drug transport. *Br J Pharmacol* **160**:1453-1463.

Kwatra D, Budda B, Vadlapudi AD, Vadlapatla RK, Pal D and Mitra AK (2012) Transfected MDCK Cell Line with Enhanced Expression of CYP3A4 and P-Glycoprotein as a Model To Study Their Role in Drug Transport and Metabolism. *Mol Pharm*.

Lambotte O, Deiva K and Tardieu M (2003) HIV-1 persistence, viral reservoir, and the central nervous system in the HAART era. *Brain Pathol* **13**:95-103.

Landowski CP, Vig BS, Song X and Amidon GL (2005) Targeted delivery to PEPT1-overexpressing cells: acidic, basic, and secondary floxuridine amino acid ester prodrugs. *Mol Cancer Ther* **4**:659-667.

Lees P, Hunter RP, Reeves PT and Toutain PL (2012) Pharmacokinetics and pharmacodynamics of stereoisomeric drugs with particular reference to bioequivalence determination. *J Vet Pharmacol Ther* **35 Suppl 1**:17-29.

Leibach FH and Ganapathy V (1996) Peptide transporters in the intestine and the kidney. *Annu Rev Nutr* **16**:99-119.

Leslie EM, Deeley RG and Cole SP (2005) Multidrug resistance proteins: role of P-glycoprotein, MRP1, MRP2, and BCRP (ABCG2) in tissue defense. *Toxicol Appl Pharmacol* **204**:216-237.

Letourneau IJ, Bowers RJ, Deeley RG and Cole SP (2005) Limited modulation of the transport activity of the human multidrug resistance proteins MRP1, MRP2 and MRP3 by nicotine glucuronide metabolites. *Toxicol Lett* **157**:9-19.

Lin J, Schyschka L, Muhl-Benninghaus R, Neumann J, Hao L, Nussler N, Dooley S, Liu L, Stockle U, Nussler AK and Ehnert S (2012) Comparative analysis of phase I and II enzyme activities in 5 hepatic cell lines identifies Huh-7 and HCC-T cells with the highest potential to study drug metabolism. *Arch Toxicol* **86**:87-95.

Lipinski CA, Lombardo F, Dominy BW and Feeney PJ (2001) Experimental and computational approaches to estimate solubility and permeability in drug discovery and development settings. *Adv Drug Deliv Rev* **46**:3-26.

Lister N, Sykes AP, Bailey PD, Boyd CA and Bronk JR (1995) Dipeptide transport and hydrolysis in isolated loops of rat small intestine: effects of stereospecificity. *J Physiol* **484 ( Pt 1)**:173-182.

Liu W, Liang R, Ramamoorthy S, Fei YJ, Ganapathy ME, Hediger MA, Ganapathy V and Leibach FH (1995) Molecular cloning of PEPT 2, a new member of the

H+/peptide cotransporter family, from human kidney. *Biochim Biophys Acta* **1235**:461-466.

Llibre JM (2009) First-line boosted protease inhibitor-based regimens in treatment-naive HIV-1-infected patients--making a good thing better. *AIDS Rev* **11**:215-222.

Lloyd C, Schevzov G and Gunning P (1992) Transfection of nonmuscle beta- and gamma-actin genes into myoblasts elicits different feedback regulatory responses from endogenous actin genes. *J Cell Biol* **117**:787-797.

Lu H and Klaassen C (2006) Tissue distribution and thyroid hormone regulation of Pept1 and Pept2 mRNA in rodents. *Peptides* **27**:850-857.

Luckner P and Brandsch M (2005) Interaction of 31 beta-lactam antibiotics with the H+/peptide symporter PEPT2: analysis of affinity constants and comparison with PEPT1. *Eur J Pharm Biopharm* **59**:17-24.

Maliepaard M, Scheffer GL, Faneyte IF, van Gastelen MA, Pijnenborg AC, Schinkel AH, van De Vijver MJ, Scheper RJ and Schellens JH (2001) Subcellular localization and distribution of the breast cancer resistance protein transporter in normal human tissues. *Cancer Res* **61**:3458-3464.

Mao Q and Unadkat JD (2005) Role of the breast cancer resistance protein (ABCG2) in drug transport. *AAPS J* **7**:E118-133.

Marchetti S, de Vries NA, Buckle T, Bolijn MJ, van Eijndhoven MA, Beijnen JH, Mazzanti R, van Tellingen O and Schellens JH (2008) Effect of the ATP-binding cassette drug transporters ABCB1, ABCG2, and ABCC2 on erlotinib hydrochloride (Tarceva) disposition in in vitro and in vivo pharmacokinetic studies employing Bcrp1-/-/Mdr1a/1b-/- (triple-knockout) and wild-type mice. *Mol Cancer Ther* **7**:2280-2287.

Markowitz M, Saag M, Powderly WG, Hurley AM, Hsu A, Valdes JM, Henry D, Sattler F, La Marca A, Leonard JM and et al. (1995) A preliminary study of ritonavir, an inhibitor of HIV-1 protease, to treat HIV-1 infection. *N Engl J Med* **333**:1534-1539.

McComsey G, Bhumbra N, Ma JF, Rathore M and Alvarez A (2003) Impact of protease inhibitor substitution with efavirenz in HIV-infected children: results of the First Pediatric Switch Study. *Pediatrics* **111**:e275-281.

Michaud V, Simard C and Turgeon J (2010) Characterization of CYP3A Isozymes involved in the Metabolism of Domperidone: Role of Cytochrome b(5) and Inhibition by Ketoconazole. *Drug Metab Lett* **4**:95-103.

Miners JO, Knights KM, Houston JB and Mackenzie PI (2006) In vitro-in vivo correlation for drugs and other compounds eliminated by glucuronidation in humans: pitfalls and promises. *Biochem Pharmacol* **71**:1531-1539.

Mitsuoka K, Kato Y, Kubo Y and Tsuji A (2007) Functional expression of stereoselective metabolism of cephalexin by exogenous transfection of oligopeptide transporter PEPT1. *Drug Metab Dispos* **35**:356-362.

Nelson DR, Koymans L, Kamataki T, Stegeman JJ, Feyereisen R, Waxman DJ, Waterman MR, Gotoh O, Coon MJ, Estabrook RW, Gunsalus IC and Nebert DW (1996) P450 superfamily: update on new sequences, gene mapping, accession numbers and nomenclature. *Pharmacogenetics* **6**:1-42.

Nguyen LA, He H and Pham-Huy C (2006) Chiral drugs: an overview. *Int J Biomed Sci* **2**:85-100.

Nies AT and Keppler D (2007) The apical conjugate efflux pump ABCC2 (MRP2). *Pflugers Arch* **453**:643-659.

Noble S and Faulds D (1996) Saquinavir. A review of its pharmacology and clinical potential in the management of HIV infection. *Drugs* **52**:93-112.

O'Brien K, Nixon S, Glazier RH and Tynan AM (2004) Progressive resistive exercise interventions for adults living with HIV/AIDS. *Cochrane Database Syst Rev*:CD004248.

Ocheltree SM, Shen H, Hu Y, Xiang J, Keep RF and Smith DE (2004) Role of PEPT2 in the choroid plexus uptake of glycylsarcosine and 5-aminolevulinic acid: studies in wild-type and null mice. *Pharm Res* **21**:1680-1685.

Ojakian GK and Herzlinger DA (1984) Analysis of epithelial cell surface polarity with monoclonal antibodies. *Fed Proc* **43**:2208-2216.

Omkvist DH, Brodin B and Nielsen CU (2010) Ibuprofen is a non-competitive inhibitor of the peptide transporter hPEPT1 (SLC15A1): possible interactions between hPEPT1 substrates and ibuprofen. *Br J Pharmacol* **161**:1793-1805.

Ouattara DA, Choi SH, Sakai Y, Pery AR and Brochot C (2011) Kinetic modelling of in vitro cell-based assays to characterize non-specific bindings and ADME processes in a static and a perfused fluidic system. *Toxicol Lett* **205**:310-319.

Ouyang H, Andersen TE, Chen W, Nofsinger R, Steffansen B and Borchardt RT (2009) A comparison of the effects of p-glycoprotein inhibitors on the blood-brain barrier permeation of cyclic prodrugs of an opioid peptide (DADLE). *J Pharm Sci* **98**:2227-2236.

Paine MF, Hart HL, Ludington SS, Haining RL, Rettie AE and Zeldin DC (2006) The human intestinal cytochrome P450 "pie". *Drug Metab Dispos* **34**:880-886.

Paine MF, Khalighi M, Fisher JM, Shen DD, Kunze KL, Marsh CL, Perkins JD and Thummel KE (1997) Characterization of interintestinal and intraintestinal variations in human CYP3A-dependent metabolism. *J Pharmacol Exp Ther* **283**:1552-1562.

Pal D, Kwatra D, Minocha M, Paturi DK, Budda B and Mitra AK (2011) Efflux transporters- and cytochrome P-450-mediated interactions between drugs of abuse and antiretrovirals. *Life Sci* **88**:959-971.

Pal D and Mitra AK (2006) MDR- and CYP3A4-mediated drug-drug interactions. *J Neuroimmune Pharmacol* **1**:323-339.

Pan Y, Wong EA, Bloomquist JR and Webb KE, Jr. (2001) Expression of a cloned ovine gastrointestinal peptide transporter (oPepT1) in Xenopus oocytes induces uptake of oligopeptides in vitro. *J Nutr* **131**:1264-1270.

Pang KS (2003) Modeling of intestinal drug absorption: roles of transporters and metabolic enzymes (for the Gillette Review Series). *Drug Metab Dispos* **31**:1507-1519.

Pang KS, Weiss M and Macheras P (2007) Advanced pharmacokinetic models based on organ clearance, circulatory, and fractal concepts. *AAPS J* **9**:E268-283.

Parker AJ and Houston JB (2008) Rate-limiting steps in hepatic drug clearance: comparison of hepatocellular uptake and metabolism with microsomal metabolism of saquinavir, nelfinavir, and ritonavir. *Drug Metab Dispos* **36**:1375-1384.

Patel K, Trivedi S, Luo S, Zhu X, Pal D, Kern ER and Mitra AK (2005) Synthesis, physicochemical properties and antiviral activities of ester prodrugs of ganciclovir. *Int J Pharm* **305**:75-89.

Paumi CM, Chuk M, Snider J, Stagljar I and Michaelis S (2009) ABC transporters in Saccharomyces cerevisiae and their interactors: new technology advances the biology of the ABCC (MRP) subfamily. *Microbiol Mol Biol Rev* **73**:577-593.

Penzak SR and Chuck SK (2002) Management of protease inhibitor-associated hyperlipidemia. *Am J Cardiovasc Drugs* **2**:91-106.

Peters BS and Conway K (2010) Therapy for HIV: past, present, and future. *Adv Dent Res* **23**:23-27.

Peters BS and Conway K (2011) Therapy for HIV: past, present, and future. *Adv Dent Res* **23**:23-27.

Peters TJ (1970) Intestinal peptidases. *Gut* **11**:720-725.

Peters WH and Kremers PG (1989) Cytochromes P-450 in the intestinal mucosa of man. *Biochem Pharmacol* **38**:1535-1538.

Pieri M, Christian HC, Wilkins RJ, Boyd CA and Meredith D (2010) The apical (hPepT1) and basolateral peptide transport systems of Caco-2 cells are regulated by AMP-activated protein kinase. *Am J Physiol Gastrointest Liver Physiol* **299**:G136-143.

Plosker GL and Scott LJ (2003) Saquinavir: a review of its use in boosted regimens for treating HIV infection. *Drugs* **63**:1299-1324.

Pochopin NL, Charman WN and Stella VJ (1994) Pharmacokinetics of dapsone and amino acid prodrugs of dapsone. *Drug Metab Dispos* **22**:770-775.

Pollard VW and Malim MH (1998) The HIV-1 Rev protein. *Annu Rev Microbiol* **52**:491-532.

Putnam WS, Pan L, Tsutsui K, Takahashi L and Benet LZ (2002) Comparison of bidirectional cephalexin transport across MDCK and caco-2 cell monolayers: interactions with peptide transporters. *Pharm Res* **19**:27-33.

Rao VV, Dahlheimer JL, Bardgett ME, Snyder AZ, Finch RA, Sartorelli AC and Piwnica-Worms D (1999) Choroid plexus epithelial expression of MDR1 P glycoprotein and multidrug resistance-associated protein contribute to the blood-cerebrospinal-fluid drug-permeability barrier. *Proc Natl Acad Sci U S A* **96**:3900-3905.

Rathbun RC and Rossi DR (2002) Low-dose ritonavir for protease inhibitor pharmacokinetic enhancement. *Ann Pharmacother* **36**:702-706.

Rautio J, Kumpulainen H, Heimbach T, Oliyai R, Oh D, Jarvinen T and Savolainen J (2008) Prodrugs: design and clinical applications. *Nat Rev Drug Discov* **7**:255-270.

Richman DD (2001) HIV chemotherapy. *Nature* **410**:995-1001.

Robertson DL, Hahn BH and Sharp PM (1995) Recombination in AIDS viruses. *J Mol Evol* **40**:249-259.

Roe AL, Snawder JE, Benson RW, Roberts DW and Casciano DA (1993) HepG2 cells: an in vitro model for P450-dependent metabolism of acetaminophen. *Biochem Biophys Res Commun* **190**:15-19.

Rossi C, Guantario B, Ferruzza S, Guguen-Guillouzo C, Sambuy Y, Scarino ML and Bellovino D (2012) Co-cultures of enterocytes and hepatocytes for retinoid transport and metabolism. *Toxicol In Vitro* **26**:1256-1264.

Rouquayrol M, Gaucher B, Roche D, Greiner J and Vierling P (2002) Transepithelial transport of prodrugs of the HIV protease inhibitors saquinavir, indinavir, and nelfinavir across Caco-2 cell monolayers. *Pharm Res* **19**:1704-1712.

Rubio-Aliaga I and Daniel H (2008) Peptide transporters and their roles in physiological processes and drug disposition. *Xenobiotica* **38**:1022-1042.

Saito H, Okuda M, Terada T, Sasaki S and Inui K (1995) Cloning and characterization of a rat H+/peptide cotransporter mediating absorption of beta-lactam antibiotics in the intestine and kidney. *J Pharmacol Exp Ther* **275**:1631-1637.

Saitoh H and Aungst BJ (1995) Possible involvement of multiple P-glycoprotein-mediated efflux systems in the transport of verapamil and other organic cations across rat intestine. *Pharm Res* **12**:1304-1310.

Salama NN, Fasano A, Thakar M and Eddington ND (2005) The impact of DeltaG on the oral bioavailability of low bioavailable therapeutic agents. *J Pharmacol Exp Ther* **312**:199-205.

Sanderson IR (1999) The physicochemical environment of the neonatal intestine. *Am J Clin Nutr* **69**:1028S-1034S.

Sawada K, Terada T, Saito H, Hashimoto Y and Inui KI (1999) Recognition of L-amino acid ester compounds by rat peptide transporters PEPT1 and PEPT2. *J Pharmacol Exp Ther* **291**:705-709.

Sawada K, Terada T, Saito H and Inui K (2001) Distinct transport characteristics of basolateral peptide transporters between MDCK and Caco-2 cells. *Pflugers Arch* **443**:31-37.

Scow JS, Madhavan S, Chaudhry RM, Zheng Y, Duenes JA and Sarr MG (2011) Differentiating passive from transporter-mediated uptake by PepT1: a comparison and evaluation of four methods. *J Surg Res* **170**:17-23.

Severijnen R, Bayat N, Bakker H, Tolboom J and Bongaerts G (2004) Enteral drug absorption in patients with short small bowel : a review. *Clin Pharmacokinet* **43**:951-962.

Shah LK and Amiji MM (2006) Intracellular delivery of saquinavir in biodegradable polymeric nanoparticles for HIV/AIDS. *Pharm Res* **23**:2638-2645.

Sharom FJ (1997) The P-glycoprotein efflux pump: how does it transport drugs? *J Membr Biol* **160**:161-175.

Sharom FJ (2008) ABC multidrug transporters: structure, function and role in chemoresistance. *Pharmacogenomics* **9**:105-127.

Shimakura J, Terada T, Shimada Y, Katsura T and Inui K (2006) The transcription factor Cdx2 regulates the intestine-specific expression of human peptide transporter 1 through functional interaction with Sp1. *Biochem Pharmacol* **71**:1581-1588.

Siccardi D, Kandalaft LE, Gumbleton M and McGuigan C (2003) Stereoselective and concentration-dependent polarized epithelial permeability of a series of phosphoramidate triester prodrugs of d4T: an in vitro study in Caco-2 and Madin-Darby canine kidney cell monolayers. *J Pharmacol Exp Ther* **307**:1112-1119.

Simon V, Ho DD and Abdool Karim Q (2006) HIV/AIDS epidemiology, pathogenesis, prevention, and treatment. *Lancet* **368**:489-504.

Smith SW (2009) Chiral toxicology: it's the same thing...only different. *Toxicol Sci* **110**:4-30.

Song H, Griesgraber GW, Wagner CR and Zimmerman CL (2002) Pharmacokinetics of amino acid phosphoramidate monoesters of zidovudine in rats. *Antimicrob Agents Chemother* **46**:1357-1363.

Spaulding A, Rutherford GW and Siegfried N (2011) Stavudine or zidovudine in three-drug combination therapy for initial treatment of HIV infection in antiretroviral-naive individuals. *Cochrane Database Syst Rev*:CD008651.

Steffansen B, Nielsen CU, Brodin B, Eriksson AH, Andersen R and Frokjaer S (2004) Intestinal solute carriers: an overview of trends and strategies for improving oral drug absorption. *Eur J Pharm Sci* **21**:3-16.

Stock I (2011) [Infections with human immunodeficiency viruses. Part II: Antiretroviral drugs, therapeutic options, and diagnostics]. *Med Monatsschr Pharm* **34**:234-244; quiz 245-236.

Strassburg CP, Kneip S, Topp J, Obermayer-Straub P, Barut A, Tukey RH and Manns MP (2000) Polymorphic gene regulation and interindividual variation of UDP-glucuronosyltransferase activity in human small intestine. *J Biol Chem* **275**:36164-36171.

Sunner T, Schneider C, Strauss M, Huggenberger A, Wiener D, Hofling S, Kamp M and Forchel A (2008) Scalable fabrication of optical resonators with embedded site-controlled quantum dots. *Opt Lett* **33**:1759-1761.

Svarovskaia ES, Cheslock SR, Zhang WH, Hu WS and Pathak VK (2003) Retroviral mutation rates and reverse transcriptase fidelity. *Front Biosci* **8**:d117-134.

Taipalensuu J, Tornblom H, Lindberg G, Einarsson C, Sjoqvist F, Melhus H, Garberg P, Sjostrom B, Lundgren B and Artursson P (2001) Correlation of gene expression of ten drug efflux proteins of the ATP-binding cassette transporter family in normal human jejunum and in human intestinal epithelial Caco-2 cell monolayers. *J Pharmacol Exp Ther* **299**:164-170.

Takakura Y, Hinoi T, Oue N, Sasada T, Kawaguchi Y, Okajima M, Akyol A, Fearon ER, Yasui W and Ohdan H (2010) CDX2 regulates multidrug resistance 1 gene expression in malignant intestinal epithelium. *Cancer Res* **70**:6767-6778.

Takano M, Yumoto R and Murakami T (2006) Expression and function of efflux drug transporters in the intestine. *Pharmacol Ther* **109**:137-161.

Talluri RS, Samanta SK, Gaudana R and Mitra AK (2008) Synthesis, metabolism and cellular permeability of enzymatically stable dipeptide prodrugs of acyclovir. *Int J Pharm* **361**:118-124.

Tamai I, Ling HY, Timbul SM, Nishikido J and Tsuji A (1988) Stereospecific absorption and degradation of cephalexin. *J Pharm Pharmacol* **40**:320-324.

Tamura K, Bhatnagar PK, Takata JS, Lee CP, Smith PL and Borchardt RT (1996a) Metabolism, uptake, and transepithelial transport of the diastereomers of Val-Val in the human intestinal cell line, Caco-2. *Pharm Res* **13**:1213-1218.

Tamura K, Lee CP, Smith PL and Borchardt RT (1996b) Metabolism, uptake, and transepithelial transport of the stereoisomers of Val-Val-Val in the human intestinal cell line, Caco-2. *Pharm Res* **13**:1663-1667.

Tang F, Horie K and Borchardt RT (2002a) Are MDCK cells transfected with the human MDR1 gene a good model of the human intestinal mucosa? *Pharm Res* **19**:765-772.

Tang F, Horie K and Borchardt RT (2002b) Are MDCK cells transfected with the human MRP2 gene a good model of the human intestinal mucosa? *Pharm Res* **19**:773-779.

Taub ME, Podila L, Ely D and Almeida I (2005) Functional assessment of multiple P-glycoprotein (P-gp) probe substrates: influence of cell line and modulator concentration on P-gp activity. *Drug Metab Dispos* **33**:1679-1687.

Temesgen Z, Cainelli F, Poeschla EM, Vlahakis SA and Vento S (2006) Approach to salvage antiretroviral therapy in heavily antiretroviral-experienced HIV-positive adults. *Lancet Infect Dis* **6**:496-507.

Terada T and Inui K (2004) Peptide transporters: structure, function, regulation and application for drug delivery. *Curr Drug Metab* **5**:85-94.

Terada T, Sawada K, Ito T, Saito H, Hashimoto Y and Inui K (2000) Functional expression of novel peptide transporter in renal basolateral membranes. *Am J Physiol Renal Physiol* **279**:F851-857.

Thamotharan M, Lombardo YB, Bawani SZ and Adibi SA (1997) An active mechanism for completion of the final stage of protein degradation in the liver, lysosomal transport of dipeptides. *J Biol Chem* **272**:11786-11790.

Thelen K and Dressman JB (2009) Cytochrome P450-mediated metabolism in the human gut wall. *J Pharm Pharmacol* **61**:541-558.

Thomson MM, Perez-Alvarez L and Najera R (2002) Molecular epidemiology of HIV-1 genetic forms and its significance for vaccine development and therapy. *Lancet Infect Dis* **2**:461-471.

Thuerauf N and Fromm MF (2006) The role of the transporter P-glycoprotein for disposition and effects of centrally acting drugs and for the pathogenesis of CNS diseases. *Eur Arch Psychiatry Clin Neurosci* **256**:281-286.

Thummel KE, O'Shea D, Paine MF, Shen DD, Kunze KL, Perkins JD and Wilkinson GR (1996) Oral first-pass elimination of midazolam involves both gastrointestinal and hepatic CYP3A-mediated metabolism. *Clin Pharmacol Ther* **59**:491-502.

Tomaru A, Takeda-Morishita M, Banba H and Takayama K (2013) Analysis of the pharmacokinetic boosting effects of ritonavir on oral bioavailability of drugs in mice. *Drug Metab Pharmacokinet* **28**:144-152.

Treijtel N, van Eijkeren JC, Nijmeijer S, de Greef-van der Sandt IC and Freidig AP (2009) Clearance and clearance inhibition of the HIV-1 protease inhibitors ritonavir and saquinavir in sandwich-cultured rat hepatocytes and rat microsomes. *Toxicol In Vitro* **23**:185-193.

Tsume Y, Vig BS, Sun J, Landowski CP, Hilfinger JM, Ramachandran C and Amidon GL (2008) Enhanced absorption and growth inhibition with amino acid monoester prodrugs of floxuridine by targeting hPEPT1 transporters. *Molecules* **13**:1441-1454.

Tusnady GE, Bakos E, Varadi A and Sarkadi B (1997) Membrane topology distinguishes a subfamily of the ATP-binding cassette (ABC) transporters. *FEBS Lett* **402**:1-3.

Ungell AL, Nylander S, Bergstrand S, Sjoberg A and Lennernas H (1998) Membrane transport of drugs in different regions of the intestinal tract of the rat. *J Pharm Sci* **87**:360-366.

Usansky HH, Hu P and Sinko PJ (2008) Differential roles of P-glycoprotein, multidrug resistance-associated protein 2, and CYP3A on saquinavir oral absorption in Sprague-Dawley rats. *Drug Metab Dispos* **36**:863-869.

van Asperen J, van Tellingen O, Sparreboom A, Schinkel AH, Borst P, Nooijen WJ and Beijnen JH (1997) Enhanced oral bioavailability of paclitaxel in mice treated with the P-glycoprotein blocker SDZ PSC 833. *Br J Cancer* **76**:1181-1183.

van Wijk H, Donachie P, Mann DL, McMahon H and Robb D (2001) A novel bile duct cannulation method with tail cuff exteriorization allowing continuous intravenous infusion and enterohepatic recirculation in the unrestrained rat. *Lab Anim* **35**:325-333.

van Zyl GU, van der Merwe L, Claassen M, Zeier M and Preiser W (2011) Antiretroviral resistance patterns and factors associated with resistance in adult patients failing NNRTI-based regimens in the Western Cape, South Africa. *J Med Virol* **83**:1764-1769.

Vella S (1995) Clinical experience with saquinavir. *AIDS* **9 Suppl 2**:S21-S25.

Vollmann K, Qurishi R, Hockemeyer J and Muller CE (2008) Synthesis and properties of a new water-soluble prodrug of the adenosine A 2A receptor antagonist MSX-2. *Molecules* **13**:348-359.

Volpe DA (2008) Variability in Caco-2 and MDCK cell-based intestinal permeability assays. *J Pharm Sci* **97**:712-725.

von Bonsdorff CH, Fuller SD and Simons K (1985) Apical and basolateral endocytosis in Madin-Darby canine kidney (MDCK) cells grown on nitrocellulose filters. *EMBO J* **4**:2781-2792.

von Moltke LL, Greenblatt DJ, Duan SX, Daily JP, Harmatz JS and Shader RI (1998) Inhibition of desipramine hydroxylation (Cytochrome P450-2D6) in vitro by quinidine and by viral protease inhibitors: relation to drug interactions in vivo. *J Pharm Sci* **87**:1184-1189.

Vyas TK, Shahiwala A and Amiji MM (2008) Improved oral bioavailability and brain transport of Saquinavir upon administration in novel nanoemulsion formulations. *Int J Pharm* **347**:93-101.

Wacher VJ, Silverman JA, Zhang Y and Benet LZ (1998) Role of P-glycoprotein and cytochrome P450 3A in limiting oral absorption of peptides and peptidomimetics. *J Pharm Sci* **87**:1322-1330.

Wang Q, Rager JD, Weinstein K, Kardos PS, Dobson GL, Li J and Hidalgo IJ (2005) Evaluation of the MDR-MDCK cell line as a permeability screen for the blood-brain barrier. *Int J Pharm* **288**:349-359.

Wang Y, Cao J, Wang X and Zeng S (2010) Stereoselective transport and uptake of propranolol across human intestinal Caco-2 cell monolayers. *Chirality* **22**:361-368.

Wang Z, Pal D and Mitra AK (2012) Stereoselective evasion of P-glycoprotein, cytochrome P450 3A, and hydrolases by peptide prodrug modification of saquinavir. *J Pharm Sci* **101**:3199-3213.

Wang Z, Pal D, Patel A, Kwatra D and Mitra AK (2013) Influence of overexpression of efflux proteins on the function and gene expression of endogenous peptide transporters in MDR-transfected MDCKII cell lines. *Int J Pharm* **441**:40-49.

Washington CB, Duran GE, Man MC, Sikic BI and Blaschke TF (1998) Interaction of anti-HIV protease inhibitors with the multidrug transporter P-glycoprotein (P-gp) in human cultured cells. *J Acquir Immune Defic Syndr Hum Retrovirol* **19**:203-209.

Watkins PB, Wrighton SA, Schuetz EG, Molowa DT and Guzelian PS (1987) Identification of glucocorticoid-inducible cytochromes P-450 in the intestinal mucosa of rats and man. *J Clin Invest* **80**:1029-1036.

Westerink WM and Schoonen WG (2007) Cytochrome P450 enzyme levels in HepG2 cells and cryopreserved primary human hepatocytes and their induction in HepG2 cells. *Toxicol In Vitro* **21**:1581-1591.

White TA, Bartesaghi A, Borgnia MJ, Meyerson JR, de la Cruz MJ, Bess JW, Nandwani R, Hoxie JA, Lifson JD, Milne JL and Subramaniam S (2008) Molecular architectures of trimeric SIV and HIV-1 envelope glycoproteins on intact viruses: strain-dependent variation in quaternary structure. *PLoS Pathog* **6**:e1001249.

Williams GC, Liu A, Knipp G and Sinko PJ (2002) Direct evidence that saquinavir is transported by multidrug resistance-associated protein (MRP1) and canalicular multispecific organic anion transporter (MRP2). *Antimicrob Agents Chemother* **46**:3456-3462.

Williams GC and Sinko PJ (1999) Oral absorption of the HIV protease inhibitors: a current update. *Adv Drug Deliv Rev* **39**:211-238.

Wu CY, Benet LZ, Hebert MF, Gupta SK, Rowland M, Gomez DY and Wacher VJ (1995) Differentiation of absorption and first-pass gut and hepatic metabolism in humans: studies with cyclosporine. *Clin Pharmacol Ther* **58**:492-497.

Wyatt R and Sodroski J (1998) The HIV-1 envelope glycoproteins: fusogens, antigens, and immunogens. *Science* **280**:1884-1888.

Xiao Y, Davidson R, Smith A, Pereira D, Zhao S, Soglia J, Gebhard D, de Morais S and Duignan DB (2006) A 96-well efflux assay to identify ABCG2 substrates using a stably transfected MDCK II cell line. *Mol Pharm* **3**:45-54.

Yang C, Tirucherai GS and Mitra AK (2001) Prodrug based optimal drug delivery via membrane transporter/receptor. *Expert Opin Biol Ther* **1**:159-175.

Yang CY, Dantzig AH and Pidgeon C (1999) Intestinal peptide transport systems and oral drug availability. *Pharm Res* **16**:1331-1343.

Youle M (2007) Overview of boosted protease inhibitors in treatment-experienced HIV-infected patients. *J Antimicrob Chemother* **60**:1195-1205.

Zaman GJ, Flens MJ, van Leusden MR, de Haas M, Mulder HS, Lankelma J, Pinedo HM, Scheper RJ, Baas F, Broxterman HJ and et al. (1994) The human multidrug resistance-associated protein MRP is a plasma membrane drug-efflux pump. *Proc Natl Acad Sci U S A* **91**:8822-8826.

Zappella M, Meloni I, Longo I, Canitano R, Hayek G, Rosaia L, Mari F and Renieri A (2003) Study of MECP2 gene in Rett syndrome variants and autistic girls. *Am J Med Genet B Neuropsychiatr Genet* **119B**:102-107.

Zhang M, Mathur A, Zhang Y, Xi S, Atay S, Hong JA, Datrice N, Upham T, Kemp CD, Ripley RT, Wiegand G, Avital I, Fetsch P, Mani H, Zlott D, Robey R, Bates SE, Li X, Rao M and Schrump DS (2012) Mithramycin represses basal and cigarette smoke-induced expression of ABCG2 and inhibits stem cell signaling in lung and esophageal cancer cells. *Cancer Res* **72**:4178-4192.

Zheng YH, Lovsin N and Peterlin BM (2005) Newly identified host factors modulate HIV replication. *Immunol Lett* **97**:225-234.

Zhou M, Duan H, Engel K, Xia L and Wang J (2010) Adenosine transport by plasma membrane monoamine transporter: reinvestigation and comparison with organic cations. *Drug Metab Dispos* **38**:1798-1805.

Zhu P, Chertova E, Bess J, Jr., Lifson JD, Arthur LO, Liu J, Taylor KA and Roux KH (2003) Electron tomography analysis of envelope glycoprotein trimers on HIV and simian immunodeficiency virus virions. *Proc Natl Acad Sci U S A* **100**:15812-15817.

# VITA

Zhiying Wang was born on January 30th, 1976 in Shenyang, China. She obtained her Bachelor of Science degree in Pharmacy from China Pharmaceutical University (Nanjing, China) in July 1998. In September 2000, she joined Peking University Health Science Center (Beijing, China), and received her Master's degree in Pharmaceutics in 2003. Later Zhiying Wang joined Dr. Ashim K. Mitra's labortary at University of Missouri-Kansas City in the fall semester 2006 in persuit of an interdisciplinary doctorate degree in Pharmaceutical Sciences and Chemistry.

Zhiying Wang is a member of American Association of Pharmaceutical Scientists (AAPS). She received a travelship award from Drug Design and Discovery (DDD) Section of AAPS to present her work at the AAPS Annual Meeting (New Orleans, LA) in 2011. She also received the Outstanding Poster Award from Health Sciences Student Research Summit (Kansas City, MO) in 2013. She has authored/co-authored several peer-reviewed research articles in reputed international journals and presentations at national conferences.